

# FedCut: A Spectral Analysis Framework for Reliable Detection of Byzantine Colluders

Hanlin Gu, Lixin Fan, *Member, IEEE*, XingXing Tang, and Qiang Yang, *Fellow, IEEE*

**Abstract**—This paper proposes a general *spectral analysis* framework that thwarts a security risk in federated Learning caused by *groups of malicious Byzantine attackers or colluders*, who conspire to upload vicious model updates to severely debase global model performances. The proposed framework delineates the strong consistency and temporal coherence between Byzantine colluders' model updates from a spectral analysis lens, and, formulates the detection of Byzantine misbehaviours as a *community detection* problem in weighted graphs. The modified normalized graph cut is then utilized to discern attackers from benign participants. Moreover, the *Spectral heuristics* is adopted to make the detection robust against various attacks. The proposed Byzantine colluder resilient method, i.e., FedCut, is guaranteed to converge with bounded errors. Extensive experimental results under a variety of settings justify the superiority of FedCut, which demonstrates extremely robust model performance (MP) under various attacks. It was shown that FedCut's averaged MP is 2.1% to 16.5% better than that of the state of the art Byzantine-resilient methods. In terms of the worst-case model performance (MP), FedCut is 17.6% to 69.5% better than these methods.

**Index Terms**—Byzantine colluders; Byzantine resilient; Spectral analysis; Normalized cut; Spectral heuristics; Graph; Federated learning; privacy preserving computing;



## 1 INTRODUCTION

FEDERATED learning (FL) [40], [66] is a suite of privacy-preserving machine learning techniques that allow multiple parties to collaboratively train a global model, yet, without gathering or exchanging *privacy* for the sake of compliance with private data protection regulation rules such as GDPR<sup>1</sup>. It is the *upgraded global model performance* that motivates multiple parties to join FL, however, the risk of potential malicious attacks aiming to degrade FL model performances cannot be discounted. It was shown that even a *single* attacker (aka a Byzantine worker) may prevent the convergence of a naive FL aggregation rule by submitting vicious model updates to outweigh benign workers (see Lemma 1 of [6]). A great deal of research effort was then devoted to developing numerous Byzantine-resilient methods which can effectively detect and attenuate such misbehaviours [6], [68], [45], [13], [61], [65], [21]. Nevertheless, recent research pointed out that a *group of attackers or colluders* may conspire to cause more damages than these Byzantine-resilient methods can deal with (see [4], [63], [18]). It is the misbehavior of such Byzantine *colluders* that motivate our research to analyze their influences on global model performances from a spectral analysis framework, and based on our findings, an effective defense algorithm to do away with Byzantine colluders is proposed.

There are two main challenges brought by Byzantine colluders. First, colluders may conspire to *misbehave consistently* and introduce *statistical bias* to break down *Robust Statistics* (RS) based resilient methods (e.g., [4], [18], [63]). Consequently, the global model performances may deteriorate significantly. Second, Byzantine colluders may conspire to violate the assumption that all malicious model updates form one group while benign ones form the other, which is invariably assumed by most clustering-based Byzantine-resilient methods [54], [51], [20]. By submitting multiple groups of such detrimental yet disguised model updates, colluders therefore can evade clustering-based methods and degrade the global model performance significantly.

In order to address the challenges brought by colluders, we propose in this article a spectral analysis framework, called FedCut, which admits effective detection of Byzantine colluders in a variety of settings and provide the spectral analysis of different types of Byzantine behaviours especially for Byzantine colluders (see Sect. 4). The essential ingredients of the proposed framework are as follows. First, we build the Spatial-Temporal graph with all clients' model updates over multiple learning iterations as nodes, and similarities between respective pairs of model updates as edge weights (see Sect. 5.1). Second, an extension of the *normalized cut* (Ncut) [55], [42] provides the optimal c-partition Ncut (see Sect. 5.2), which allows to detect colluders with consistent behaviour efficiently. Third, *spectral heuristics* [70] are used to determine the type of Byzantine attackers, the unknown number of colluder groups and the appropriate scaling factor  $\sigma$  of Gaussian kernels used for measuring similarities between model updates (see Sect. 5.3). By leveraging the aforementioned techniques together within the unified spectral analysis framework, we thus propose in Sect. 5 the FedCut method which demonstrates superior robustness in the presence of different types of colluder attacks. Its

- Hanlin Gu and Lixin Fan are with WeBank AI Lab, WeBank, China. E-mail: {allengu, lixinfan}@webank.com, {ghlts123, Lixin.Fan01}@gmail.com.
- Xingxing Tang is with the Department of Computer Science and Engineering, Hong Kong University of Science and Technology, Hong Kong. E-mail: xtangav@connect.ust.hk
- Qiang Yang is with the Department of Computer Science and Engineering, Hong Kong University of Science and Technology, Hong Kong and WeBank AI Lab, WeBank, China. E-mail: qyang@cse.ust.hk.

Corresponding author: Lixin Fan.

1. GDPR is applicable as of May 25th, 2018 in all European member states to harmonize data privacy laws across Europe. <https://gdpr.eu/>

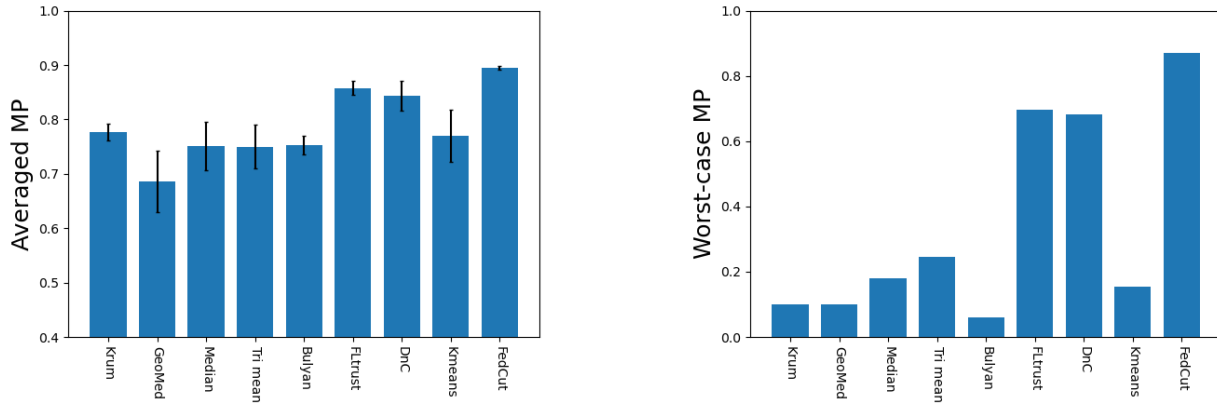


Fig. 1: Averaged (left) and worst-case (right) model performances under all attacks for different Byzantine-resilient methods (Krum [6], GeoMedian [13], Median, Trimmed mean [68], Bulyan [21], FLtrust [10], DnC [52], Kmeans [54] and our proposed FedCut) with IID setting and 30 Byzantine clients for classification of Fashion MNIST (FedCut – the proposed method, see more details in Sect. 7.1).

convergence is theoretically proved in Sect. 6 and it compares favorably to the state of arts Byzantine-resilient methods in thorough empirical evaluations of model performances in Sect. 7. Our contributions are three folds.

- First, we provide the spectral analysis of Byzantine attacks, especially, those launched by colluders. Specifically, we formulate existing Byzantine attacks as four types and gain a deeper understanding of colluders’ attacks in the lens of spectral. Moreover, we delineate root causes of failure cases of existing Byzantine-resilient methods in the face of colluder attacks (see Sect. 4.3).
- Second, we propose the spectral analysis framework, called FedCut, which distinguishes benign clients from multiple groups of Byzantine colluders. Specifically, the *normalized cut*, *temporal consistency* and the *spectral heuristics* are adopted to address challenges brought by colluders. Moreover, we provide the theoretical analysis of convergence of the proposed algorithm FedCut.
- Finally, we propose to thoroughly investigate both *averaged* and *worst-case* model performances of different Byzantine-resilient methods with extensive experiments under a variety of settings, including different types of models, datasets, extents of Non-IID, the fraction of attackers, combinations of colluders groups. It was then demonstrated that the proposed FedCut consistently outperforms existing methods under all different settings (see Fig. 1 and Tab. 1).

## 2 RELATED WORK

Related work are abundant in the literature and we briefly review them below.

**Byzantine attacks** can be broadly categorized as Non-Collusion and Collusion attacks. The former attacks were proposed to degrade global model performances by uploading Gaussian noise or flipping gradients [6], [35]. The latter type launched consistent attacks to induce misclassifications of Byzantine attackers [4], [18], [63].

**Robust statistics based aggregation** approaches treated

malicious model updates as *outliers*, which are far away from benign clients, and filter out outliers via robust statistics accordingly. For example, the coordinate-wise Median and some variants of Median, such as geometric Median, were proposed to remove outliers [68], [45], [61]. Moreover, Blanchard et al. assumed few outliers were far away from benign updates. Therefore, they used the Krum function to select model updates that are very close to at least half the other updates [6] as benign updates. However, the aforementioned methods are vulnerable to attacks with collusion which may conspire to induce *biased* estimations [4], [18], [63]. A different line of approaches [52], [16], [15] used the concentration filter to remove the outliers which are far away from concentration (such as the mean) [52], [16], [15]. For instance, Shejwalkar et al. applied SVD to the covariance matrix of model updates and filtered out outliers that largely deviate from the empirical mean of model updates towards the principle direction [52]. However, the effectiveness of the concentration filter may deteriorate in the presence of collusion attacks (see Sect. 4.3), and moreover, the time complexity of this approach is high  $\tilde{O}(d^3)$  when the dimension of updates  $d$  is large.

**Clustering based robust aggregation** grouped all clients into two clusters according to pairwise similarities between clients’ updates and regarded the cluster with a smaller number as the Byzantine cluster. For instance, some methods applied *Kmeans* into clustering benign and byzantine clients [54], [9] and Sattler et al. separated benign and byzantine clients by minimizing *cosine similarity* of updates among two groups [51], [50]. Moreover, Ghosh et al. made use of iterative Kmeans clustering to remove the byzantine attackers [20]. However, the adopted naive clustering such as Kmeans, Kmedian [26], [38] have two shortcomings: 1) being *inefficient* and easily trapped into *local minima*; 2) breaking down when the number of colluder groups is unknown to the the clustering method (see details in Sect. 4).

**Server based robust aggregation** assumed *the server had an extra training dataset* which was used to evaluate uploaded model updates. Either abnormal updates with low scores

TABLE 1: Overview of the performance for various Byzantine-resilient methods (Robust statistics based: Krum [6], Median, Trimmed Mean [68] and DnC [52]; Clustering based: Kmeans [54]; Server based: FLtrust [10]; Spectral based: FedCut, see more details in Sect. 2) under different Byzantine attacks (Non-Collusion attack: [6], label flipping [15] and sign flipping [15], Collusion-diff attack: same value attack [35], Fang-v1 (design for trimmed mean) [18] and our designed Multi-collusion attack, Collusion-mimic attack: Mimic [28] and Lie [4], see more details in Sect. 4.2). ✓, Δ and ✗ denotes the drop of model performance less than 3%, from 3% to 10% and above 10% on Fashion MNIST respectively (see more comparisons in Sect. 7)

		Robust statistics based				Clustering based	Server based	Spectral based
		Krum	Median	Tri mean	DnC	Kmeans	FLtrust	FedCut(Ours)
Non-Collusion	Gaussian[6]	Δ	✓	✓	✗	✗	✓	✓
	label flipping[15]	Δ	✗	✗	✓	✓	✓	✓
	sign flipping[15]	Δ	Δ	Δ	✗	✗	Δ	✓
Collusion-diff	same value[35]	Δ	✗	✗	✓	✓	✓	✓
	Fang-v1[18]	Δ	✗	✗	✓	✓	Δ	✓
	Multi-collusion	Δ	✗	✗	Δ	✗	✓	✓
Collusion-mimic	Mimic[28]	✗	Δ	Δ	Δ	✓	✓	✓
	Lie [4]	Δ	✗	✗	✗	✓	✗	✓

were filtered out [10], [62], [48], [46] or minority Byzantine updates were filtered out through majority votes [12], [47], [22]. However, this approach is not applicable to the case when the server-side data is not available, or it might break down if the distribution of server’s data deviates far from that of training data of clients.

**Historical Information based byzantine robust methods** made use of historical information (such as distributed Momentums [17]) to help correct the statistical bias brought by colluders during the training, and thus lead to the convergence of optimization of federated learning [3], [27], [2], [11], [29], [19].

**Other byzantine robust methods** used signs of the gradients [5], [56], optimization strategy [35] or sampling methods [28] to achieve robust aggregation. Recently, some work studied Byzantine-robust algorithms in the decentralized setting without server [21], [44], [24] and asynchronous setting with heterogeneous communication delays [14], [64], [67].

**Community detection in graph.** In the proposed framework, the detection of Byzantine colluders is treated as the detection of multiple subgraphs or *communities* in a large weighted graph (see Sect. 5.1). Existing approaches [41] could be applied to detect the byzantine colluders. One important technique is to detect specific features of graph such as clustering coefficients [59]. Another important technique is to leverage the spectral property of graph based on the *adjacency matrix* or *normalized Laplacian matrix* and so on [53], [49], [8]. Moreover, the number of communities can be determined based on the eigengap of these matrix [70] (see Sect. 5.3).

### 3 PRELIMINARY

#### 3.1 Federated Learning

We consider a *horizontal federated learning* [66], [40] setting consisting of one server and  $K$  clients. We assume  $K$  clients<sup>2</sup> have their local dataset  $\mathcal{D}_i = \{(\mathbf{x}_{i,j}, y_{i,j})\}_{j=1}^{n_i}, i = 1 \cdots K$ , where  $\mathbf{x}_{i,j}$  is the input data,  $y_{i,j}$  is the label and  $n_i$  is the total number of data points for  $i_{th}$  client. The training in federated

learning is divided into three steps which iteratively run until the learning converges:

- The  $i_{th}$  client takes empirical risk minimization as:

$$\min_{\mathbf{w}_i} F_i(\mathbf{w}_i, \mathcal{D}_i) = \min_{\mathbf{w}_i} \frac{1}{n_i} \sum_{j=1}^{n_i} \ell(\mathbf{w}_i, \mathbf{x}_{i,j}, y_{i,j}), \quad (1)$$

where  $\mathbf{w}_i \in \mathbb{R}^d$  is the  $i_{th}$  client’s local model weight and  $\ell(\cdot)$  is a loss function that measures the accuracy of the prediction made by the model on each data point.

- Each client sends respective local model updates  $\nabla F_i$  to the server and the server updates the *global model*  $\mathbf{w}$  as  $\mathbf{w} = \mathbf{w} - \eta \frac{1}{K} \sum_{i=1}^K \nabla F_i$ , where  $\eta$  is learning rate.
- The server distributes the updated global model  $\mathbf{w}$  to all clients.

#### 3.2 Byzantine Attack in Federated Learning

We assume a malicious threat mode where an unknown number of participants out of  $K$  clients are Byzantine, i.e., they may upload arbitrarily corrupt updates  $\mathbf{g}_b$  to degrade the global model performance (MP). Under this assumption, behaviours of Byzantine clients and the rest of benign clients can be summarized as follows:

$$\mathbf{g}_i = \begin{cases} \nabla F_i & \text{Benign clients} \\ \mathbf{g}_b & \text{Byzantine clients} \end{cases} \quad (2)$$

Note that under the assumed threat mode, each adversarial node has access to updates of all clients during the training procedure. They are aware of the adoption of Federated Learning Byzantine-resilient methods [6], [4], [63], and conspire to upload specially designed model updates that may overwhelm existing defending methods. Byzantine clients who behave consistently as such are referred to as *colluders* throughout this article. Moreover, we assume the server to be honest and try to defend the Byzantine attacks.

### 4 FAILURE CASES CAUSED BY BYZANTINE COLLUDERS

The challenge brought by colluders is detrimental to Byzantine-resilient algorithms in different ways. We first

2. In this article we use terms "client", "node", "participant" and "party" interchangeably.

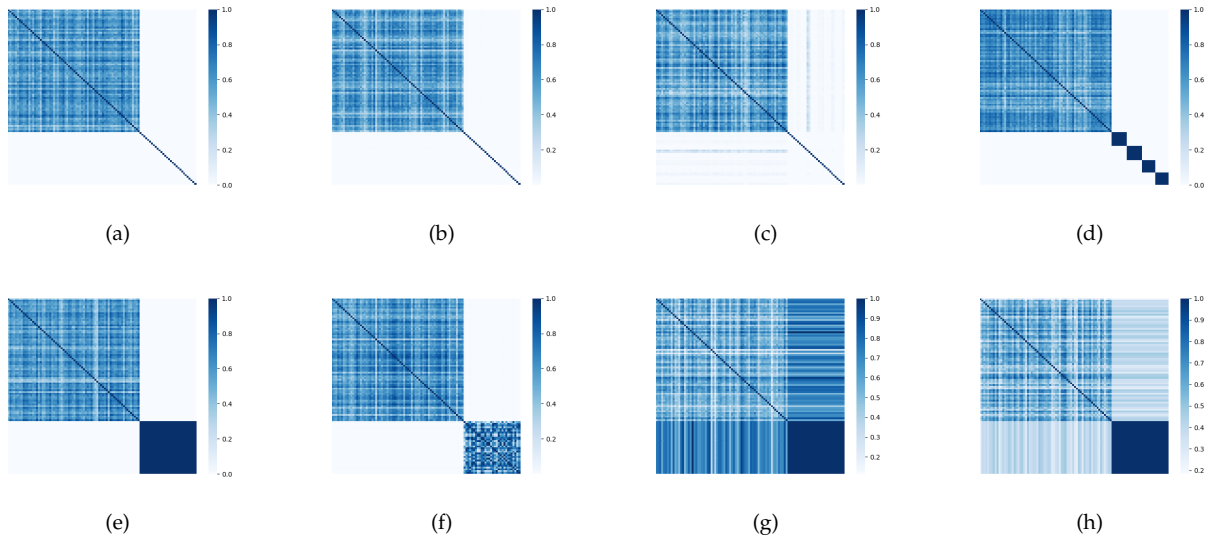


Fig. 2: Heatmap of adjacency matrices for 8 types of attack (in Sect. 7.1) of 100 client including 30 attackers at  $1000_{th}$  iteration under IID setting. In each subfigure, benign clients form a single coherent cluster residing in the upper-left block of the adjacent matrix, while attackers reside in the bottom-right parts of the adjacent matrix. The scaling factor  $\sigma^2 = 10$  and the task is logistic regression for MNIST dataset. From left to right, top to bottom, attack methods are Gaussian attack [6], label flipping [15], sign flipping [15], our designed multi-collision attack, same value attack [35], Fang-v1 (design for trimmed mean) [18], Mimic attack, and Lie [4] respectively.

analyze below behaviours of representative Byzantine attackers from a graph theoretic perspective. Then we demonstrate a toy example to showcase that existing Byzantine-resilient methods are vulnerable to collusion attacks.

#### 4.1 Weighted Undirected Graph in Federated Learning

We regard model updates contributed by  $K$  clients as an undirected graph  $G = (V, E)$ , where  $V = v_1, \dots, v_K$  represent  $K$  model updates,  $E$  is a set of weighted edge representing similarities between uploaded model updates corresponding to clients in  $V$ . We assume that the graph  $G = (V, E)$  is weighted, and each edge between two nodes  $v_i$  and  $v_j$  carries a non-negative weight, e.g.,  $A_{ij} = \exp(-\|\mathbf{g}_i - \mathbf{g}_j\|^2/2\sigma^2) \geq 0$ , where  $\mathbf{g}_i$  is uploaded gradient for  $i_{th}$  client and  $\sigma$  is the Gaussian scaling factor. Let  $G_R = (V_R, E_R)$  and  $G_B = (V_B, E_B)$  respectively denote *two* subgraphs of  $G$  representing benign and Byzantine clients.

Moreover, Byzantine problem [32] could be regarded as finding a optimal graph-cut for  $G$  to distinguish the Byzantine and benign model updates. Since model updates from colluders form specific patterns (see Fig. 3 for examples), the aforementioned graph-cut can be generalized to the so called *community-detection problem* [41] in which multiple subsets of closely connected nodes are to be separated from each other.

#### 4.2 Spectral Graph Analysis for Byzantine Attackers

We illustrate the spectral analysis of representative Byzantine attacks, especially, those launched by colluders. For example, Fig. 2 shows adjacency matrices with elements representing pairwise similarities between *70 benign clients* under IID setting and *30 attackers* (the darker the element the higher the pairwise similarity is). It is clear in each subfigure that benign

clients form a single coherent cluster residing in the upper-left block of the adjacent matrix<sup>3</sup>, while attackers reside in the bottom-right parts of the adjacent matrix. We observe the following characteristics pertaining to benign as well as Byzantine model updates.

First, benign model updates form a single group (upper-left block of Fig. 2), which is formally illustrated by Assumption 1, i.e., they all lie in the group (circle) with center  $\nabla F$  and radius  $\kappa$ . Specifically, when the local datasets are homogeneous (IID),  $\kappa$  is small, indicating the strong similarity among benign model updates. When the local data of clients becomes heterogeneous, the radius  $\kappa$  becomes larger. Note that Assumption 1 has been widely used to bound differences between model updates of benign clients, e.g., in [37], [69].

**Assumption 1.** Assume the difference of local gradients  $\nabla F_i$  and the mean of benign model update  $\nabla F = \frac{1}{|V_R|} \sum_{i \in V_R} \nabla F_i$  is bounded ( $V_R$  is the set of benign clients), i.e., there exists a finite  $\kappa$ , such that

$$\|\nabla F_i - \nabla F\| \leq \kappa^4.$$

Second, Byzantine model updates can be categorized into four types (Fig. 3):

- Non-Collusion:  $\|\mathbf{g}_b - \nabla F\| > \kappa$  and malicious updates ( $\mathbf{g}_b$ ) are far away from each other (e.g., Gaussian attack [6], label flipping [15] and sign flipping [15] attacks in Fig. 2(a), (b) and (c)).
- Collusion-diff:  $\|\mathbf{g}_b - \nabla F\| > \kappa$  and malicious updates ( $\mathbf{g}_b$ ) form one or multiple clusters (small intra-cluster distance) (e.g., our designed collusion attack (see Sect. 7.1), same

3. Note that the order of the nodes illustrated in Fig. 2 is irrelevant and we separate benign nodes from Byzantine nodes only for better visual illustration.

4.  $\|\cdot\|$  in the paper represents the  $\ell_2$  norm

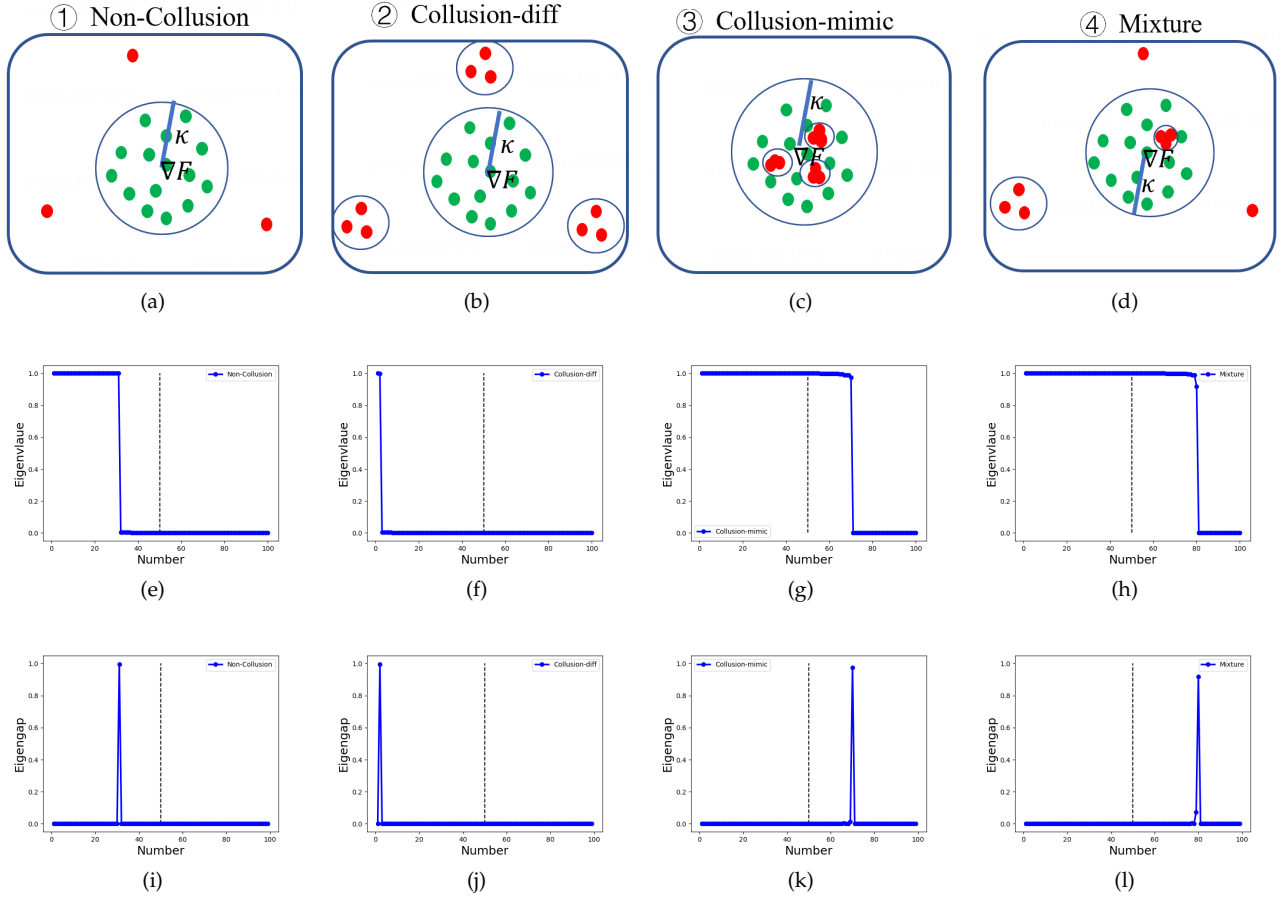


Fig. 3: Spectral analysis of four types of Byzantine attackers (Each column represents one type of attack), including Non-Collusion, Collusion-diff, Collusion-mimic and Mixture attacks. We take one example of 100 clients consisting of 70 benign clients and 30 attackers, view the model updates as nodes, and compute the pair-wise similarities as edges. The first row provides an overview of four attacks ((a), (b), (c) and (d) represents Non-Collusion, Collusion-diff, Collusion-mimic and Mixture attacks respectively where green and red points represent benign and Byzantine updates respectively), while the second and third rows show the eigenvalue and eigengap of the normalized adjacency matrix (see Def. 4).

value attack [35], Fang-v1 [18] attacks in Fig. 2(d), (e) and (f)).

- Collusion-mimic:  $\|\mathbf{g}_b - \nabla F\| < \kappa$  and  $\mathbf{g}_b$  of different attackers are almost identical ( $\|\mathbf{g}_b^i - \mathbf{g}_b^j\| \ll \kappa$ ). It represents adversaries with strong connections form one or multiple clusters (small intra-cluster distance), and their behaviours are very similar to the few selected benign clients but are different from the rest of benign clients (e.g., Mimic attack [28] and Lie [4] in Fig. 2(g) and (h)).
- Mixture: adversaries may combine Non-collusion, Collusion-diff, and Collusion-mimic arbitrarily to obtain a mixture attack.

In order to address the complex types of both benign and Byzantine model updates, we adopt the eigengap technique [53], [70] to reliably detect benign and Byzantine clusters (or communities). We provide the following proposition to elucidate characteristics of different types of Byzantine attacks in the lens of spectral analysis. The proof of Proposition 1 is deferred to Appendix C.

**Proposition 1.** Suppose  $K$  clients consist of  $m$  benign clients and  $q$  attackers ( $q < m - 1$ ). If Assumption 1 holds for Non-collusion and Collusion-diff attacks, then only the first  $c$  eigenvalues are

close to 1 and

- $c = 1 + q < \frac{K}{2}$  for Non-collusion attacks provided that  $\|\mathbf{g}_b - \nabla F\| \gg \kappa$  and malicious updates ( $\mathbf{g}_b$ ) are far away from each other;
- $c = 1 + B < \frac{K}{2}$  for Collusion-diff attacks provided that malicious updates form  $B$  groups and  $\|\mathbf{g}_b - \nabla F\| \gg \kappa$ ;
- $c > \frac{K}{2}$  for Collusion-mimic attacks that  $\|\mathbf{g}_b - \nabla F\| < \kappa$  and malicious updates are almost identical.

**Remark 1.** Proposition 1 illustrates that the eigenvalue 1 has multiplicity  $c$ , and then there is a large gap to the  $(c + 1)$ th eigenvalue  $\lambda_{c+1} < 1$ . Therefore, we can use the position of the pronounced eigengap to elucidate the number of community clusters. Specifically, we use the largest eigengap to determine the number of the community clusters in our proposed method. Moreover, Proposition 1 demonstrates that the position of the pronounced eigengap for Non-collusion and Collusion-diff attacks is less than  $\frac{K}{2}$  while larger than  $\frac{K}{2}$  for Collusion-mimic attack. This property is used in the proposed method to distinguish Collusion-mimic attacks from other types of attacks (see Sect. 5.3.3).

We illustrate with a concrete example the different spectra of four types of attacks in Fig. 3, in which each column represents one type of attack. We observe the following



properties (all of the examples include 70 benign clients and 30 attackers):

- for Non-Collusion attack, we use the Gaussian attack [35] to upload largely different random updates following  $\mathcal{N}(0, 200)$ . Fig. 3(e) and (i) show the eigenvalue of adjacency matrix  $L$  drops abruptly between index 30 and 31, i.e., the largest eigengap lies in index 31. It indicates the number of different communities is 31 with 70 benign clients forming a close group and 30 individual attackers forming other groups;
- for Collusion-diff attack, we use the same-value attack [35] to upload updates consisting of all one elements, Fig. 3(f) and (j) illustrate the largest eigengap lies in 2 elucidating that benign clients form one group and colluders with strong connections form the other group;
- for Collusion-mimic attack, we use the mimic attack [28] to upload updates that mimic one benign update, the largest eigengap is 70 because Byzantine colluders and mimicked benign clients form a group while the rest of 69 benign clients form 69 groups separately as Fig. 3(g) and (k) illustrate. It is because the connection among mimic colluders is much stronger than benign clients.
- for Mixture attack, we combine the Gaussian attack (5 attackers), same-value attack (5 attackers), and mimic attack (20 attackers). Fig. 3(h) and (l) reveal that the largest eigengap is 80, in which mimic colluders and one mimicked benign client form a group. In contrast, 69 benign clients and 10 attackers form 79 groups separately. This example showcase that the mimic attack dominates the spectral characteristics of the Mixture attack. Therefore, for the proposed method, the Collusion-mimic type attack is first detected and removed, followed by the detection of other two types of attack (see Algo. 3 in Sect. 5.3.3 and line 3-4 of Algo. 2 in Sect. 5.2).

### 4.3 Failure Case Analysis

We evaluate two types of representative Byzantine-resilient methods (Robust statistics and the clustering based aggregation methods) and the proposed FedCut method (see Sect. 5.2) under four typical Byzantine Attacks mentioned in Sect. 4.2, in terms of their Byzantine Tolerance Rates (BTR) defined below. Specifically, we assume 10 benign model updates following 1D Gaussian distribution  $\mathcal{N}(0.1, 0.1)$  and see four types Byzantine attacks (**S1-S4**) as illustrated in Tab. 2.

TABLE 2: four scenarios (**S1-S4**) of Byzantine Attacks. **S1** represents the **Non-Collusion** type; **S2-s** and **S2-m** represent **Collusion-diff** and the difference is **S2-s** only has a single cluster of colluders while **S2-m** consists multiple clusters of colluders; **S3** denotes the **Collusion-mimic** scenario; **S4** denotes a mixture scenario comprising the **Non-Collusion**, **Collusion-diff** and **Collusion-mimic** type.

Scenario	Attack Type	Attack Distribution	Number
<b>S1</b>	Non-Collusion	$\mathcal{N}(0.1, 1)$	8
<b>S2-s</b>	Collusion-diff	$\mathcal{N}(-2, 0.01)$	8
<b>S2-m</b>	Collusion-diff	$\mathcal{N}(-2, 0.01)$	4
		$\mathcal{N}(4, 0.01)$	4
<b>S3</b>	Collusion-mimic	$\mathcal{N}(\mu, 0.01)^5$	8
<b>S4</b>	Mixture	$\mathcal{N}(-2, 0.01)$	3
		$\mathcal{N}(\mu, 0.01)$	3
		$\mathcal{N}(0.1, 1)$	1

5.  $\mu$  is the minimum elements of 10 benign model updates

Next, we provide a toy example of four types of Byzantine attacks mentioned above to illustrate failure cases of existing Byzantine-resilient methods.

In order to evaluate different Byzantine-resilient methods under the four scenarios, we define the Byzantine Tolerant Rate representing the fraction of Byzantine Tolerant cases over repeated runs against attacks as follows:

**Definition 1.** (*Byzantine Tolerant Rate*) Suppose the server receives  $(K - q)$  correct gradients  $\mathcal{V} = \{v_1, \dots, v_{K-q}\}$  and  $q$  Byzantine gradients  $\mathcal{U} = \{u_1, \dots, u_q\}$ . A Byzantine robust method  $\mathcal{A}$  is said to be **Byzantine Tolerant** to certain attacks [63] if

$$< \mathbb{E}[\mathcal{V}], \mathbb{E}[\mathcal{A}(\mathcal{V} \cup \mathcal{U})] > \geq 0 \quad (3)$$

Moreover, the **Byzantine Tolerant Rate (BTR)** for  $\mathcal{A}$  is the fraction of Byzantine Tolerant cases over repeated runs against attacks.

Tab. 3 summarized toy example results for different Byzantine-resilient methods under four types of Byzantine attacks mentioned above. We can draw following conclusions:

- First, for Non-Collusion attack (**S1**), all Byzantine-resilient methods except Kmeans [54] perform well (i.e., the BTR is higher than 90%), which indicates that Non-Collusion attack is easy to be defended.
- Second, for Collusion-diff attack (**S2**), Robust Statistics based methods such as Krum [6], Median, Trimmed Mean [68] and DnC [52] are vulnerable to **S2-s**. This failure is mainly ascribed to the wrong estimation of sample *mean* or *median* misled by biased model updates from colluders. Moreover, the clustering based method i.e., Kmeans [54] fails in the **S2-m**, with BTR as low as 3.5%. This is because the clustering based method relies on the assumption that only one group of colluders exists, but two or more groups of colluders in **S2-m** are misclassified by naive clustering-based methods with wrong assumptions.
- Third, for Collusion-mimic attack (**S3**), both Robust Statistics based methods and clustering based method fail, with BTR lower than 52.9%. The main reason is that colluders would introduce statistical bias for benign updates and similar behaviours of colluders are hard to detect.
- Finally, the proposed FedCut method is able to defend against all attacks with high BTR (more than 95%) by using a Spatial-Temporal framework and *spectral heuristics* illustrated in Sect. 5.

It is worth mentioning that the toy example used in this Section only showcases some simplified failure cases that might defeat existing Byzantine-resilient methods. Instead, the attacking methods evaluated in Sect. 7 is more complex and detrimental, and we refer readers to thorough experimental results in Sect. 7 and Appendix B.

## 5 FEDCUT: SPECTRAL ANALYSIS AGAINST BYZANTINE COLLUDERS

This section illustrates the proposed spectral analysis framework (see Algo. 1) in which distinguishing benign clients from *one or more groups of Byzantine colluders* is formulated as a *community detection problem* in Spatial-Temporal graphs [53], in which nodes represent all model updates and weighted

TABLE 3: four scenarios (S1-S4) of Byzantine Attacks are repeated 1000 runs to evaluate 5 representative Byzantine-resilient methods and the proposed FedCut method, in terms of their Byzantine Tolerance Rates (BTR) in Def. 1

BTR	Krum [6]	Median [68]	Trimmed Mean [68]	DnC [52]	Kmeans [54]	FedCut (ours)
S1	96.0%	96.2%	92.6%	95.3%	70.5%	<b>96.2%</b>
S2-s	34.5%	29.5%	27.5%	89.6%	99.0%	<b>99.0%</b>
S2-m	86.1%	89.3%	88.2%	99.4%	3.5%	<b>99.6%</b>
S3	29.6%	36.9%	37.7%	52.9%	33.7%	<b>98.7%</b>
S4	59.5%	61.5%	67.6%	53.1%	85.6%	<b>95.9%</b>

edges represent similarities between respective pairs of model update over all training iterations (see Sect. 5.1). The *normalized graph cut* with temporal consistency [55], [42] (called FedCut) is adopted to ensure that a global optimal clustering is found (see Sect. 5.2). Moreover, the *spectral heuristics* [70] is then used to determine the Gaussian scaling factor, the number of colluder groups and the attack type (see Sect. 5.3). The gist of the proposed method is how to discern colluders from benign clients, by scrutinizing similarities between their respective model updates (see Fig. 4 for an overview).

---

#### Algorithm 1 FedCut Framework

---

**Input:**  $K$  clients with local training datasets  $\mathcal{D}_i, i = 1, 2, \dots, |\mathcal{D}_i|$ ; number of global iterations  $T$ ; learning rate  $\eta$  and batch size  $b$ .

**Output:** Global model  $\mathbf{w}$ .

- 1:  $\mathbf{w} \leftarrow$  random initialization,  $\tilde{L}^0 = \mathbf{0} \in \mathbb{R}^{K \times K}$ .
  - 2: **for**  $t = 1, 2, \dots, T$  **do**
  - 3:   **Step I:** The server sends the global model  $\mathbf{w}$  to all clients  $i = v_1, v_2, \dots, v_K$ .
  - 4:   **Step II:** Training local models and server model.
  - 5:   **for**  $i = v_1, v_2, \dots, v_K$  **do in parallel**
  - 6:      $\mathbf{g}_i^t = \text{ModelUpdate}(\mathbf{w}, \mathcal{D}_i, b, \eta)$ .
  - 7:     Send  $\mathbf{g}_i$  to the server.
  - 8:   **end for**
  - 9:   **Step III:** Updating the global model via FedCut
  - 10:  $\mathcal{I}_R, \tilde{L}^t = \mathbf{C}\text{-Ncut}(\mathbf{g}_{\mathcal{I}_R}^t, \tilde{L}^{t-1})$
  - 11:  $\mathbf{g}^t = \mathbf{Aggregate}(\mathbf{g}_{\mathcal{I}_R}^t)$ , where  $\mathbf{g}_{\mathcal{I}_R}^t = \{\mathbf{g}_i^t | v_i \in \mathcal{I}_R\}$
  - 12:  $\mathbf{w} \leftarrow \mathbf{w} - \eta \mathbf{g}^t$ .
  - 13: **end for**
  - 14: **return**  $\mathbf{w}$ .
- 

### 5.1 A Spatial-Temporal Graph in Federated Learning

In order to use all information during the training, we define a Spatial-Temporal graph by considering behaviours of clients among all training iterations:

**Definition 2.** (*Spatial-Temporal Graph*) Define a Spatial-Temporal graph  $G = (V, E)$  as a sequence of snapshots  $\langle G^1, \dots, G^T \rangle$ , where  $G^t = (V, E^t)$  is an undirected graph at iteration  $t$ .  $V$  denotes a fixed set of  $K$  vertexes representing model updates belonging to  $K$  clients.  $E^t$  is a set of weighted edge representing similarities between model updates corresponding to clients in  $V$  at iteration  $t$ , where related adjacency matrix of the graph is  $A^t$ .

Given a set of model updates from  $K$  clients over  $T$  iterations during federated learning, one is able to construct

such a Spatial-Temporal graph by assigning edge weights as the measured pair-wise similarity between model updates.

The construction of the Spatial-Temporal graph with historical information is motivated by a common shortcoming of Byzantine-resilient methods, e.g., reported in [29], which showed that methods without using historical information during the training might lead to deteriorated global model performances in the presence of colluders. Our ablation study in Appendix B also confirmed the importance of using the Spatial-Temporal graph.

### 5.2 FedCut

As mentioned in Sect. 5.1, we have defined a Spatial-Temporal graph  $G = \langle G^1, \dots, G^T \rangle$  according to the model updates from  $K$  clients over  $T$  iterations during federated learning. Byzantine problem is then regarded as to find an *optimal cut* for  $G$  such that the inter-cluster similarities (between benign clients and colluders) are as small as possible and intra-cluster similarities are as large as possible<sup>6</sup>. One optimal cut as such is known as the *Normalized cut (Ncut)* and has been initially applied to image segmentation [55], [42]. We adopt the Ncut approach to identify those colluders which have large intra-cluster similarities. Moreover, we extend the notion of *Ncut* to cater for the proposed Spatial-Temporal Graph over all iterations to make the detection of Byzantine colluders more consistent over multiple iterations. The *c-partition Ncut for Spatial-Temporal Graph* is thus defined as follows:

**Definition 3.** (*c-partition Ncut for Spatial-Temporal Graph*) Let  $G = (V, E)$  be a Spatial-Temporal graph as Def. 2. Denote the *c-partition* for graph  $G$  as  $V = B_1 \cup \dots \cup B_c$  and  $B_i \cap B_j = \emptyset$  for any  $i, j$ , *c-partition Ncut for Spatial-Temporal Graph* aims to optimize:

$$\min_{(B_1 \cup \dots \cup B_c) = V} \sum_{t=1}^T \sum_{i=1}^c \frac{W^t(B_i, \bar{B}_i)}{\text{Vol}^t(B_i)}, \quad (4)$$

where  $\bar{B}_i$  is the complement of  $B_i$ ,  $W^t(B_i, B_j) := \frac{1}{2} \sum_{i \in B_i, j \in B_j} A_{ij}^t$ , and  $A_{ij}^t$  is edge weight of  $B_i$  and  $B_j$ , and  $\text{Vol}^t(B_i) := \sum_{i \in B} \sum_{j \in V} A_{ij}^t$ .

The proposed FedCut (Algo. 2) is used to get rid of malicious updates before model updates are aggregated. FedCut computes adjacent matrix according to the uploaded gradients over all training iterations and then takes the *normalized cut* to distinguish benign clients and colluders.

<sup>6</sup> We view the cluster with the largest numbers as benign clients which constitute the largest community among all clients.

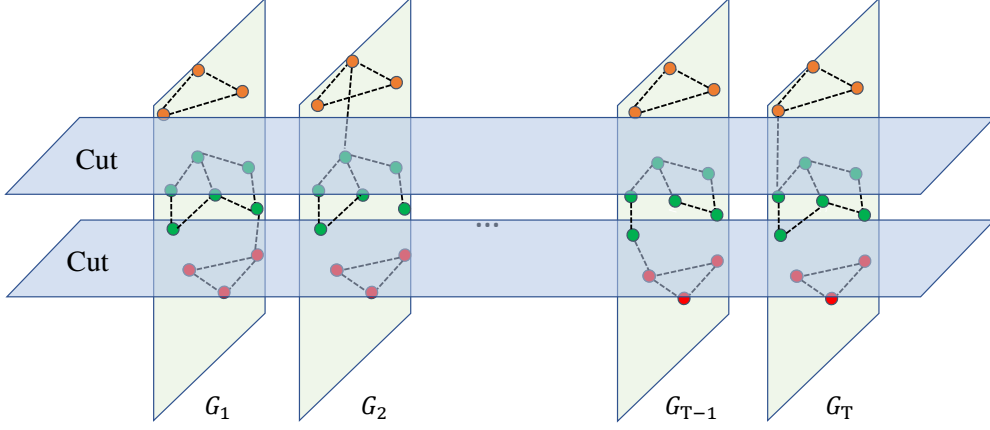


Fig. 4: FedCut: provide a temporal spatial cut to separate benign clients (green point) two-parties colluders (orange and red point) among all iterations.

Specifically, three important parameters including the appropriate Gaussian kernel  $\sigma_*$ , the cluster number  $c$  and the set of mimic colluders  $\mathcal{I}$  (who behave similarly to benign clients) need to be firstly determined (see Algo. 3). Then we calculate the adjacency matrix  $A^t$  at  $t_{th}$  iteration to remove the mimic colluders, i.e., set the connection between the mimic colluders and benign clients to be zero (line 2-7 in Algo. 2). We further compute normalized adjacency matrix  $\tilde{L}^t$  by induction over  $t$  iterations (line 8-9 in Algo. 2). Finally, we implement NCut into normalized adjacency matrix  $\tilde{L}^t$  to choose the clusters of benign clients (line 10-12 in Algo. 2).

It is worth noting that FedCut runs over multiple learning iterations and, as shown by Proposition 2, it is guaranteed to provide the optimal  $c$ -partition  $Ncut$  defined by Eq. (4) (See Proof in Appendix C).

**Proposition 2.** *FedCut (Algo. 2) solves the  $c$ -partition  $Ncut$  for Spatial-Temporal Graph i.e., it obtains a optimal solution by:*

$$\arg \min_{(B_1 \cup \dots \cup B_c) = V} \sum_{t=1}^T \sum_{i=1}^c \frac{W^t(B_i, \bar{B}_i)}{Vol^t(B_i)}$$

### 5.3 Spectral Heuristics

The determination of three parameters (i.e., the scaling parameter of Gaussian kernels  $\sigma_*$ , the number of clusters  $c$  and mimic colluders  $\mathcal{I}$ ) are critical in thwarting Byzantine Collusion attacks as illustrated in Sect. 4.3. We adopt the *Spectral Heuristics* about the following definition of eigengap to determine these three important parameters.

**Definition 4.** *The  $i_{th}$  eigengap is defined as  $|\lambda_i - \lambda_{i+1}|$  for which eigenvalues of the the normalized adjacency matrix  $L = D^{-1/2}AD^{-1/2}$  are ranked in descending order, where  $D = \text{diag}(\text{Sum}(A))$ . Let  $\delta$  be the largest eigengap among  $|\lambda_i - \lambda_{i+1}|$ .*

#### 5.3.1 Gaussian Kernel Determination

The Gaussian kernel scaling parameter  $\sigma$  in similarity function  $A_{ij} = \exp(-\|\mathbf{g}_i - \mathbf{g}_j\|^2/2\sigma^2)$  controls how rapidly the  $A_{ij}$  falls off with the distance between  $\mathbf{g}_i$  and  $\mathbf{g}_j$ . An

---

#### Algorithm 2 c-NCut: $c$ -partition $Ncut$ for the Spatial-Temporal Graph

---

- Input:** The uploaded gradients of  $K$  clients at  $t_{th}$  iteration:  $\{\mathbf{g}_i^t\}_{i=1}^K$ , normalized adjacency matrix averaged over the first  $t-1$  iterations:  $\tilde{L}^{t-1}$ ;
- Output:** The set of benign clients:  $\mathcal{I}_R$ ; normalized adjacency matrix averaged over  $t$  iterations:  $\tilde{L}^t$ .
- 1:  $c, \sigma_*, \mathcal{I} = \text{PDSH}(\{\mathbf{g}_i^t\}_{i=1}^K)$ ;
  - 2: Compute the adjacency matrix  $A^t$  as:
  - 3: **if** Client  $i \in \mathcal{I}$  **then**
  - 4:    $A_{ij}^t = 0$  ( $i \neq j$ )
  - 5: **else**
  - 6:    $A_{ij}^t = \exp(-\|\mathbf{g}_i^t - \mathbf{g}_j^t\|^2/2\sigma_*^2)$
  - 7: **end if**
  - 8:  $D = \text{diag}(\text{Sum}(A^t))$ ,  $L^t = D^{-1/2}A^tD^{-1/2}$ ;
  - 9:  $\tilde{L}^t = \frac{t-1}{t}\tilde{L}^{t-1} + \frac{1}{t}L^t$ ;
  - 10: Eigen decomposition:  $\tilde{L}^t = Q\Lambda Q^{-1}$ ;
  - 11: Apply  $K$ means into top  $c$  normalized eigenvectors ( $Q$ ) to assign  $K$  clients into  $c$  clusters.
  - 12:  $\mathcal{I}_R$  is the cluster with the largest number of clients;
  - 13: **return**  $\mathcal{I}_R$  and  $\tilde{L}^t$ .
- 

appropriate  $\sigma$  is crucial for distinguishing Byzantine and benign clients. The following analysis shows that if the maximum eigengap  $\delta$  (see Def. 4) is sufficiently large, a small perturbation on the normalized adjacency matrix  $L$  or will only affect the eigenvectors with bounded influence, and thus the clustering of  $c$  clusters via top  $c$  eigenvectors are stable.

**Proposition 3** (Stability [57]). *Let  $\lambda$ ,  $Y$  and  $\delta$  be eigenvalue, principle eigenvectors and the maximum eigengap of  $L$  separately. Define a matrix small perturbation for  $L$  as  $\tilde{L} = L + E$  so that  $\|E\|_2$  is small enough, let  $\tilde{\lambda}$ ,  $\tilde{Y}$  be eigenvalue and principle eigenvectors of  $\tilde{L}$ . If the maximum eigengap  $\delta$  is large enough, then*

$$\|Y - \tilde{Y}\| \leq \frac{4\|E\|}{\delta - \sqrt{2}\|E\|} \quad (5)$$

It is noted that the error bound  $\|Y - \tilde{Y}\|$  in the principle eigenvectors is affected by two factors: the perturbation  $\|E\|$  in the affinity matrix, and the maximal eigengap  $\delta$ . While the



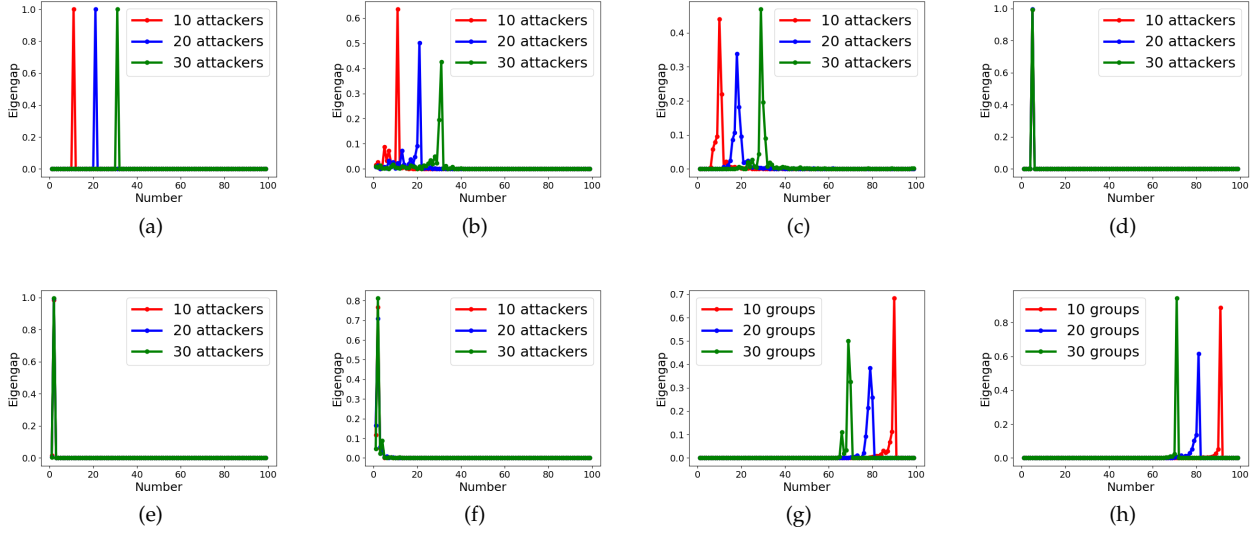


Fig. 5: The change of eigengap for different attacks with different number of attackers under IID setting for MNIST dataset. From left to right, top to bottom, attack methods are Gaussian attack [6], label flipping [15], sign flipping [15], our designed collusion attack (see Appendix A), same value attack [35], Fang-v1 (design for trimmed mean) [18], Mimic attack [28], and Lie [4] respectively.

---

**Algorithm 3** Parameter Determination via Spectral Heuristics (PDSH)

---

**Input:** The uploaded gradients of  $K$  clients at  $t_{th}$  iteration:  $\{\mathbf{g}_i^t\}_{i=1}^K$ , a preselected set of  $\sigma: \{\sigma_1, \dots, \sigma_n\}$ , where  $\sigma_0 \ll \sigma_1$

**Output:** The cluster number  $c$ , the appropriate Gaussian kernel  $\sigma_*$ , the set of mimic colluders  $\mathcal{I}$ ;

- 1: Initialize  $\mathcal{I} = \emptyset$
  - 2: **while**  $\sigma \in \{\sigma_1, \dots, \sigma_n\}$  **do**
  - 3:   Compute the adjacency matrix  $A^t$ , where  $A_{ij}^t =$
  - 4:    $\exp(-\|\mathbf{g}_i^t - \mathbf{g}_j^t\|^2 / 2\sigma^2)$ .
  - 5:    $D = \text{diag}(\text{Sum}(A^t))$ ,  $L^t = D^{-1/2} A^t D^{-1/2}$ .
  - 6:   Eigen decomposition:  $L^t = P \Lambda P^{-1}$ ;
  - 7:   Compute eigengap  $\Delta_i = \lambda_i - \lambda_{i+1}$ , where  $\lambda_i$  is the
  - 8:    $i_{th}$  eigenvalue;
  - 9:    $j = \arg \max_i \Delta_i$ ,  $\Delta_\sigma = \Delta_j$ ,  $c_\sigma = j$ ;
  - 10: **end while**
  - 11:  $\sigma_* = \arg \max_\sigma \Delta_\sigma$ ,  $c = c_{\sigma_*}$ ;
  - 12: **if**  $c > \frac{K}{2}$  **then**
  - 13:   Apply Kmeans into top  $c$  normalized eigenvectors
  - 14:   to assign  $K$  clients into  $c$  clusters;
  - 15:    $\mathcal{I}$  are the clusters with number larger than 1.
  - 16: **end if**
  - 17:  $\sigma_* = \arg \max_\sigma \{\Delta_\sigma | c_\sigma < \frac{K}{2}\}$ ,  $c = c_{\sigma_*}$ ;
  - 18: **return**  $c$ ,  $\sigma_*$  and the set of mimic colluders  $\mathcal{I}$ .
- 

perturbation is unknown and unable to modify for a given matrix  $\tilde{L}$ , one can seek to maximize the eigengap  $\delta$  so that the recovered principle eigenvectors are as stable as possible. According to proposition 3, we select the optimal parameter  $\sigma_*$  by maximizing the maximum eigengap, i.e.,

$$\sigma_* = \arg \max_\sigma \delta(\sigma) \quad (6)$$

We implement this strategy in Algo. 3. Fig. 6 shows that one can select  $\sigma$  as such that the largest eigengap is up

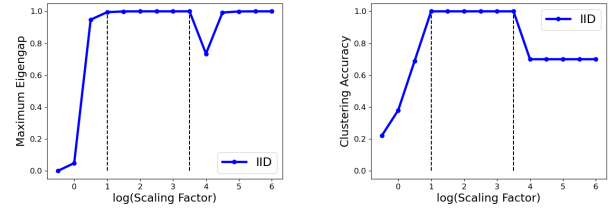


Fig. 6: The change of the maximum eigengap of normalized adjacency matrix and clustering accuracy with different scaling factor  $\sigma$  for the Gaussian attack [35], where the normalized adjacency matrix  $L = D^{-1/2} A D^{-1/2}$ ,  $D = \text{diag}(\text{Sum}(A))$  and  $A_{ij} = \exp(-\|\mathbf{g}_i - \mathbf{g}_j\|^2 / 2\sigma^2)$ . The clustering accuracy is calculated by NCut on the normalized adjacency matrix with 100 client including 70 benign clients and 30 Byzantine clients.

to its maximal (e.g.,  $\log(\sigma)$  is in the range (1,3.5) for the Gaussian attack), provided that the clustering accuracy achieves the largest value (100%) in this range. Also noted that the clustering accuracy drops in the extreme case (i.e., the  $\sigma \geq 1e^4$ ) even the maximum eigengap is still large. Therefore, we select the optimal  $\sigma$  at one reasonable range with removing the extreme case (see detailed range in Sect. 7.1).

### 5.3.2 Determination of the Number of Clusters

The assumption made by many clustering-based Byzantine-resilient methods that model updates uploaded by all Byzantine attackers form a *single group* might be violated in the presence of collusion (as shown by the toy example in Sect. 4.3 and experimental results in Sect. 7). Therefore, it is necessary to discover the number of clusters, and one possible way is to analyze the spectrum of the adjacency matrix, normalized adjacency matrix or correlation matrix [53]. According to the spectral property in Sect. 4.2, we

determine the clustering number  $c$  (see line 3-11 in Algo. 3) based on the position of the largest eigengap of normalized adjacency matrix, i.e.,

$$c = \operatorname{argmax}_k |\lambda_k - \lambda_{k+1}| \quad (7)$$

Fig. 5 displays the change of eigengap under different attacks, which shows that the index of the largest eigengap is a good estimation of the number of clusters. Specifically,

- for Non-Collusion attack (i.e., Gaussian attack [6], label flipping [15] and sign flipping [15]), the largest eigengap in Fig. 5(a), (b) and (c) consisting of 10, 20 and 30 attackers lies in 11, 21, and 31 with benign clients forming one group and 10, 20 and 30 individual attackers;
- for Collusion-diff attack, the largest eigengap of Fig. 5(e) and (f) lies in between second and third largest eigenvalues. The position of the largest eigengap indicates that there are two clusters (one cluster represents benign clients while the other cluster represents colluders);
- for Collusion-mimic attack, the largest eigengap in Fig. 5(a), (b), and (c) of 10, 20 and 30 attackers lies in 90, 80, and 70 indicating that cluster numbers are 90, 80, and 70 (colluders form one group while other benign clients form 90, 80, and 70 groups separately);

In addition, Our empirical results in Appendix B also demonstrates the effectiveness of estimating the number of communities via the largest eigengap even for heterogeneous dataset among clients.

### 5.3.3 Mimic Colluders Detection

Colluders may mimic the behaviours of some benign clients towards over-emphasizing some clients and render other model updates useless. Therefore, it is hard to distinguish the mimic colluders and benign clients. The existing byzantine-resilient methods could not defend the Collusion-mimic attack (see Sect. 4.3 for **S3** case). We leverage the spectral property to detect the mimic colluders if the position of the largest eigengap is larger than  $\frac{K}{2}$  (Proposition 1). Specifically, when the position of the largest eigengap is larger than  $\frac{K}{2}$ , we pick the clusters with number of clients larger than two as mimic colluders sets (see line 12-15 in Algo. 3).

## 6 CONVERGENCE ANALYSIS

We prove the convergence of such an iterative FedCut algorithm. The proof for Theorem 2 uses the similar technique as [15] (see details in Appendix C).

**Assumption 2.** For malicious updates  $\mathbf{g}_b$  provided that  $\|\mathbf{g}_b - \nabla F\| > \kappa$ , the difference between the mean of benign updates and colluders' updates has at least  $C\kappa$  distance, where  $C$  is a large constant, i.e.,

$$\|\mathbf{g}_b - \nabla F\| > C\kappa.$$

**Remark 2.**  $C$  in the Assumption 2 is greatly larger than 1, which demonstrates a large distance between colluders and the mean of benign updates. If the single attacker uploads gradients within  $\kappa$  distance from the mean of benign updates, we can regard this attacker as one benign client. For mimic colluders who introduce the statistical bias, we detect these colluders and remove them according to spectral heuristics (see Sect. 5.3.3).

**Theorem 1.** Suppose an  $0 < \alpha < \frac{1}{2}$  fraction of clients are Byzantine attackers. If Assumption 1 and 2 holds, we can find the estimate of  $\hat{\mathbf{g}}$  according to line 11 in Algo. 1 and with the probability  $1 - \tilde{O}(\sqrt{Z_1})$ , such that  $\|\hat{\mathbf{g}} - \nabla F\| \leq \tilde{O}(\alpha\kappa)$ , where

$$Z_1 = \frac{4K\sqrt{\alpha(1-\alpha)Z\frac{C^2}{4}}}{\delta - K\sqrt{2\alpha(1-\alpha)Z\frac{C^2}{4}}}, Z = \exp(-2\kappa^2/\sigma^2).$$

**Remark 3.** The Theorem 1 illustrates that the distance between estimated gradients  $\hat{\mathbf{g}}$  via FedCut and benign averaged gradients  $\bar{\mathbf{g}}$  is bounded by  $\tilde{O}(\alpha\kappa)$ . Moreover,  $\alpha(1-\alpha)$  is increasing w.r.t.  $\alpha$  when  $\alpha < \frac{1}{2}$ , and  $Z_1$  is increasing w.r.t.  $\alpha(1-\alpha)$ . Therefore,  $Z_1$  is increasing w.r.t.  $\alpha$ , which indicates that the probability  $1 - \tilde{O}(Z_1)$  decreases as the number of Byzantine attackers increases. In addition, for the larger  $C$ ,  $Z_1$  tends to zero since  $Z < 1$ . Consequently,  $\|\hat{\mathbf{g}} - \nabla F\| \leq \tilde{O}(\kappa)$  with a high probability close to 1.

**Assumption 3.** The stochastic gradients sampled from any local dataset have uniformly bounded variance over  $\mathcal{D}_i$  for all benign clients, i.e., there exists a finite  $\sigma_0$ , such that for all  $\mathbf{x}_{i,j} \in \mathcal{D}_i, i \in [K]$ , we have

$$\mathbb{E}_j \|\nabla F_i(\mathbf{w}_i, \mathbf{x}_{i,j}) - \nabla F_i(\mathbf{w}_i)\|^2 \leq \sigma_0^2, \quad (8)$$

where  $\nabla F_i(\mathbf{w}_i) = \mathbb{E}_j \nabla F_i(\mathbf{w}_i, x_{i,j})$ .

**Remark 4.** The difference between Assumption 1 and 3 is that the former bounds the variance across gradient estimates within the same client while the latter bounds the variance between model updates across clients.

**Assumption 4.** We assume that  $F(x)$  is  $L$ -smooth and has  $\mu$ -strong convex.

**Theorem 2.** Suppose an  $0 < \alpha < \frac{1}{2}$  fraction of clients are corrupted. For a global objective function  $F: \mathbb{R}^d \rightarrow \mathbb{R}$ , the server obtains a sequence of iterates  $\{\mathbf{w}^t: t \in [0:T]\}$  (see Algo. 1) when run with a fixed step-size  $\eta < \min\{\frac{1}{4L}, \frac{1}{\mu}\}$ . If Assumption 1, 2, 3 and 4 holds, the sequence of average iterates  $\{\mathbf{w}^t: t \in [0:T]\}$  satisfy the following convergence guarantees:

$$\|\mathbf{w}^T - \mathbf{w}^*\|^2 \leq (1 - \frac{C_1\mu}{L})^T \|\mathbf{w}^0 - \mathbf{w}^*\|^2 + \frac{\Gamma}{\mu^2}, \quad (9)$$

where  $\Gamma = \tilde{O}(\sigma_0^2 + \kappa^2 + \alpha^2\kappa^2)$ ,  $C_1$  is a constant and  $\mathbf{w}^*$  is the global optimal weights in federated learning.

Theorem 2 provides the convergence guarantee of FedCut framework in the strong convex case. As  $T$  tends to infinity, the upper bound of  $\|\mathbf{w}^T - \mathbf{w}^*\|^2$  becomes large with the increasing of  $\sigma_0$  (variance of gradients within the same client),  $\kappa$  (variance between model updates across benign clients) and  $\alpha$  (the ratio of Byzantine attackers).

## 7 EXPERIMENTAL RESULTS

This section illustrates the proposed FedCut method's experimental results compared with eight existing Byzantine-robust methods. We refer to Appendix A and B for the full report of extensive experimental results.

### 7.1 Setup and Evaluation Metrics

- **Models:** logistic regression, LeNet [34] and AlexNet [25] three models are used in all experiment settings. (see results for other models and datasets in supplementary material).

- **Datasets:** *MNIST* [33], *Fashion-MNIST* [60] and *CIFAR10* [30] are used for image classification tasks. To simulate Non-IID settings, class labels assigned to clients follows a Dirichlet distribution  $Dir(\beta)$  [36].
- **Federated Learning Settings:** We simulate a horizontal federated learning system with  $K = 100$  clients in a stand-alone machine with 8 Tesla V100-SXM2 32 GB GPUs and 72 cores of Intel(R) Xeon(R) Gold 61xx CPUs. In each communication round, the clients update the weight updates, and the server adopts *Fedavg* [40] algorithm to aggregate the model updates. The detailed experimental hyper-parameters are listed in Appendix A.
- **Byzantine attacks:** We set 10%, 20% and 30% clients, i.e., 10, 20, and 30 out of 100 clients are Byzantine attackers. The following attacking methods are used in experiments:
  - the *same value attack*: model updates of attackers are replaced by the all ones' vector;
  - the *sign flipping attack*: local gradients of attackers are shifted by a scaled value  $-4$ ;
  - the *gaussian attack*: local gradients at clients are replaced by independent Gaussian random vectors  $\mathcal{N}(0, 200)$ ;
  - the *Lie attack*: it was designed in [4];
  - the *Fang-v1 attack* and *Fang-v2 attack*: they were designed in [18] for coordinate-wise trimmed mean [68] and Krum

TABLE 4: Model performances of different Byzantine-resilient methods under different Byzantine attacks (with IID setting 30 Byzantine clients for classification of MNIST, Fashion MNIST and CIFAR10). Moreover, the baseline of FedAvg [40] without any attacks achieve the model performance 92.5%, 90.1 % and 69.4% for MNIST, Fashion MNIST and CIFAR10 respectively.

		Krum[6]	GeoMedian[13]	Median[68]	Trimmed[68]	Bulyan[21]	FLtrust[10]	DnC[52]	Kmeans[54]	FedCut(Ours)
M N I S T	No attack	90.5±0.1	92.4±0.0	90.5±0.1	90.3±0.1	89.6±0.1	89.4±0.1	92.2±0.3	92.4±0.3	92.5±0.1
	Lie [4]	90.5±0.0	84.4±0.6	84.0±0.3	83.6±0.8	73.6±1.0	89.5±0.1	92.2±0.3	92.2±0.2	92.3±0.2
	Fang-v1 [18]	90.2±0.1	45.8±0.5	43.4±1.5	37.8±2.6	85.5±0.3	75.8±3.5	92.3±0.3	92.3±0.2	92.3±0.1
	Fang-v2 [18]	41.1±7.4	53.4±2.1	39.0±2.3	42.4±2.8	18.8±6.1	79.7±0.8	92.0±0.6	88.2±0.4	92.3±0.1
	Same value [35]	90.6±0.1	85.6±0.0	77.0±0.4	75.1±0.6	88.8±0.4	89.8±0.3	92.3±0.2	92.2±0.3	92.2±0.1
	Gaussian [6]	90.4±0.1	92.4±0.1	90.6±0.1	90.8±0.1	89.6±0.3	87.0±1.0	74.3±0.4	22.4±4.3	92.3±0.1
	sign flipping [15]	90.6±0.1	91.3±0.1	90.2±0.1	90.2±0.1	89.6±0.2	72.2±5.5	90.7±0.1	49.9±1.3	91.9±0.2
	label flipping [15]	90.4±0.1	89.4±0.1	85.6±0.2	85.4±0.4	89.5±0.4	89.3±0.6	92.2±0.2	92.1±0.2	92.1±0.4
	minic [28]	86.1±0.4	86.3±0.9	88.3±0.3	89.7±0.2	85.5±0.5	90.5±0.1	92.2±0.4	92.1±0.1	92.3±0.1
	Collusion (Ours)	90.3±0.2	83.9±2.1	79.5±0.7	78.0±0.8	89.7±0.3	89.4±0.1	90.2±0.3	43.2±20.8	92.3±0.1
Averaged	85.1±0.9	80.5±0.7	76.8±0.6	76.3±0.9	80.0±1.0	85.3±1.2	90.1±0.3	75.7±2.8	<b>92.2±0.2</b>	
Worst-case	41.1±7.4	45.8±0.5	39.0±2.3	37.8±2.6	18.8±6.1	72.2±5.5	74.3±0.4	22.4±4.3	<b>91.9±0.2</b>	
F M N I S T	No attack	84.6±0.5	89.5±0.3	88.2±0.4	88.6±0.4	87.3±0.3	88.2±0.5	90.3±0.2	90.0±0.3	90.1±0.3
	Lie [4]	85.3±0.6	60.7±12.9	50.5±22.7	68.9±6.9	55.5±10.3	75.8±4.3	78.4±5.0	89.0±0.8	89.7±0.6
	Fang-v1 [18]	85.4±0.3	82.5±1.0	73.1±4.1	69.1±4.6	84.8±0.9	86.6±1.3	89.5±0.6	89.7±0.3	89.7±0.5
	Fang-v2 [18]	10.0±11.1	12.6±4.8	64.2±3.3	46.6±16.6	10.5±2.4	80.1±2.3	71.5±10.4	69.3±1.4	89.3±0.4
	Same value [35]	85.6±0.6	59.9±14.3	69.8±0.8	66.5±3.6	86.7±0.3	88.1±0.7	89.4±0.6	88.8±0.6	89.6±0.4
	Gaussian [6]	85.5±0.3	89.5±0.5	87.5±0.5	88.2±0.4	87.1±0.8	87.9±0.7	69.8±7.7	17.9±27.3	89.7±0.2
	sign flipping [15]	85.2±0.8	85.9±1.2	86.2±0.6	86.3±0.5	87.1±0.4	84.0±1.4	76.9±1.1	52.8±3.0	87.5±0.9
	label flipping [15]	85.5±0.2	89.6±0.3	72.6±5.1	78.5±4.8	87.1±0.3	87.9±0.6	89.8±0.3	89.9±0.4	89.1±0.3
	minic [28]	79.7±0.6	81.2±0.4	83.0±1.3	86.7±0.8	79.8±0.7	87.7±0.2	88.8±0.2	89.1±0.4	89.4±0.7
	Collusion (Ours)	84.7±0.5	35.9±22.7	71.2±6.3	69.5±1.8	86.8±0.6	88.4±0.3	85.5±1.7	76.9±13.6	90.0±0.5
Averaged	77.2±1.6	68.7±5.8	74.6±4.5	74.9±4.0	75.3±1.7	85.5±1.2	83.0±2.8	75.3±4.8	<b>89.4±0.5</b>	
Worst-case	10.0±11.1	12.6±4.8	50.5±22.7	46.6±16.6	10.5±2.4	75.8±4.3	69.8±7.7	17.9±27.3	<b>87.5±0.9</b>	
C I F A R 10	No attack	64.6±0.1	64.9±2.1	39.0±25.2	66.6±1.6	29.5±6.6	68.3±0.0	69.7±0.9	68.6±0.6	68.0±0.4
	Lie [4]	63.9±2.1	10.0±0.2	10.2±0.2	9.8±0.2	10.0±0.1	12.4±4.2	11.9±3.3	20.4±22.0	68.4±0.4
	Fang-v1 [18]	64.4±0.5	63.9±0.3	11.2±2.1	17.5±12.3	17.3±3.4	68.1±0.8	66.8±0.3	68.0±0.9	67.7±3.9
	Fang-v2 [18]	9.9±0.1	15.0±4.1	11.0±1.3	11.3±1.4	10.0±0.1	61.8±4.2	67.0±0.6	53.4±12.7	68.5±1.5
	Same value [35]	64.8±0.7	50.2±0.3	10.0±0.0	10.0±0.0	54.8±0.2	29.2±33.3	65.1±5.2	65.3±11.3	66.4±1.8
	Gaussian [6]	63.5±1.1	62.1±4.3	48.4±4.8	65.4±0.2	17.1±6.2	68.1±0.6	31.8±2.3	12.6±1.3	65.3±0.7
	sign flipping [15]	65.0±0.5	58.6±12.5	16.6±5.6	51.9±1.7	40.2±14.9	28.7±32.4	47.5±9.4	17.7±22.6	63.1±5.5
	label flipping [15]	63.7±1.4	36.1±22.7	18.6±3.3	50.2±2.1	13.0±2.7	61.3±2.5	57.1±0.8	58.3±1.5	63.8±2.0
	minic [28]	44.1±0.9	65.0±0.5	56.4±1.0	66.0±0.8	42.2±2.8	48.0±32.9	65.9±1.7	66.6±3.6	68.8±0.2
	Collusion (Ours)	63.3±0.6	10.0±0.1	9.7±0.1	10.2±0.0	19.4±1.2	67.9±0.7	29.5±13.4	10.5±0.3	67.0±1.7
Averaged	56.7±0.8	43.6±4.7	23.1±4.4	35.9±2.0	25.3±3.8	51.4±11.2	51.2±3.8	44.1±7.7	<b>66.7±1.8</b>	
Worst-case	9.9±0.1	10.0±0.2	9.7±0.1	9.8±0.2	10.0±0.1	12.4±4.2	11.9±3.3	10.5±0.3	<b>63.1±5.5</b>	

[6] respectively;

- Mimic attack: Colluders may mimic the behaviours of some benign clients towards over-emphasizing some clients and under-representing others [28].
- Our designed *multi-collusion attack*: adversaries are separated into 4 groups, and the same group has similar values. For example, each group is sampled from  $\mathcal{N}(\mu + \mu_i, 0.0001)$ , and different group has different  $\mu_i$ , where  $\mu$  is the mean of uploaded gradients of all other benign clients.
- **Byzantine-resilient methods:** *Nine* existing methods i.e., Statistic-based methods: Krum [6], Median [68], Trimmed Mean [68], Bulyan [21] and DnC [52], Serve-evaluating methods: FLtrust [10], Clustering-based methods: Kmeans [54] and the proposed method *FedCut* are compared in terms of following metrics.
- **Gaussian kernel scaling parameters of FedCut:** the pre-selected set of  $\sigma: \{\sigma_1, \dots, \sigma_n\}$  in Algo. 3 is the geometric sequence with common ratio 2 of  $(1, 10\sqrt{10})$  for MNIST,  $(1, 10\sqrt{10})$  for Fashion-MNIST and  $(0.1, 10\sqrt{10})$  for CIFAR10.

**Evaluation metric:** two types of metrics are used in our evaluation.

- *Model Performance (MP)* of the federated model is used to evaluate defending capabilities of different methods. In order to elucidate robustness of each defending method, we also report respective *averaged* and *worst-case* model performances under all possible attacks.
- For methods including DnC [52], Kmeans [54] and FedCut, which detect benign clients before aggregation, *detection accuracy* among all iterations is used to quantify their defending capabilities. Note that this accuracy is measured against *ground-truth Byzantine attackers' membership*, and

it should not be confused with the image classification accuracy of the main task.

## 7.2 Comparison with Other Byzantine-resilient Methods

Tab. 4 summarizes Model Performances (MP) of 8 existing methods as well as the proposed FedCut method for classification of MNIST, Fashion MNIST, and CIFAR10 using logistic regression, LeNet, and AlexNet respectively under IID setting and 30 attackers (see Appendix B for more results with other settings). There are four noticeable observations.

- FedCut performs robustly under almost all attacks with worst-case MP above 92.0% for MNIST, 87.5% for Fashion MNIST and 63.1% for CIFAR10. This robust performance is in sharp contrast with eight existing methods, each of which has a *worst-case MP degradation* ranging from 18.2% (i.e., DnC by Gaussian attack reaching 74.3% MP) to 73.7% (i.e., Bulyan by Fang-v2 merely having 18.8% MP) on MNIST.
- In terms of averaged MP, it is clearly observed that FedCut outperformed eight existing methods by noticeable margins ranging between 2.1% to 16.5% on MNIST, 3.9% to 20.7% on Fashion MNIST and 10.0% to 43.6% on CIFAR10.
- Robust Statistics based methods (e.g., Krum, GeoMedian, Median, and Trimmed Mean) were overwhelmed by Collusion-diff and Collusion-mimic attacks (such as the MP drops 49.1% for Median under Fang-v1 attack and the MP drops 51.4% for Krum under Fang-v2 attack), incurred a significant MP degradation on MNIST. In contrast, all Collusion attacks cause a minor MP loss of less than 0.5% to FedCut.
- Existing clustering-based method, i.e., Kmeans performs robustly in the presence of single-group colluders but

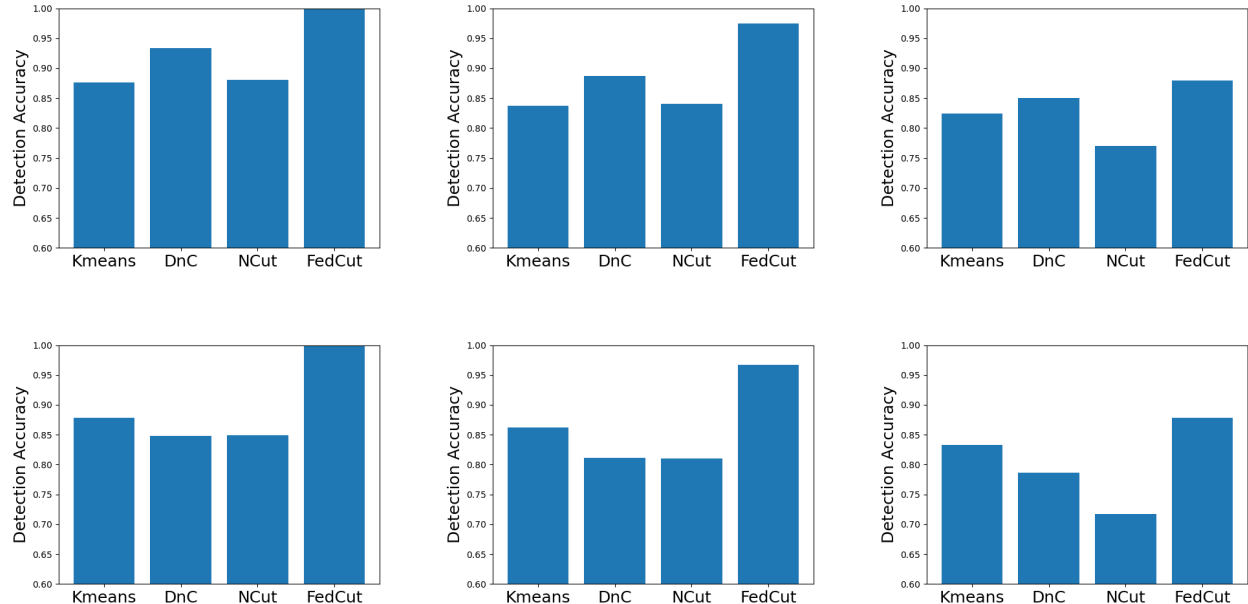


Fig. 7: The Detection accuracy of different Byzantine-resilient methods (Kmeans, DnC, NCut and FedCut) among all 8 attacks with different Non-IID extent (left: IID, middle: Non-IID with  $\beta = 0.5$ , right: Non-IID with  $\beta = 0.1$ ) on MNIST (first row) and Fashion MNIST (second row).

with MP degradation less than 2% (e.g., Kmeans for Same Value attack on MNIST, Fashion MNIST and CIFAR10), but incurred significant MP degradation more than 50% in the face of multi-group colluders attackers (e.g., Kmeans for the Multi-Collusion attack on MNIST and Gaussian attack on Fashion MNIST). In contrast, multi-group collusion doesn't cause significant MP loss to the proposed FedCut, which adopts spectral heuristics to make an estimation of the number of colluder groups (see Sect. 5.3). Correspondingly, the detection accuracy of FedCut is higher than other methods, as Fig. 7 shows. For instance, the detection accuracy of FedCut on MNIST in the IID setting is 99.9%, while the detection accuracy of DnC and Kmeans drop to 93.6% and 87.5% separately.

### 7.3 Robustness

In this subsection, we demonstrate the robustness of our FedCut framework under different byzantine numbers, the Non-IID extent of clients' local data, and multiple collusion attacks.

#### 7.3.1 Robustness under Varying Numbers of Attackers.

Fig. 8 shows the model performance (MP) for different Byzantine-resilient methods under different types of attacks for different Byzantine attackers, i.e., 10, 20, and 30 attackers. The result shows that the MP of FedCut doesn't drop with the increase of Byzantine numbers while the MP of others drops seriously (e.g., the averaged MP of Median [68] drops to 74.6% from 88.6% in Fashion MNIST dataset). Clearly, our proposed method, FedCut, is robust for the the number of byzantine attackers.

#### 7.3.2 Robustness under Heterogeneous dataset

Fig. 9 shows the model performance (MP) for different Byzantine resilient methods under different types of attacks for different Non-IID extent of clients' datasets. The result demonstrates that the MP of FedCut drops no more than 3% as the clients' local dataset becomes more heterogeneous while the MP of others drops seriously (e.g., the averaged MP of trimmed mean [68] drops to 55.4% from 74.9% in Fashion MNIST dataset)

#### 7.3.3 Robustness against the Multi-Collusion attack

In the former part, we design the 'Multi-Collusion attack' in which adversaries are separated into four groups, and the

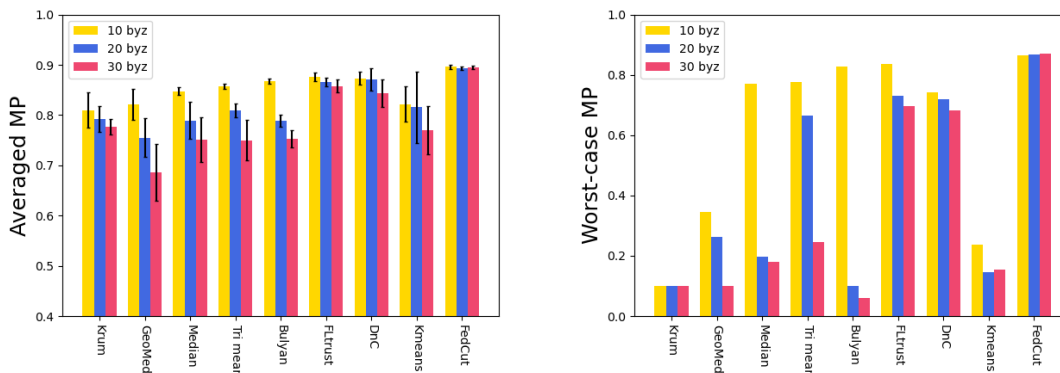


Fig. 8: Averaged and worst-case model performance among all 8 attacks of different Byzantine-resilient methods with IID setting for different byzantine numbers (yellow: 10 attackers, blue: 20 attackers, green: 30 attackers) on Fashion MNIST.

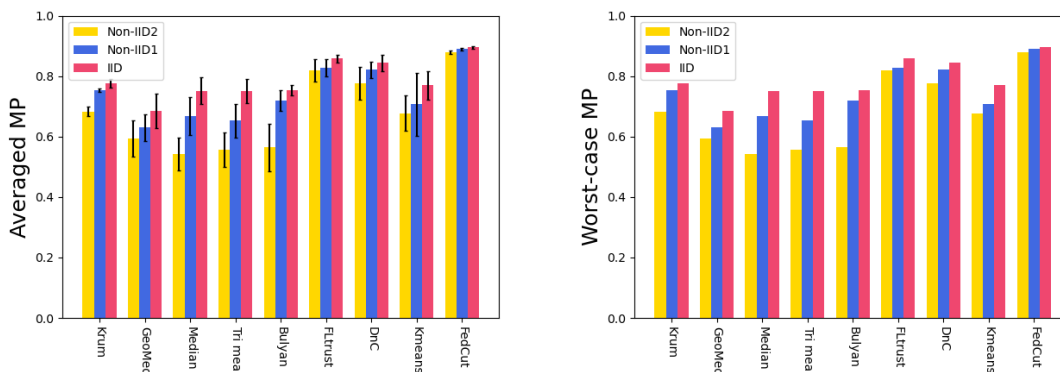


Fig. 9: Averaged and worst-case model performance among all 8 attacks of different Byzantine-resilient methods with 30 Byzantine attackers for different Non-IID extent (yellow: Non-IID with  $\beta = 0.1$ , blue: Non-IID with  $\beta = 0.5$ , green: IID) on Fashion MNIST.

TABLE 5: Computation Time complexity for different Byzantine resilient methods, where  $K$  is the number of client,  $d$  is the dimension of updates,  $T'$  is training time of the server's data for FLtrust.

<b>Defense</b>	Krum [6]	GeoMedian [13]	Median [68]	Trimmed [68]	Bulyan [21]
<b>Time Complexity</b>	$\tilde{O}(K^2d)$	$\tilde{O}(K^2d)$	$\tilde{O}(K^2d+)$	$\tilde{O}(K^2d)$	$\tilde{O}(Kd)$
<b>Defense</b>	FLtrust [10]	DnC [52]	Kmeans [54]	FedCut (Ours)	
<b>Time Complexity</b>	$\tilde{O}(Kd + T')$	$\tilde{O}(d^3 + K^2d)$	$\tilde{O}(K^2d)$	$\tilde{O}(K^2d + K^3)$	

same group has similar values. For example, each group is sampled from  $\mathcal{N}(\mu + \mu_i, 0.0001)$ , and different groups have different  $\mu_i$ , where  $\mu$  is the mean of uploaded gradients of all other benign clients. We further design more 'collusion attacks' with a various number of colluders' parties as follows: 30 attackers are separated into 1) two groups with each group having 15 attackers; 2) three groups with each group having ten attackers 3) four groups with each group having 8, 8, 7, 7 attackers respectively; 4) five groups with each group has six attackers.

Tab. 7 and 6 displays the model performances under different 'collusion attacks,' which illustrates that various collusion attacks do not influence FedCut and NCut while other byzantine resilient methods such as Kmeans are affected seriously by collusion attack. Note that DnC performs well with 2-groups collusion, but MP drops when colluders' groups increase.

TABLE 6: Model performances of different Byzantine-resilient methods under different groups of collusion attacks (with Non-IID setting  $\beta = 0.5$  and 30 attackers for classification of MNIST).  $i$  – groups represent the number of colluders.

	Krum [6]	GeoMedian [13]	Median [68]	Trimmed [68]	Bulyan [21]	FLtrust [10]	DnC [52]	Kmeans [54]	FedCut (Ours)
2-groups	89.2±0.4	79.2±0.0	71.9±0.1	69.0±0.2	89.1±0.2	88.5±0.1	<b>91.9±0.1</b>	45.7±0.0	91.7±0.0
3-groups	88.9±0.1	81.1±0.0	73.4±0.0	70.7±0.1	88.9±0.1	88.0±0.1	87.2±0.8	45.9±0.1	<b>91.6±0.1</b>
4-groups	89.0±0.5	82.2±1.2	73.6±1.2	72.3±1.2	86.7±1.2	89.2±0.5	89.4±0.5	31.2±2.2	<b>92.1±0.1</b>
5-groups	88.8±1.1	84.2±0.1	78.0±0.1	75.1±0.0	88.7±0.1	88.4±0.1	89.0±0.3	54.1±0.0	<b>91.7±0.1</b>

TABLE 7: Model performances of different Byzantine-resilient methods under different groups of collusion attacks (with IID and 30 attackers for classification of MNIST).  $i$  – groups represent the number of colluders' clusters.

	Krum [6]	GeoMedian [13]	Median [68]	Trimmed [68]	Bulyan [21]	FLtrust [10]	DnC [52]	Kmeans [54]	FedCut (Ours)
2-groups	90.8±0.0	80.2±0.4	73.3±0.1	72.7±0.3	90.1±0.0	88.8±0.1	<b>92.0±0.1</b>	46.4±0.1	<b>91.8±0.0</b>
3-groups	90.6±0.1	82.3±0.4	77.2±0.7	75.7±0.3	90.1±0.1	88.9±0.1	89.0±1.4	49.5±0.1	<b>91.8±0.0</b>
4-groups	90.3±0.2	83.9±2.1	79.5±0.7	78.0±0.8	89.7±0.3	89.4±0.1	90.2±0.3	43.2±8.4	<b>92.2±0.2</b>
5-groups	90.7±0.1	84.4±0.4	79.3±0.1	78.9±0.1	90.1±0.1	88.6±0.6	89.4±0.1	51.9±0.1	<b>91.9±0.0</b>

## 7.4 Computation Complexity

We compare the computation time complexity for different Byzantine resilient methods for each iteration on the server as Tab. 5. It shows that the computation complexity of our proposed method FedCut is  $\tilde{O}(K^2d + K^3)$ , where implementing the singular vector decomposition (SVD) needs  $\tilde{O}(K^3)$

[23] and computing the adjacency matrix requires  $\tilde{O}(K^2d)$ . The time complexity of FedCut is comparable to statistic-based methods such as Krum [6] ( $\tilde{O}(K^2d)$ ) and median [68] ( $\tilde{O}(K^2d)$ ) when the dimension of model  $d$  is greatly larger than number of participants  $K$ .

Empirically, the proposed FedCut method allows the training of a DNN model (AlexNet) with 100 clients to run in three hours, under a simulated environment (see Appendix A for details). We regard this time complexity is reasonable for practical federated learning applications across multiple institutions. For cross-devices application scenarios in which  $K$  might be up to millions, randomized SVD [23] can be adopted to improve the time complexity from  $\tilde{O}(K^3)$  to  $\tilde{O}(K)$  if the normalized adjacency matrix has low rank. Applying randomized SVD to cross-device FL scenarios is one of our future work.

## 8 DISCUSSION AND CONCLUSION

This paper proposed a novel spectral analysis framework, called FedCut, to detect Byzantine colluders robustly and efficiently from the graph perspective. Specifically, our proposed algorithm FedCut ensures the optimal separation of benign clients and colluders in the spatial-temporal graph constructed from uploaded model updates over different iterations. We analyze existing Byzantine attacks and Byzantine-resilient methods in the lens of spectral analysis. It was shown that existing Byzantine-resilient methods may suffer from failure cases in the face of Byzantine colluders. Moreover, spectral heuristics are used in FedCut to determine the number of colluder groups, the scaling factor and mimic colluders, which significantly improves the Byzantine tolerance in colluders detection.

Our extensive experiments on multiple datasets and theoretical convergence analysis demonstrate that our proposed framework can achieve drastic improvements over the FL baseline in terms of model performance under various Byzantine attacks.

Finally, the proposed and many existing Byzantine-resilient methods assume that the server could access to clients' model updates to compute the similarity. However, the leakage of model updates allows a semi-honest server to infer some information of the private data [72]. Therefore, Byzantine problem should be considered when implementing FL for privacy-preserving applications. In future work, we will explore to what extent FedCut can be used in conjunction with Differential Privacy [1] or Homomorphic Encryption mechanisms [71].



## REFERENCES

- [1] Martin Abadi, Andy Chu, Ian Goodfellow, H Brendan McMahan, Ilya Mironov, Kunal Talwar, and Li Zhang. Deep learning with differential privacy. In *Proceedings of the 2016 ACM SIGSAC conference on computer and communications security*, pages 308–318, 2016.
- [2] Dan Alistarh, Zeyuan Allen-Zhu, and Jerry Li. Byzantine stochastic gradient descent. *Advances in Neural Information Processing Systems*, 31, 2018.
- [3] Zeyuan Allen-Zhu, Faeze Ebrahimiaghazani, Jerry Li, and Dan Alistarh. Byzantine-resilient non-convex stochastic gradient descent. In *International Conference on Learning Representations*, 2020.
- [4] Gilad Baruch, Moran Baruch, and Yoav Goldberg. A little is enough: Circumventing defenses for distributed learning. *Advances in Neural Information Processing Systems*, 32, 2019.
- [5] Jeremy Bernstein, Jiawei Zhao, Kamyar Azizzadenesheli, and Anima Anandkumar. signsgd with majority vote is communication efficient and fault tolerant. In *International Conference on Learning Representations*, 2018.
- [6] Peva Blanchard, El Mahdi El Mhamdi, Rachid Guerraoui, and Julien Stainer. Machine learning with adversaries: Byzantine tolerant gradient descent. *Advances in Neural Information Processing Systems*, 30, 2017.
- [7] Stephen Boyd, Stephen P Boyd, and Lieven Vandenbergh. *Convex optimization*. Cambridge university press, 2004.
- [8] Andries E Brouwer and Willem H Haemers. *Spectra of graphs*. Springer Science & Business Media, 2011.
- [9] Saikiran Bulusu, Venkata Gandikota, Arya Mazumdar, Ankit Singh Rawat, and Pramod K Varshney. Byzantine resilient distributed clustering with redundant data assignment. In *2021 IEEE International Symposium on Information Theory (ISIT)*, pages 2143–2148. IEEE, 2021.
- [10] Xiaoyu Cao, Minghong Fang, Jia Liu, and Neil Zhenqiang Gong. Fltrust: Byzantine-robust federated learning via trust bootstrapping. *arXiv preprint arXiv:2012.13995*, 2020.
- [11] Chen Chen, Lingjuan Lyu, Yuchen Liu, Fangzhao Wu, Chaochao Chen, and Gang Chen. Byzantine-resilient federated learning via gradient memorization.
- [12] Lingjiao Chen, Hongyi Wang, Zachary Charles, and Dimitris Papailiopoulos. Draco: Byzantine-resilient distributed training via redundant gradients. In *International Conference on Machine Learning*, pages 903–912. PMLR, 2018.
- [13] Yudong Chen, Lili Su, and Jiaming Xu. Distributed statistical machine learning in adversarial settings: Byzantine gradient descent. *Proceedings of the ACM on Measurement and Analysis of Computing Systems*, 1(2):1–25, 2017.
- [14] Georgios Damaskinos, Rachid Guerraoui, Richeek Patra, Mahsa Taziki, et al. Asynchronous byzantine machine learning (the case of sgd). In *International Conference on Machine Learning*, pages 1145–1154. PMLR, 2018.
- [15] Deepesh Data and Suhas Diggavi. Byzantine-resilient high-dimensional sgd with local iterations on heterogeneous data. In *International Conference on Machine Learning*, pages 2478–2488. PMLR, 2021.
- [16] Ilias Diakonikolas, Gautam Kamath, Daniel Kane, Jerry Li, Ankur Moitra, and Alistair Stewart. Robust estimators in high-dimensions without the computational intractability. *SIAM Journal on Computing*, 48(2):742–864, 2019.
- [17] El Mahdi El Mhamdi, Rachid Guerraoui, and Sébastien Louis Alexandre Rouault. Distributed momentum for byzantine-resilient stochastic gradient descent. In *9th International Conference on Learning Representations (ICLR)*, number CONF, 2021.
- [18] Minghong Fang, Xiaoyu Cao, Jinyuan Jia, and Neil Gong. Local model poisoning attacks to {Byzantine-Robust} federated learning. In *29th USENIX Security Symposium (USENIX Security 20)*, pages 1605–1622, 2020.
- [19] Sadegh Farhadkhani, Rachid Guerraoui, Nirupam Gupta, Rafael Pinot, and John Stephan. Byzantine machine learning made easy by resilient averaging of momentums. *arXiv preprint arXiv:2205.12173*, 2022.
- [20] Avishek Ghosh, Justin Hong, Dong Yin, and Kannan Ramchandran. Robust federated learning in a heterogeneous environment. *arXiv preprint arXiv:1906.06629*, 2019.
- [21] Rachid Guerraoui, Sébastien Rouault, et al. The hidden vulnerability of distributed learning in byzantium. In *International Conference on Machine Learning*, pages 3521–3530. PMLR, 2018.
- [22] Nirupam Gupta, Think T Doan, and Nitin Vaidya. Byzantine fault-tolerance in federated local sgd under 2f-redundancy. *arXiv preprint arXiv:2108.11769*, 2021.
- [23] Nathan Halko, Per-Gunnar Martinsson, and Joel A Tropp. Finding structure with randomness: Probabilistic algorithms for constructing approximate matrix decompositions. *SIAM review*, 53(2):217–288, 2011.
- [24] Lie He, Sai Praneeth Karimireddy, and Martin Jaggi. Byzantine-robust decentralized learning via self-centered clipping. *arXiv preprint arXiv:2202.01545*, 2022.
- [25] Forrest N Iandola, Song Han, Matthew W Moskewicz, Khalid Ashraf, William J Dally, and Kurt Keutzer. Squeezenet: Alexnet-level accuracy with 50x fewer parameters and < 0.5 mb model size. *arXiv preprint arXiv:1602.07360*, 2016.
- [26] Anil K Jain and Richard C Dubes. *Algorithms for clustering data*. Prentice-Hall, Inc., 1988.
- [27] Peter Kairouz, H Brendan McMahan, Brendan Avent, Aurélien Bellet, Mehdi Bennis, Arjun Nitin Bhagoji, Kallista Bonawitz, Zachary Charles, Graham Cormode, Rachel Cummings, et al. Advances and open problems in federated learning. *Foundations and Trends® in Machine Learning*, 14(1–2):1–210, 2021.
- [28] Sai Praneeth Karimireddy, Lie He, and Martin Jaggi. Byzantine-robust learning on heterogeneous datasets via bucketing. *arXiv preprint arXiv:2006.09365*, 2020.
- [29] Sai Praneeth Karimireddy, Lie He, and Martin Jaggi. Learning from history for byzantine robust optimization. In *International Conference on Machine Learning*, pages 5311–5319. PMLR, 2021.
- [30] Alex Krizhevsky, Geoffrey Hinton, et al. Learning multiple layers of features from tiny images. 2009.
- [31] Alex Krizhevsky, Ilya Sutskever, and Geoffrey E Hinton. Imagenet classification with deep convolutional neural networks. *Advances in neural information processing systems*, 25, 2012.
- [32] Leslie Lamport, Robert Shostak, and Marshall Pease. The byzantine generals problem. In *Concurrency: the Works of Leslie Lamport*, pages 203–226. 2019.
- [33] Yann LeCun, Léon Bottou, Yoshua Bengio, and Patrick Haffner. Gradient-based learning applied to document recognition. *Proceedings of the IEEE*, 86(11):2278–2324, 1998.
- [34] Yann LeCun et al. Lenet-5, convolutional neural networks. URL: <http://yann.lecun.com/exdb/lenet>, 20(5):14, 2015.
- [35] Liping Li, Wei Xu, Tianyi Chen, Georgios B Giannakis, and Qing Ling. Rsa: Byzantine-robust stochastic aggregation methods for distributed learning from heterogeneous datasets. In *Proceedings of the AAAI Conference on Artificial Intelligence*, volume 33, pages 1544–1551, 2019.
- [36] Qinbin Li, Yiqun Diao, Quan Chen, and Bingsheng He. Federated learning on non-iid data silos: An experimental study. *arXiv preprint arXiv:2102.02079*, 2021.
- [37] Xiang Li, Wenhao Yang, Shusen Wang, and Zhihua Zhang. Communication efficient decentralized training with multiple local updates. *arXiv preprint arXiv:1910.09126*, 5, 2019.
- [38] Stuart Lloyd. Least squares quantization in pcm. *IEEE transactions on information theory*, 28(2):129–137, 1982.
- [39] Helmut Lutkepohl. Handbook of matrices. *Computational statistics and data analysis*, 2(25):243, 1997.
- [40] Brendan McMahan, Eider Moore, Daniel Ramage, Seth Hampson, and Blaise Aguera y Arcas. Communication-efficient learning of deep networks from decentralized data. In *Artificial intelligence and statistics*, pages 1273–1282. PMLR, 2017.
- [41] Mark EJ Newman. Detecting community structure in networks. *The European physical journal B*, 38(2):321–330, 2004.
- [42] Andrew Ng, Michael Jordan, and Yair Weiss. On spectral clustering: Analysis and an algorithm. *Advances in neural information processing systems*, 14, 2001.
- [43] Rafail Ostrovsky, Yuval Rabani, Leonard J Schulman, and Chaitanya Swamy. The effectiveness of lloyd-type methods for the k-means problem. *Journal of the ACM (JACM)*, 59(6):1–22, 2013.
- [44] Jie Peng and Qing Ling. Byzantine-robust decentralized stochastic optimization. In *ICASSP 2020-2020 IEEE International Conference on Acoustics, Speech and Signal Processing (ICASSP)*, pages 5935–5939. IEEE, 2020.
- [45] Krishna Pillutla, Sham M Kakade, and Zaid Harchaoui. Robust aggregation for federated learning. *arXiv preprint arXiv:1912.13445*, 2019.
- [46] Saurav Prakash and Amir Salman Avestimehr. Mitigating byzantine attacks in federated learning. *arXiv preprint arXiv:2010.07541*, 2020.

- [47] Shashank Rajput, Hongyi Wang, Zachary Charles, and Dimitris Papailiopoulos. Detox: A redundancy-based framework for faster and more robust gradient aggregation. *Advances in Neural Information Processing Systems*, 32, 2019.
- [48] Jayanth Reddy Regatti, Hao Chen, and Abhishek Gupta. Bygars: Byzantine sgd with arbitrary number of attackers using reputation scores.
- [49] Camellia Sarkar and Sarika Jalan. Spectral properties of complex networks. *Chaos: An Interdisciplinary Journal of Nonlinear Science*, 28(10):102101, 2018.
- [50] Felix Sattler, Klaus-Robert Müller, and Wojciech Samek. Clustered federated learning: Model-agnostic distributed multitask optimization under privacy constraints. *IEEE transactions on neural networks and learning systems*, 32(8):3710–3722, 2020.
- [51] Felix Sattler, Klaus-Robert Müller, Thomas Wiegand, and Wojciech Samek. On the byzantine robustness of clustered federated learning. In *ICASSP 2020-2020 IEEE International Conference on Acoustics, Speech and Signal Processing (ICASSP)*, pages 8861–8865. IEEE, 2020.
- [52] Virat Shejwalkar and Amir Houmansadr. Manipulating the byzantine: Optimizing model poisoning attacks and defenses for federated learning. In *NDSS*, 2021.
- [53] Hua-Wei Shen and Xue-Qi Cheng. Spectral methods for the detection of network community structure: a comparative analysis. *Journal of Statistical Mechanics: Theory and Experiment*, 2010(10):P10020, 2010.
- [54] Shiqi Shen, Shruti Tople, and Prateek Saxena. Auror: Defending against poisoning attacks in collaborative deep learning systems. In *Proceedings of the 32nd Annual Conference on Computer Security Applications*, pages 508–519, 2016.
- [55] Jianbo Shi and Jitendra Malik. Normalized cuts and image segmentation. *IEEE Transactions on pattern analysis and machine intelligence*, 22(8):888–905, 2000.
- [56] Jy-yong Sohn, Dong-Jun Han, Beongjun Choi, and Jaekyun Moon. Election coding for distributed learning: Protecting signsgd against byzantine attacks. *Advances in Neural Information Processing Systems*, 33:14615–14625, 2020.
- [57] Gilbert W Stewart. Matrix perturbation theory. 1990.
- [58] Ulrike Von Luxburg. A tutorial on spectral clustering. *Statistics and computing*, 17(4):395–416, 2007.
- [59] Duncan J Watts and Steven H Strogatz. Collective dynamics of ‘small-world’ networks. *nature*, 393(6684):440–442, 1998.
- [60] Han Xiao, Kashif Rasul, and Roland Vollgraf. Fashion-mnist: a novel image dataset for benchmarking machine learning algorithms. *arXiv preprint arXiv:1708.07747*, 2017.
- [61] Cong Xie, Oluwasanmi Koyejo, and Indranil Gupta. Generalized byzantine-tolerant sgd. *Journal of Environmental Sciences (China) English Ed*, 2018.
- [62] Cong Xie, Oluwasanmi Koyejo, and Indranil Gupta. Zeno: Byzantine-suspicious stochastic gradient descent. *arXiv preprint arXiv:1805.10032*, 24, 2018.
- [63] Cong Xie, Oluwasanmi Koyejo, and Indranil Gupta. Fall of empires: Breaking byzantine-tolerant sgd by inner product manipulation. In *Uncertainty in Artificial Intelligence*, pages 261–270. PMLR, 2020.
- [64] Cong Xie, Sanmi Koyejo, and Indranil Gupta. Zeno++: Robust fully asynchronous sgd. In *International Conference on Machine Learning*, pages 10495–10503. PMLR, 2020.
- [65] Haibo Yang, Xin Zhang, Minghong Fang, and Jia Liu. Byzantine-resilient stochastic gradient descent for distributed learning: A lipschitz-inspired coordinate-wise median approach. In *2019 IEEE 58th Conference on Decision and Control (CDC)*, pages 5832–5837. IEEE, 2019.
- [66] Qiang Yang, Yang Liu, Tianjian Chen, and Yongxin Tong. Federated machine learning: Concept and applications. *ACM Transactions on Intelligent Systems and Technology (TIST)*, 10(2):1–19, 2019.
- [67] Yi-Rui Yang and Wu-Jun Li. Basgd: Buffered asynchronous sgd for byzantine learning. In *International Conference on Machine Learning*, pages 11751–11761. PMLR, 2021.
- [68] Dong Yin, Yudong Chen, Ramchandran Kannan, and Peter Bartlett. Byzantine-robust distributed learning: Towards optimal statistical rates. In *International Conference on Machine Learning*, pages 5650–5659. PMLR, 2018.
- [69] Hao Yu, Rong Jin, and Sen Yang. On the linear speedup analysis of communication efficient momentum sgd for distributed non-convex optimization. In *International Conference on Machine Learning*, pages 7184–7193. PMLR, 2019.
- [70] Lihi Zelnik-Manor and Pietro Perona. Self-tuning spectral clustering. *Advances in neural information processing systems*, 17, 2004.
- [71] Chengliang Zhang, Suyi Li, Junzhe Xia, Wei Wang, Feng Yan, and Yang Liu. {BatchCrypt}: Efficient homomorphic encryption for {Cross-Silo} federated learning. In *2020 USENIX annual technical conference (USENIX ATC 20)*, pages 493–506, 2020.
- [72] Ligeng Zhu, Zhijian Liu, and Song Han. Deep leakage from gradients. *Advances in neural information processing systems*, 32, 2019.

Hyper-parameter	Logistic Regression	LeNet	AlexNet
Activation function	ReLU	ReLU	ReLU
Optimization method	Adam	Adam	Adam
Learning rate	0.0005	0.001	0.001
Weight Decay	0.001	0.002	0.001
Batch size	32	32	64
Data Distribution	IID and Non-IID ( $\beta = 0.5, 0.1$ )		IID
Iterations	2000	3000	3000
Number of Clients	100	100	30
Numbers of Attackers	10, 20, 30	10, 20, 30	6

TABLE 8: Training parameters

## APPENDIX A EXPERIMENT SETTING

This section illustrates the experiment settings of the empirical study of the proposed FedCut framework in comparison with existing Byzantine resilient methods.

**Model Architectures** The architectures we investigated include the well-known Logistic regression, LeNet [34] and AlexNet [31].

**Dataset** We evaluate Federated learning model performances with classification tasks on standard MNIST, Fashion MNIST [60] and CIFAR10 dataset. The MNIST database of 10-class handwritten digits has a training set of 60,000 examples, and a test set of 10,000 examples. Fashion MNIST is fashion product of MNIST including 60,000 images and the test set has 10,000 images. The CIFAR-10 dataset consists of 60000  $32 \times 32$  colour images in 10 classes, with 6000 images per class. Respectively, we conduct stand image classification tasks of MNIST, Fashion MNIST and CIFAR10 with logistic regression, LeNet and AlexNet. According to the way we split the dataset for clients in federated learning, the experiments are divided into IID setting and Non-IID setting. Specifically, We consider *lable-skew* Non-IID federated learning setting, where we assume each client’s training examples are drawn with class labels following a *dirichlet distribution* ( $Dir(\beta)$ ) [36], with which  $\beta > 0$  is the concentration parameter controlling the identicalness among users (we use  $\beta = 0.1$  &  $0.5$  in the following).

**Federated Learning Settings** We simulate a horizontal federated learning system with  $K = 100$  clients in a stand-alone machine with 8 Tesla V100-SXM2 32 GB GPUs and 72 cores of Intel(R) Xeon(R) Gold 61xx CPUs. In each communication round, the clients update the weight updates, and the server adopts *Fedavg* [40] algorithm to aggregate the model updates. The detailed experimental hyper-parameters are listed in Tab. 8.

**Attack:** We set 10%, 20% and 30% clients, i.e., 10, 20 and 30 out of 100 clients be Byzantine attackers. The following attacking methods are used in experiments:

- 1) the ‘same value attack’, where model updates of attackers are replaced by the all ones vector;
- 2) the ‘label flipping attack’, where attackers use the wrong label to generate the gradients to upload;
- 3) the ‘sign flipping attack’, where local gradients of attackers are shifted by a scaled value  $-4$ ;
- 4) the ‘gaussian attack’, where local gradients at clients are replaced by independent Gaussian random vectors  $\mathcal{N}(0, 200)$ .
- 5) the ‘Lie attack’, which was designed in [4];
- 6) the ‘Fang-v1 attack’, which was designed in [18] for coordinate-wise trimmed mean [68] and Krum [6] (Fang-v2 attack);
- 7) the ‘Fang-v2 attack’, which was designed in [18] for Krum [6];
- 8) Our designed ‘collusion attack’ that adversaries are separated into 4 groups and same group has the similar values. For example, each groups is sampled from  $\mathcal{N}(\mu + \mu_i, 0.0001)$  and different groups has different  $\mu_i$ , where  $\mu$  is mean of uploaded gradients of all other benign clients.

**Byzantine-resilient methods** The following Byzantine resilient methods are evaluated in experiments:

- 1) Krum [6], we adopt codes from <https://github.com/vrt1shjwlkr/NDSS21-Model-Poisoning/tree/main/femnist>
- 2) Median [68], we adopt codes from <https://github.com/Liepill/RSA-Byzantine>
- 3) Trimmed Mean [68], we adopt codes from <https://github.com/vrt1shjwlkr/NDSS21-Model-Poisoning/tree/main/femnist>
- 4) Bulyan [21], we adopt codes from <https://github.com/vrt1shjwlkr/NDSS21-Model-Poisoning/tree/main/femnist>
- 5) DnC [52], we adopt codes from <https://github.com/vrt1shjwlkr/NDSS21-Model-Poisoning/tree/main/femnist>
- 6) FLtrust [10], we adopt codes from <https://people.duke>

edu/~zg70/code/fltrust.zip

- 7) Kmeans [54], we adopt codes from <https://scikit-learn.org/stable/modules/generated/sklearn.cluster.KMeans.html>
- 8) Ncut [42], we adopt Ncut in each iteration separately for ablation study.
- 9) FedCut, the proposed FedCut method applied to the Spatial-Temporal network.

## APPENDIX B ABLATION STUDY

In this section, we report more experimental results on different extent Non-IID (e.g.,  $\beta=0.1$  and  $\beta=0.5$ ), number of byzantine attackers (e.g., 10, 20 and 30), model (e.g., logistic regression, LeNet and AlexNet) and dataset (e.g., MNIST, Fashion MNIST and CIFAR10).

### B.1 More Experimental Results

Tab. 9-26 show the model performance (MP) for different Byzantine resilient methods under different types of attacks in various settings. All results show that the proposed method FedCut achieve the best model performances compared to other byzantine resilient methods when the Non-IID extent increases from  $\beta = 0.5$  to 0.1 and byzantine attackers numbers increases from 10 to 30. As shown by the ablation study, the MP of NCut is not as stable as that of the proposed FedCut (e.g., MP drops to 31.7 % with Non-IID setting and 30 attackers under Fang-v1 attack).

### B.2 FedCut v.s. FedCut without Temporal Consistency

In this part, we compare FedCut and NCut, which remove the temporal consistency. Fig. 10 shows the averaged MP of FedCut and NCut, which demonstrates the stability of FedCut while the averaged MP of NCut is highly influenced by the Non-IID extent of clients' data (e.g., the MP of Ncut drops to 80% with Non-IID parameter  $\beta = 0.1$ ). The reason temporal consistency would help to distinguish benign and byzantine clients during the training process.

### B.3 Robustness for Spectral Heuristics in Heterogeneous Dataset

In this part, we demonstrate the effectiveness of estimating the number of communities, Gaussian scaling factors via the

largest eigengap even for the heterogeneous dataset among clients.

Fig. 11 and 12 display the position of the largest eigengap for Non-IID dataset ( $q = 0.1, 0.5$ ), which illustrates the largest eigengap is also a good estimation for the number of communities. Moreover, Fig. 13 also shows the eigengap and clustering accuracy could reach the optimal at the same time even for Non-IID dataset ( $q = 0.1, 0.5$ ), which demonstrates we could select the Gaussian scaling factor according to the largest eigengap.

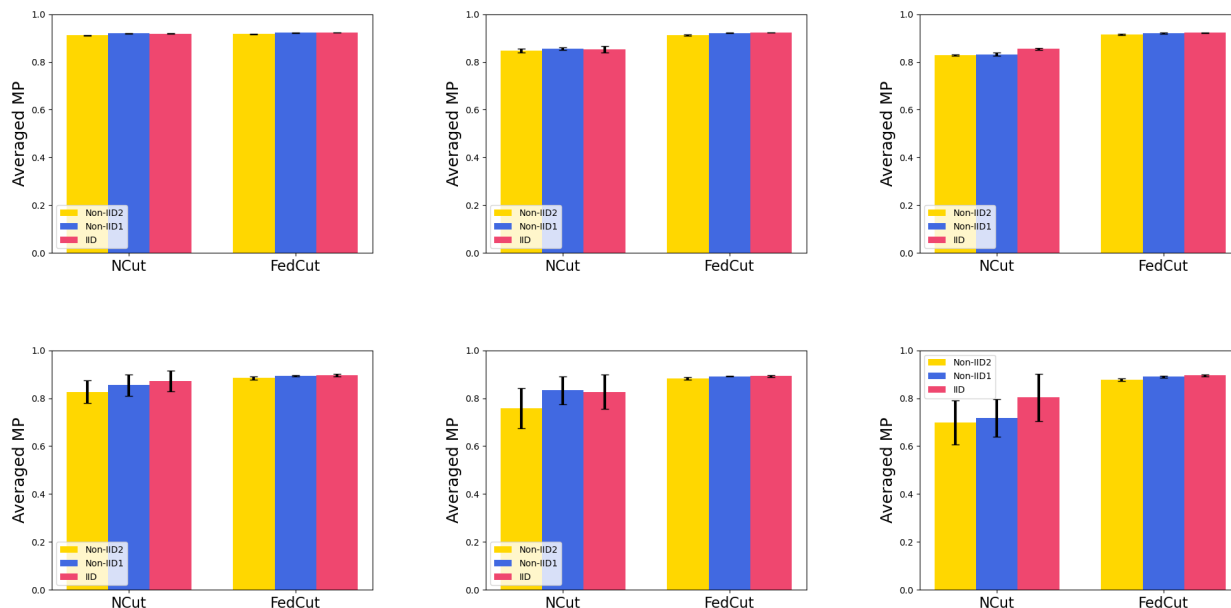


Fig. 10: Average MP of FedCut and Ncut (FedCut without temporal consistency) among all 8 attacks with different byzantine numbers (left: 10 attackers, middle: 20 attackers and right: 30 attackers) on MNIST (first row) and Fashion MNIST (second row).

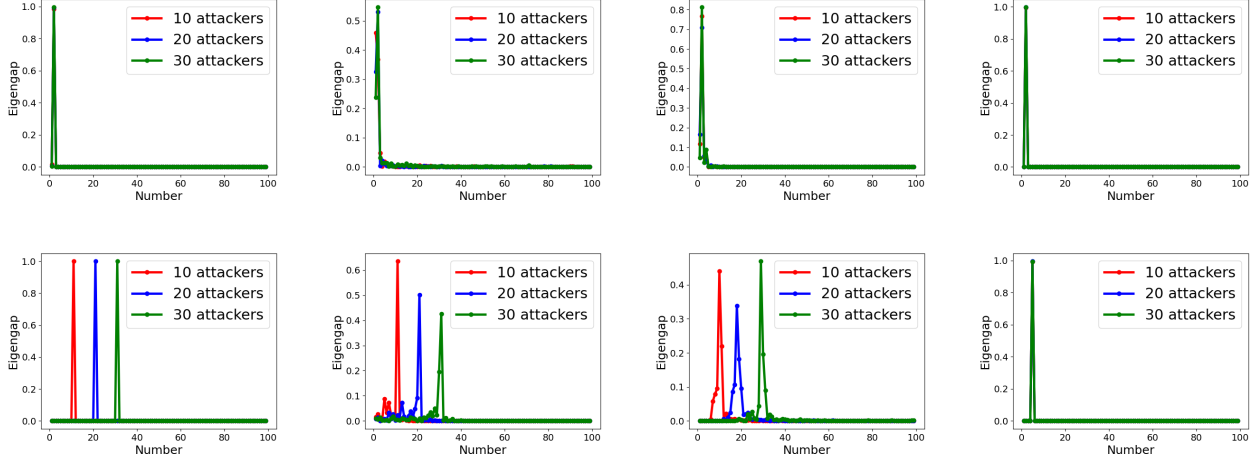


Fig. 11: The change of eigengap for different attacks with different number of attackers under IID setting for MNIST dataset.

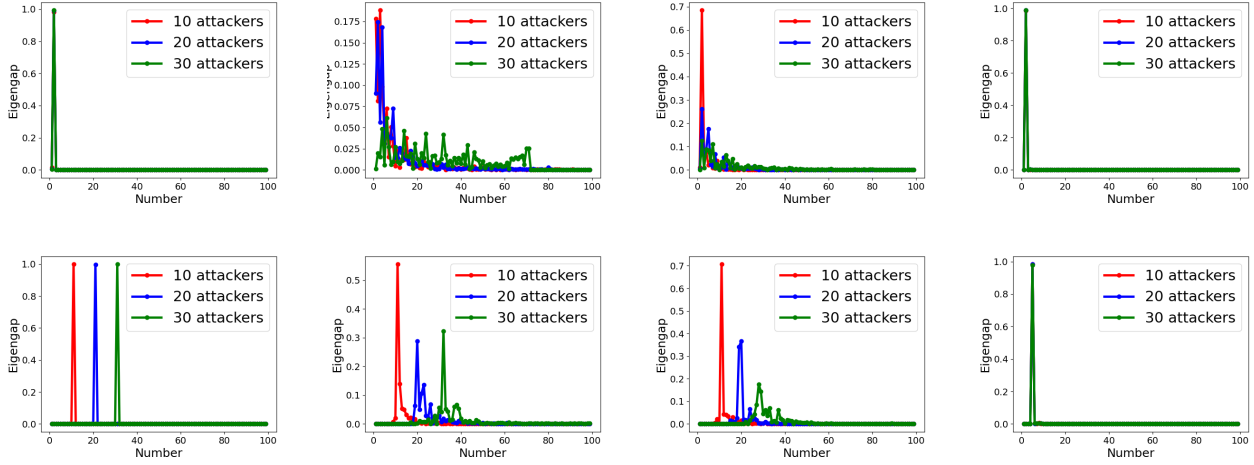


Fig. 12: The change of eigengap for different attacks with different number of attackers under Non-IID with  $\beta = 0.1$  setting for MNIST dataset.

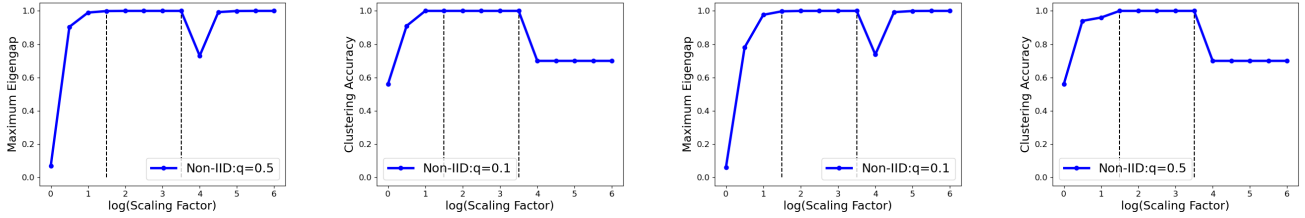


Fig. 13: The change of the maximum eigengap of normalized adjacency matrix and clustering accuracy with different scaling factor  $\sigma$  for the Gaussian attack [35] on different Non-IID dataset ( $q = 0.1, 0.5$ ), where the normalized adjacency matrix  $L = D^{-1/2}AD^{-1/2}$ ,  $D = \text{diag}(\text{Sum}(A))$  and  $A_{ij} = \exp(-\|\mathbf{g}_i - \mathbf{g}_j\|^2/2\sigma^2)$ . The clustering accuracy is calculated by NCut on the normalized adjacency matrix with 100 client including 70 benign clients and 30 Byzantine clients.



		Krum [6]	GeoMeidan [13]	Median [68]	Trimmed [68]	Bulyan [21]	FLtrust [10]	DnC [52]	Kmeans [54]	FedCut (Ours)
F M N I S T	No attack	75.7±1.1	88.5±0.9	76.5±4.0	81.6±1.4	75.5±1.5	85.6±1.6	89.1±0.4	88.7±0.7	88.9±1.0
	Lie [4]	73.8±0.7	78.9±1.7	40.0±28.6	47.4±22.8	72.1±5.0	83.0±2.9	75.3±3.8	81.1±0.9	88.7±0.8
	Fang-v1 [18]	75.4±2.3	86.7±1.1	64.7±7.7	62.3±17.1	74.4±3.3	83.9±3.0	89.9±0.2	76.6±8.1	89.2±1.4
	Fang-v2 [18]	10.0±0.0	43.4±5.7	68.8±3.6	59.5±13.0	56.8±11.3	84.9±0.7	88.4±1.9	88.8±0.4	88.9±0.1
	Same value [35]	75.8±1.2	75.0±1.6	78.3±4.9	78.5±3.5	76.7±2.9	85.9±2.0	89.5±0.2	89.2±0.5	89.3±0.6
	Gaussian [6]	77.2±0.8	88.2±0.7	78.2±30.8	74.8±7.9	64.8±15.5	86.3±0.9	80.4±4.2	40.6±24.2	89.6±0.4
	sign flipping [15]	75.9±2.4	87.4±1.1	78.9±2.9	72.4±14.3	67.7±15.6	85.3±1.3	85.5±1.3	54.9±10.0	84.4±0.9
	label flipping [15]	76.6±0.9	88.1±0.9	69.0±7.5	78.7±1.6	60.2±20.9	85.8±1.3	89.4±0.5	87.8±1.0	88.0±0.4
	minic [28]	75.5±1.4	87.9±0.6	77.1±2.1	86.0±0.3	79.3±0.3	87.4±0.4	88.9±0.3	88.9±0.2	88.9±0.7
	Collusion (Ours)	75.9±1.6	34.9±11.2	72.7±1.1	69.3±2.2	71.8±4.4	87.1±0.1	66.6±6.6	56.6±22.3	89.1±0.4
	Averaged	69.2±1.2	75.9±2.6	70.4±9.3	71.1±8.4	69.9±8.1	85.5±1.4	84.3±1.9	75.3±6.8	88.5±0.7
Worst-case	10.0±0.0	34.9±11.2	40.0±28.6	47.4±22.8	56.8±11.3	83.0±2.9	66.6±6.6	40.6±24.2	84.4±0.9	

TABLE 9: Model performances of different Byzantine-resilient methods under different attacks (with Non-IID setting  $\beta = 0.1$  and 10 attackers for classification of Fashion MNIST).

		Krum [6]	GeoMeidan [13]	Median [68]	Trimmed [68]	Bulyan [21]	FLtrust [10]	DnC [52]	Kmeans [54]	FedCut (Ours)
F M N I S T	No attack	83.2±0.6	89.9±0.3	84.5±0.9	84.3±1.9	83.6±2.3	87.4±0.9	90.0±0.4	89.6±0.5	90.0±0.4
	Lie [4]	83.5±0.7	84.3±0.6	55.1±18.7	75.8±6.0	82.6±1.8	83.6±2.5	71.0±29.0	80.2±1.3	89.9±0.6
	Fang-v1 [18]	83.7±0.4	89.1±0.4	79.8±3.4	79.7±3.5	84.1±1.8	85.3±1.6	90.2±0.3	89.6±1.5	89.6±0.3
	Fang-v2 [18]	10.0±0.0	60.3±6.3	72.2±2.3	73.1±1.5	73.0±2.0	85.7±1.0	89.0±1.3	88.7±0.5	89.2±0.4
	Same value [35]	83.5±0.3	76.3±0.5	84.2±0.6	83.4±1.4	83.8±1.3	87.1±0.5	89.8±0.2	89.9±0.2	90.0±0.5
	Gaussian [6]	83.1±0.4	89.7±0.3	84.5±1.3	85.3±1.2	79.9±4.6	87.2±0.6	78.1±4.6	49.6±16.0	89.8±0.1
	sign flipping [15]	83.7±0.7	88.9±0.7	82.8±3.8	84.6±1.8	80.8±2.7	86.7±1.5	88.2±0.5	71.7±10.6	86.4±0.6
	label flipping [15]	83.6±0.8	89.5±0.4	81.1±3.4	83.4±3.4	81.1±2.5	87.5±0.6	90.0±0.2	89.6±0.2	89.8±0.3
	minic [28]	83.6±0.5	89.4±0.1	81.5±6.3	88.4±0.6	85.1±0.8	88.7±0.6	89.4±0.1	89.7±0.2	89.2±0.3
	Collusion (Ours)	84.3±0.6	27.8±24.8	75.2±1.9	75.5±1.4	81.9±2.8	88.7±0.6	84.2±0.7	54.5±12.6	90.1±0.1
	Averaged	76.2±0.5	78.5±3.4	78.1±4.3	81.4±2.3	81.6±2.3	86.8±1.0	86.0±3.7	79.3±4.4	89.4±0.4
Worst-case	10.0±0.0	27.8±24.8	55.1±18.7	73.1±1.5	73.0±2.0	83.6±2.5	71.0±29.0	49.6±16.0	86.4±0.6	

TABLE 10: Model performances of different Byzantine-resilient methods under different attacks (with Non-IID setting  $\beta = 0.5$  and 10 attackers for classification of Fashion MNIST).

		Krum [6]	GeoMeidan [13]	Median [68]	Trimmed [68]	Bulyan [21]	FLtrust [10]	DnC [52]	Kmeans [54]	FedCut (Ours)
F M N I S T	No attack	84.7±0.7	90.0±0.4	87.9±0.4	88.2±0.4	87.0±0.6	88.0±0.6	90.2±0.2	89.8±0.4	90.2±0.1
	Lie [4]	85.1±0.3	66.8±22.2	81.9±2.2	82.7±0.9	85.1±0.5	85.2±1.1	80.0±3.8	78.6±3.2	90.0±0.4
	Fang-v1 [18]	84.9±0.6	88.7±0.7	86.5±0.4	86.6±0.6	86.9±0.4	87.4±1.0	89.9±0.4	90.1±0.2	87.8±2.1
	Fang-v2 [18]	47.7±31.0	78.2±1.8	78.0±0.3	84.7±0.8	84.8±1.0	84.3±0.8	89.6±0.9	89.3±0.2	90.3±0.4
	Same value [35]	85.3±0.5	76.9±0.4	85.5±0.5	85.1±0.7	87.2±0.5	88.2±0.9	90.2±0.6	90.3±0.2	90.3±0.1
	Gaussian [6]	85.1±0.9	90.0±0.4	87.8±0.5	88.1±0.4	87.5±0.4	88.3±0.8	76.3±5.2	30.2±26.5	90.3±0.2
	sign flipping [15]	85.0±0.4	89.4±0.3	87.9±0.4	88.2±0.4	87.1±0.4	86.5±1.9	89.3±0.6	87.7±0.6	89.4±1.0
	label flipping [15]	84.9±0.5	89.9±0.2	85.6±1.1	85.1±0.7	87.1±0.4	88.2±0.8	90.4±0.4	90.1±0.2	88.0±0.2
	minic [28]	85.3±0.2	89.4±0.4	87.9±0.7	89.4±0.5	86.9±0.3	89.1±0.3	89.8±0.4	89.9±0.2	89.8±0.2
	Collusion (Ours)	85.3±0.5	54.7±4.5	79.1±1.3	78.1±0.4	87.5±0.4	88.7±0.2	85.0±0.5	67.6±2.9	90.1±0.0
	Averaged	81.3±3.6	81.4±3.1	84.8±0.8	85.6±0.6	86.7±0.5	87.4±0.8	87.1±1.3	80.4±3.5	89.6±0.5
Worst-case	47.7±31.0	54.7±4.5	78.0±0.3	78.1±0.4	84.8±1.0	84.3±0.8	76.3±5.2	30.2±26.5	87.8±2.1	

TABLE 11: Model performances of different Byzantine-resilient methods under different attacks (with IID and 10 attackers for classification of Fashion MNIST).

		Krum [6]	GeoMeidan [13]	Median [68]	Trimmed [68]	Bulyan [21]	FLtrust [10]	DnC [52]	Kmeans [54]	FedCut (Ours)
F M N I S T	No attack	72.0±2.5	88.4±0.7	70.1±11.0	81.8±0.3	81.8±0.4	86.1±1.1	88.9±0.8	88.7±0.6	89.4±0.4
	Lie [4]	75.4±1.2	64.4±9.9	35.5±25.0	41.3±19.5	26.9±28.5	76.8±4.0	72.1±6.8	88.1±0.6	88.1±2.3
	Fang-v1 [18]	76.4±1.5	78.5±0.8	27.9±10.9	35.8±9.2	71.6±5.5	84.1±2.9	88.7±0.8	89.7±0.4	89.2±0.1
	Fang-v2 [18]	10.0±0.0	10.9±1.2	18.8±18.4	32.9±5.8	23.6±9.0	84.9±0.4	82.2±8.1	65.8±10.3	89.0±0.3
	Same value [35]	76.6±1.9	64.5±8.9	57.8±11.9	66.7±3.7	81.2±0.7	86.1±1.0	89.5±0.4	89.5±0.4	89.4±0.2
	Gaussian [6]	76.4±0.4	88.0±0.7	76.4±2.7	79.4±1.4	78.2±3.5	85.7±1.9	76.4±6.6	20.7±28.9	89.3±0.1
	sign flipping [15]	75.5±1.2	85.3±5.5	73.0±5.9	54.5±25.3	80.5±8.5	83.4±2.5	76.7±1.2	61.1±3.4	82.9±0.5
	label flipping [15]	76.5±0.7	88.3±1.0	66.8±13.1	75.5±2.9	77.3±10.4	85.6±1.2	87.3±2.0	87.0±1.2	88.5±0.5
	minic [28]	75.3±1.4	84.6±1.4	60.4±13.3	81.1±3.6	66.9±4.7	87.4±0.5	88.0±0.1	88.7±0.4	89.1±0.2
	Collusion (Ours)	75.0±1.6	55.9±11.4	67.7±2.0	70.7±0.4	71.7±2.2	86.4±0.5	86.1±0.4	32.4±20.0	89.4±0.4
	Averaged	68.9±1.2	70.9±4.2	55.4±11.4	62.0±7.2	66.0±7.3	84.7±1.6	83.6±2.7	71.2±6.6	88.4±0.5
Worst-case	10.0±0.0	10.9±1.2	18.8±18.4	32.9±5.8	23.6±9.0	76.8±4.0	72.1±6.8	20.7±28.9	82.9±0.5	

TABLE 12: Model performances of different Byzantine-resilient methods under different attacks (with Non-IID setting  $\beta = 0.1$  and 20 attackers for classification of Fashion MNIST).

		Krum [6]	GeoMeidan [13]	Median [68]	Trimmed [68]	Bulyan [21]	FLtrust [10]	DnC [52]	Kmeans [54]	FedCut (Ours)
F M N I S T	No attack	82.3±0.7	90.0±0.3	85.6±1.0	86.5±0.4	85.5±2.8	88.1±0.6	89.4±1.0	88.4±1.0	90.2±0.2
	Lie [4]	83.5±1.0	53.7±13.5	36.1±15.6	51.9±26.7	54.5±12.9	76.3±6.0	73.3±7.8	87.9±1.0	89.9±0.1
	Fang-v1 [18]	84.8±0.7	85.5±1.1	75.5±2.5	71.8±7.3	83.1±0.9	84.4±1.4	89.2±1.3	88.8±1.2	89.4±0.2
	Fang-v2 [18]	10.0±8.3	18.9±7.1	62.4±5.1	55.8±2.8	59.3±5.4	84.9±0.8	83.0±8.3	72.4±5.2	89.5±0.2
	Same value [35]	83.7±0.8	64.8±8.2	77.7±2.7	71.5±5.5	86.2±1.0	86.9±0.7	88.8±1.2	89.0±1.2	89.4±0.1
	Gaussian [6]	82.9±0.4	89.6±0.5	84.6±2.5	86.2±1.1	85.7±0.7	88.4±0.4	77.5±7.2	38.2±34.5	89.5±0.3
	sign flipping [15]	82.9±1.4	87.7±0.9	85.0±1.0	85.0±0.9	85.1±1.4	84.4±1.8	85.0±1.5	74.3±7.4	86.0±0.1
	label flipping [15]	82.4±1.1	89.9±0.4	79.4±3.4	80.4±1.8	80.3±6.6	88.1±0.2	88.4±1.2	88.6±1.5	89.3±0.3
	minic [28]	81.1±2.6	87.5±1.1	83.0±0.4	87.8±0.3	76.3±1.5	88.7±0.3	89.3±0.3	89.4±0.3	88.9±0.6
	Collusion (Ours)	84.5±1.0	41.7±17.0	72.0±1.2	61.4±15.3	81.4±5.0	88.7±0.7	86.9±0.5	56.5±9.7	89.9±0.3
	Averaged	75.8±1.8	70.9±5.0	74.1±3.5	73.8±6.2	77.7±3.8	85.9±1.3	85.1±3.0	77.4±6.3	89.2±0.2
Worst-case	10.0±8.3	18.9±7.1	36.1±15.6	51.9±26.7	54.5±12.9	76.3±6.0	73.3±7.8	38.2±34.5	86.0±0.1	

TABLE 13: Model performances of different Byzantine-resilient methods under different attacks (with Non-IID setting  $\beta = 0.5$  and 20 attackers for classification of Fashion MNIST).

		Krum [6]	GeoMeidan [13]	Median [68]	Trimmed [68]	Bulyan [21]	FLtrust [10]	DnC [52]	Kmeans [54]	FedCut (Ours)
F M N I S T	No attack	84.6±0.6	90.1±0.4	88.3±0.2	88.0±0.6	87.5±0.2	88.3±0.6	89.3±1.0	89.2±0.7	89.1±0.9
	Lie [4]	84.7±0.7	76.3±18.9	69.0±26.6	75.2±3.1	82.4±0.2	79.0±4.2	79.7±4.6	89.0±1.0	88.8±1.0
	Fang-v1 [18]	85.3±0.4	86.4±0.7	80.8±1.4	80.3±2.0	87.5±0.3	86.6±0.9	88.5±1.0	89.2±0.6	89.7±0.2
	Fang-v2 [18]	38.0±21.1	46.4±9.7	70.9±1.4	71.0±2.1	17.2±12.5	82.9±0.8	85.0±6.4	86.6±2.3	90.0±0.2
	Same value [35]	85.0±0.5	74.0±2.2	78.9±2.0	77.8±1.2	87.1±0.4	88.4±0.4	89.3±0.8	89.2±0.7	89.5±0.2
	Gaussian [6]	85.2±0.5	89.9±0.4	88.1±0.3	88.5±0.3	87.1±0.4	88.1±0.5	78.6±6.6	40.7±33.8	89.4±0.2
	sign flipping [15]	84.5±0.5	88.5±0.1	87.4±0.3	87.4±0.5	87.4±0.2	86.4±0.6	87.3±0.8	75.7±6.8	87.3±0.5
	label flipping [15]	85.5±0.6	89.9±0.6	82.3±0.8	82.0±0.5	87.3±0.2	87.3±0.9	89.2±1.1	89.8±0.7	89.7±0.1
	minic [28]	81.8±0.8	86.3±0.8	86.4±0.3	88.5±0.2	80.0±0.4	88.4±0.3	89.1±0.2	89.2±0.9	89.8±0.4
	Collusion (Ours)	84.9±0.7	35.7±5.0	76.7±1.1	69.7±2.9	87.4±0.2	88.6±0.2	86.9±0.4	66.7±22.7	89.6±1.0
	Averaged	79.9±2.6	76.4±3.9	80.9±3.4	80.8±1.3	79.1±1.5	86.4±0.9	86.3±2.3	80.5±7.0	89.3±0.5
Worst-case	38.0±21.1	35.7±5.0	69.0±26.6	69.7±2.9	17.2±12.5	79.0±4.2	78.6±6.6	40.7±33.8	87.3±0.5	

TABLE 14: Model performances of different Byzantine-resilient methods under different attacks (with IID setting and 20 attackers for classification of Fashion MNIST).

		Krum [6]	GeoMeidan [13]	Median [68]	Trimmed [68]	Bulyan [21]	FLtrust [10]	DnC [52]	Kmeans [54]	FedCut (Ours)
F M N I S T	No attack	71.7±1.9	88.6±0.7	80.6±1.2	79.5±3.7	79.4±0.9	86.2±1.5	88.6±0.2	89.3±0.2	89.3±0.5
	Lie [4]	74.4±0.8	37.9±17.2	26.9±14.5	30.1±22.4	48.0±10.9	66.5±26.1	61.4±22.2	87.7±1.8	88.1±2.3
	Fang-v1 [18]	74.5±1.9	61.3±4.6	19.5±5.4	21.3±5.3	16.7±33.8	82.0±3.0	79.1±2.4	89.1±0.4	88.6±0.6
	Fang-v2 [18]	10.0±0.0	10.0±0.0	15.3±7.7	17.6±3.1	12.3±3.0	84.4±0.4	78.0±14.6	15.0±18.6	88.7±0.2
	Same value [35]	75.6±1.0	43.2±19.2	44.5±8.2	41.0±3.5	79.6±1.1	86.0±0.4	89.2±0.7	89.4±0.3	89.0±0.5
	Gaussian [6]	76.1±2.1	87.9±0.8	75.2±3.7	80.9±1.0	78.2±3.7	85.9±1.4	76.7±11.1	13.3±29.5	88.8±0.1
	sign flipping [15]	74.1±1.0	79.3±5.6	71.1±6.1	70.0±5.1	79.6±1.0	80.7±2.2	50.2±3.2	39.4±3.8	82.1±0.5
	label flipping [15]	76.5±1.5	87.3±1.0	67.7±7.0	70.2±5.1	80.1±14.9	85.9±1.6	83.7±6.8	80.6±3.2	86.7±1.9
	minic [28]	72.6±5.5	70.3±2.2	73.8±0.7	75.9±7.8	53.6±3.6	86.9±0.7	86.9±0.5	88.9±0.2	88.9±0.1
	Collusion (Ours)	76.4±1.5	39.7±9.0	67.8±2.2	67.5±3.4	19.7±6.3	86.1±0.2	82.1±1.1	54.0±3.1	89.2±0.3
	Averaged	68.2±1.7	60.6±6.0	54.2±5.7	55.4±6.0	54.7±7.9	83.1±3.8	77.6±6.3	64.7±6.1	87.9±0.7
Worst-case	10.0±0.0	10.0±0.0	15.3±7.7	17.6±3.1	12.3±3.0	66.5±26.1	50.2±3.2	13.3±29.5	82.1±0.5	

TABLE 15: Model performances of different Byzantine-resilient methods under different attacks (with Non-IID setting  $\beta = 0.1$  and 30 attackers for classification of Fashion MNIST).

		Krum [6]	GeoMeidan [13]	Median [68]	Trimmed [68]	Bulyan [21]	FLtrust [10]	DnC [52]	Kmeans [54]	FedCut (Ours)
F M N I S T	No attack	82.6±0.8	89.6±0.7	85.4±1.5	84.4±1.9	83.7±4.3	87.3±0.8	89.5±0.4	89.1±0.6	89.7±0.2
	Lie [4]	83.0±1.0	45.4±14.6	39.0±15.9	50.9±10.5	59.5±11.1	52.6±19.5	79.8±2.7	89.6±0.7	89.3±0.3
	Fang-v1 [18]	83.3±0.3	76.6±2.2	47.6±10.2	52.1±5.9	81.2±3.1	85.0±1.6	85.5±0.2	89.6±0.3	88.8±0.8
	Fang-v2 [18]	10.0±0.0	10.0±0.0	47.4±5.5	32.4±14.8	12.3±3.3	84.6±0.9	80.8±11.8	34.6±24.0	88.8±0.6
	Same value [35]	84.2±0.7	49.9±15.9	53.5±8.0	48.3±10.3	85.8±0.9	85.4±1.7	89.4±0.1	89.3±0.4	89.1±0.5
	Gaussian [6]	83.4±1.0	89.0±0.4	84.1±1.9	86.3±1.3	85.1±1.2	87.6±0.9	73.0±8.9	17.5±29.4	89.5±0.1
	sign flipping [15]	83.0±0.4	85.3±1.7	83.6±0.8	83.5±2.0	83.1±1.6	79.7±2.1	59.6±4.3	29.7±23.1	87.9±1.6
	label flipping [15]	83.6±0.3	89.7±0.5	67.4±15.1	75.5±1.6	85.1±1.1	87.4±1.1	88.9±1.2	89.3±0.4	88.5±0.4
	minic [28]	77.0±1.7	78.3±0.7	80.6±1.0	84.1±0.7	63.0±7.4	88.3±0.3	87.9±0.6	88.9±0.6	89.4±0.5
	Collusion (Ours)	83.6±0.4	10.4±8.3	65.2±4.8	63.3±7.1	85.3±0.6	88.6±0.5	83.6±0.3	63.0±24.1	89.0±0.5
	Averaged	75.4±0.7	62.4±4.5	65.4±6.5	66.1±5.6	72.4±3.5	82.7±2.9	81.8±3.1	68.1±10.4	89.0±0.6
Worst-case	10.0±0.0	10.0±0.0	39.0±15.9	32.4±14.8	12.3±3.3	52.6±19.5	59.6±4.3	17.5±29.4	87.9±1.6	

TABLE 16: Model performances of different Byzantine-resilient methods under different attacks (with Non-IID setting  $\beta = 0.5$  and 30 attackers for classification of Fashion MNIST).

		Krum [6]	GeoMeidan [13]	Median [68]	Trimmed [68]	Bulyan [21]	FLtrust [10]	DnC [52]	Kmeans [54]	FedCut (Ours)
M N I S T	No attack	64.2±6.8	92.1±0.1	66.9±2.3	66.1±2.1	55.6±5.9	89.8±0.2	91.7±0.2	91.8±0.3	92.2±0.0
	Lie [4]	61.6±7.7	90.5±0.2	75.8±2.8	73.8±3.7	63.1±2.2	89.6±0.1	92.1±0.2	89.8±0.2	92.2±0.1
	Fang-v1 [18]	62.7±5.9	89.8±0.2	50.9±4.5	42.9±6.6	57.5±2.0	79.3±1.5	92.0±0.3	68.4±5.3	92.0±0.1
	Fang-v2 [18]	58.4±4.2	88.2±0.1	40.9±3.4	45.0±2.7	41.6±5.2	78.5±2.4	91.4±0.4	91.6±0.1	92.3±0.2
	Same value [35]	63.0±6.6	90.5±0.2	58.8±2.2	58.7±2.2	55.2±3.2	89.8±0.2	92.1±0.2	92.1±0.3	92.2±0.1
	Gaussian [6]	63.6±4.5	91.9±0.1	68.5±3.1	67.1±4.9	54.5±3.8	89.6±0.4	83.3±0.3	43.8±3.4	92.3±0.1
	sign flipping [15]	66.2±7.9	91.5±0.1	66.8±3.4	68.5±5.1	53.6±3.0	79.6±0.6	90.3±0.2	64.7±1.3	91.5±0.2
	label flipping [15]	64.8±2.1	91.3±0.1	57.3±2.5	58.1±5.4	53.0±7.2	89.9±0.4	90.5±0.2	86.4±0.7	88.8±0.1
	minic [28]	72.5±3.1	91.3±0.1	74.8±0.9	88.0±0.4	65.1±4.2	90.2±0.1	91.4±0.1	91.1±0.2	92.1±0.2
	Collusion (Ours)	66.6±4.9	89.7±0.6	69.7±7.3	70.8±6.4	58.5±9.0	89.6±0.4	89.2±1.9	79.1±0.3	92.1±0.2
	Averaged	64.4±5.4	90.7±0.2	63.0±3.2	63.9±4.0	55.8±4.6	86.6±0.6	90.4±0.4	79.9±1.2	91.8±0.1
Worst-case	58.4±4.2	88.2±0.1	40.9±3.4	42.9±6.6	41.6±5.2	78.5±2.4	83.3±0.3	43.8±3.4	88.8±0.1	

TABLE 17: Model performances of different Byzantine-resilient methods under different attacks (with Non-IID setting  $\beta = 0.1$  and 10 attackers for classification of MNIST).

		Krum [6]	GeoMeidan [13]	Median [68]	Trimmed [68]	Bulyan [21]	FLtrust [10]	DnC [52]	Kmeans [54]	FedCut (Ours)
M N I S T	No attack	89.0±0.3	92.4±0.1	85.3±0.5	84.9±0.1	81.7±1.0	89.0±0.4	92.2±0.3	92.0±0.4	92.4±0.1
	Lie [4]	89.3±0.3	91.5±0.2	87.7±0.2	88.1±0.5	85.1±0.7	88.8±0.7	92.3±0.2	91.6±0.0	92.4±0.1
	Fang-v1 [18]	89.2±0.3	91.4±0.2	72.5±1.6	72.3±1.3	80.1±0.7	78.2±2.0	92.3±0.2	92.2±0.2	92.3±0.0
	Fang-v2 [18]	38.1±5.5	88.2±0.2	70.2±1.6	70.2±2.3	60.5±1.5	80.9±0.6	91.9±0.3	91.9±0.2	92.4±0.1
	Same value [35]	89.3±0.4	91.2±0.2	79.3±0.3	78.5±1.1	81.1±0.6	88.5±0.9	92.3±0.3	92.3±0.2	92.4±0.1
	Gaussian [6]	89.2±0.4	92.3±0.2	85.7±0.2	85.5±0.3	80.6±0.6	88.5±0.5	83.5±0.7	43.3±5.3	92.3±0.1
	sign flipping [15]	89.1±0.2	92.2±0.1	86.0±0.1	85.6±0.5	81.0±0.8	78.1±0.8	92.0±0.1	81.9±8.3	91.9±0.3
	label flipping [15]	89.3±0.5	91.8±0.2	82.2±0.2	82.6±1.0	81.3±1.6	88.9±0.3	91.8±0.1	90.4±0.5	91.3±1.3
	minic [28]	89.9±0.3	92.1±0.2	88.6±0.4	91.4±0.1	85.4±0.3	90.6±0.1	92.2±0.1	92.1±0.1	92.4±0.1
	Collusion (Ours)	89.2±0.4	90.7±0.7	84.5±2.4	84.1±2.6	82.3±3.7	88.7±0.2	90.1±1.7	78.1±5.3	92.2±0.0
Averaged	84.2±0.9	91.4±0.2	82.2±0.8	82.3±1.0	79.9±1.2	86.0±0.7	91.1±0.4	84.6±2.1	92.2±0.2	
Worst-case	38.1±5.5	88.2±0.2	70.2±1.6	70.2±2.3	60.5±1.5	78.1±0.8	83.5±0.7	43.3±5.3	91.3±1.3	

TABLE 18: Model performances of different Byzantine-resilient methods under different attacks (with Non-IID setting  $\beta = 0.5$  and 10 attackers for classification of MNIST).

		Krum [6]	GeoMeidan [13]	Median [68]	Trimmed [68]	Bulyan [21]	FLtrust [10]	DnC [52]	Kmeans [54]	FedCut (Ours)
M N I S T	No attack	90.3±0.1	92.5±0.1	90.3±0.1	90.1±0.2	88.3±0.3	89.6±0.2	92.3±0.3	92.3±0.2	92.4±0.1
	Lie [4]	90.5±0.1	91.8±0.2	90.7±0.2	90.9±0.1	89.1±0.1	89.6±0.1	92.3±0.2	91.8±0.3	92.3±0.1
	Fang-v1 [18]	90.4±0.1	91.7±0.2	83.6±0.2	82.8±0.4	88.0±0.2	77.1±2.1	92.4±0.2	91.9±0.3	92.3±0.1
	Fang-v2 [18]	43.8±2.0	89.5±0.6	83.6±0.5	83.2±0.3	71.2±0.6	81.6±1.4	92.2±0.3	92.1±0.1	92.4±0.0
	Same value [35]	90.4±0.2	91.6±0.1	87.9±0.2	87.6±0.1	88.6±0.2	89.5±0.1	92.2±0.1	92.3±0.3	92.4±0.1
	Gaussian [6]	90.5±0.2	92.4±0.1	90.4±0.3	90.4±0.1	88.5±0.2	88.7±0.2	83.6±0.5	50.7±0.9	92.4±0.1
	sign flipping [15]	90.4±0.1	92.3±0.1	90.4±0.2	90.3±0.1	88.6±0.1	75.6±3.8	92.2±0.2	91.5±0.1	92.2±0.1
	label flipping [15]	90.4±0.2	91.8±0.1	89.4±0.3	89.2±0.2	88.6±0.2	89.2±0.5	92.2±0.1	92.2±0.3	92.2±0.1
	minic [28]	90.7±0.2	92.1±0.2	90.9±0.2	91.7±0.1	89.6±0.1	90.4±0.2	92.5±0.1	92.2±0.1	92.4±0.1
	Collusion (Ours)	90.5±0.2	91.0±0.4	88.9±0.8	88.6±0.8	88.7±0.6	89.0±0.4	91.7±0.4	76.5±0.7	92.2±0.2
Averaged	85.8±0.3	91.7±0.2	88.6±0.3	88.5±0.2	86.9±0.3	86.0±0.9	91.4±0.2	86.4±0.3	92.3±0.1	
Worst-case	43.8±2.0	89.5±0.6	83.6±0.2	82.8±0.4	71.2±0.6	75.6±3.8	83.6±0.5	50.7±0.9	92.2±0.1	

TABLE 19: Model performances of different Byzantine-resilient methods under different attacks (with IID and 10 attackers for classification of MNIST).

		Krum [6]	GeoMeidan [13]	Median [68]	Trimmed [68]	Bulyan [21]	FLtrust [10]	DnC [52]	Kmeans [54]	FedCut (Ours)
M N I S T	No attack	63.2±8.0	92.1±0.1	63.3±3.4	66.0±0.7	75.6±2.6	89.9±0.2	91.7±0.3	91.8±0.2	92.3±0.1
	Lie [4]	66.6±2.7	86.4±0.2	81.6±0.2	83.5±0.4	79.2±0.5	88.7±0.5	92.0±0.3	92.0±0.2	92.1±0.1
	Fang-v1 [18]	68.4±2.5	79.0±0.8	32.3±4.2	30.7±5.5	63.2±6.2	78.8±2.2	92.0±0.3	92.0±0.4	92.2±0.1
	Fang-v2 [18]	52.1±3.9	62.5±4.0	26.4±1.9	28.2±3.1	39.5±9.1	81.0±3.3	89.0±1.3	91.5±0.1	92.2±0.1
	Same value [35]	66.3±6.7	86.8±0.5	52.7±5.1	47.9±2.2	71.1±4.4	89.8±0.4	91.9±0.3	92.0±0.2	92.1±0.1
	Gaussian [6]	68.6±1.9	91.7±0.1	68.0±3.6	70.0±3.1	71.4±3.5	89.4±0.4	78.9±0.2	27.1±1.8	92.1±0.2
	sign flipping [15]	70.4±4.6	90.5±0.1	66.5±5.2	66.9±4.0	71.9±3.5	78.6±0.8	82.7±1.7	66.7±9.8	89.6±0.7
	label flipping [15]	65.3±1.5	90.0±0.1	51.4±2.3	47.9±7.2	72.2±2.9	89.7±0.5	88.2±0.7	87.1±0.2	85.4±0.4
	minic [28]	68.0±2.6	87.4±1.8	81.4±1.0	82.3±3.1	65.3±7.9	90.3±0.2	90.5±0.2	91.2±0.1	92.0±0.3
	Collusion (Ours)	65.9±4.8	84.6±0.3	69.3±5.2	69.2±7.3	76.5±6.3	89.3±0.6	91.3±0.2	41.2±2.0	92.1±0.1
Averaged	65.5±3.9	85.1±0.8	59.3±3.2	59.3±3.7	68.6±4.7	86.6±0.9	88.8±0.6	77.3±1.5	91.2±0.2	
Worst-case	52.1±3.9	62.5±4.0	26.4±1.9	28.2±3.1	39.5±9.1	78.6±0.8	78.9±0.2	27.1±1.8	85.4±0.4	

TABLE 20: Model performances of different Byzantine-resilient methods under different attacks (with Non-IID setting  $\beta = 0.1$  and 20 attackers for classification of MNIST).

		Krum [6]	GeoMeidan [13]	Median [68]	Trimmed [68]	Bulyan [21]	FLtrust [10]	DnC [52]	Kmeans [54]	FedCut (Ours)
M N I S T	No attack	89.2±0.6	92.4±0.1	84.9±0.6	84.6±0.4	86.7±0.2	89.0±0.8	92.2±0.2	92.0±0.3	92.4±0.1
	Lie [4]	89.3±0.3	88.3±0.3	86.8±0.2	86.8±0.2	86.7±0.3	89.0±0.3	92.3±0.2	92.3±0.1	92.4±0.1
	Fang-v1 [18]	89.3±0.4	80.4±1.6	53.6±4.4	52.8±2.4	82.9±1.3	78.9±1.4	92.3±0.3	92.3±0.2	92.1±0.1
	Fang-v2 [18]	47.8±5.7	70.2±2.4	50.1±4.5	47.3±4.2	34.0±2.3	80.3±0.7	90.3±0.9	91.3±0.4	92.3±0.0
	Same value [35]	89.3±0.2	88.5±0.1	69.7±1.9	70.8±1.6	85.7±0.5	88.9±0.5	92.3±0.2	92.4±0.1	92.3±0.1
	Gaussian [6]	89.4±0.4	92.1±0.2	86.1±0.4	86.2±0.6	86.7±0.2	87.9±1.1	80.3±0.6	31.1±2.2	92.3±0.0
	sign flipping [15]	89.2±0.2	91.9±0.2	86.3±0.4	86.4±0.6	86.3±0.5	76.9±2.7	91.3±0.2	76.9±1.5	91.6±0.4
	label flipping [15]	89.4±0.2	90.8±0.1	78.1±1.6	78.3±1.5	86.5±0.4	88.9±1.0	90.9±0.1	89.4±0.5	91.3±0.9
	minic [28]	86.6±4.2	89.9±0.4	88.5±1.1	90.4±0.3	75.6±1.2	90.7±0.2	92.2±0.2	92.1±0.1	92.3±0.1
	Collusion (Ours)	88.9±0.3	86.3±1.2	80.0±1.4	79.4±3.4	87.3±1.4	88.9±0.6	91.5±0.2	48.0±11.0	92.3±0.1
Averaged	84.8±1.3	87.1±0.7	76.4±1.7	76.3±1.5	79.8±0.8	85.9±0.9	90.6±0.3	79.8±1.6	92.1±0.2	
Worst-case	47.8±5.7	70.2±2.4	50.1±4.5	47.3±4.2	34.0±2.3	76.9±2.7	80.3±0.6	31.1±2.2	91.3±0.9	

TABLE 21: Model performances of different Byzantine-resilient methods under different attacks (with Non-IID setting  $\beta = 0.5$  and 20 attackers for classification of MNIST).

		Krum [6]	GeoMeidan [13]	Median [68]	Trimmed [68]	Bulyan [21]	FLtrust [10]	DnC [52]	Kmeans [54]	FedCut (Ours)
M N I S T	No attack	90.4±0.2	92.4±0.1	90.4±0.1	90.4±0.2	89.9±0.4	89.4±0.1	92.3±0.3	92.3±0.2	92.3±0.1
	Lie [4]	90.3±0.3	89.6±0.1	87.8±0.5	87.5±0.1	88.6±0.1	89.7±0.2	92.3±0.2	92.3±0.3	92.4±0.1
	Fang-v1 [18]	90.4±0.2	78.5±1.4	67.4±1.9	66.8±1.0	88.3±0.2	74.8±3.0	92.2±0.3	92.2±0.3	92.4±0.0
	Fang-v2 [18]	47.1±2.4	72.8±1.0	69.0±1.1	69.1±0.5	31.6±2.8	79.3±1.7	90.7±0.5	91.4±0.3	92.3±0.1
	Same value [35]	90.5±0.1	89.8±0.4	83.4±0.7	82.4±1.2	89.6±0.1	89.6±0.2	92.3±0.3	92.2±0.2	92.4±0.1
	Gaussian [6]	90.5±0.1	92.4±0.1	90.7±0.1	90.4±0.1	90.0±0.0	87.8±0.9	79.4±0.6	31.9±4.8	92.4±0.1
	sign flipping [15]	90.5±0.4	92.1±0.1	90.5±0.2	90.4±0.1	90.1±0.1	73.9±4.7	91.8±0.1	65.8±5.1	92.2±0.1
	label flipping [15]	90.5±0.3	90.6±0.1	88.0±0.1	87.9±0.2	90.1±0.2	89.4±0.5	92.3±0.3	92.0±0.1	92.0±0.3
	minic [28]	87.3±1.1	86.5±0.3	90.5±0.1	91.1±0.2	88.2±0.6	90.2±0.5	92.3±0.1	92.2±0.1	92.2±0.1
	Collusion (Ours)	90.4±0.2	88.0±2.0	84.7±1.7	83.5±0.4	90.0±0.2	89.1±0.7	91.5±0.2	46.9±7.1	92.1±0.1
Averaged	85.8±0.5	87.3±0.6	84.2±0.6	83.9±0.4	83.6±0.5	85.3±1.3	90.7±0.3	78.9±1.9	92.3±0.1	
Worst-case	47.1±2.4	72.8±1.0	67.4±1.9	66.8±1.0	31.6±2.8	73.9±4.7	79.4±0.6	31.9±4.8	92.0±0.3	

TABLE 22: Model performances of different Byzantine-resilient methods under different attacks (with IID and 20 attackers for classification of MNIST).

		Krum [6]	GeoMeidan [13]	Median [68]	Trimmed [68]	Bulyan [21]	FLtrust [10]	DnC [52]	Kmeans [54]	FedCut (Ours)
M N I S T	No attack	62.6±4.8	92.1±0.0	66.1±5.3	64.1±3.2	73.7±1.5	90.1±0.5	91.5±0.5	91.6±0.2	92.3±0.1
	Lie [4]	68.8±0.9	78.7±0.4	79.4±1.3	79.1±0.8	71.5±3.1	86.6±2.0	92.0±0.2	92.1±0.3	92.1±0.1
	Fang-v1 [18]	68.7±3.5	49.7±8.3	20.8±3.5	20.9±2.1	54.0±3.3	80.2±2.5	91.9±0.3	92.0±0.3	92.0±0.1
	Fang-v2 [18]	30.7±17.1	34.2±4.8	26.9±6.6	25.2±2.6	12.2±6.2	80.8±2.0	82.3±4.6	88.4±1.3	92.0±0.0
	Same value [35]	66.8±2.9	77.7±0.2	46.9±5.4	47.9±2.5	70.1±3.3	89.9±0.3	92.0±0.2	92.1±0.3	92.0±0.1
	Gaussian [6]	67.9±0.5	91.7±0.0	72.1±4.0	71.4±2.7	70.6±5.1	89.0±0.5	74.9±1.3	20.2±2.2	92.1±0.1
	sign flipping [15]	66.3±3.9	88.6±0.5	73.6±4.1	73.0±4.2	72.0±4.9	76.9±1.6	52.5±1.2	37.5±6.4	89.5±0.4
	label flipping [15]	64.1±2.0	88.6±0.3	47.2±1.4	42.7±2.8	74.2±3.5	89.9±0.6	86.7±0.8	82.9±3.3	89.6±0.4
	minic [28]	69.9±2.8	80.1±5.1	74.9±2.6	82.0±2.4	47.7±3.5	89.8±0.3	90.5±0.2	90.7±0.5	91.7±0.3
	Collusion (Ours)	69.6±6.8	79.7±1.5	66.3±2.9	66.2±3.4	75.6±7.7	89.5±0.3	88.9±1.3	39.0±16.9	91.9±0.2
Averaged	63.5±4.5	76.1±2.1	57.4±3.7	57.3±2.7	62.2±4.2	86.3±1.1	84.3±1.1	72.7±3.2	91.5±0.2	
Worst-case	30.7±17.1	34.2±4.8	20.8±3.5	20.9±2.1	12.2±6.2	76.9±1.6	52.5±1.2	20.2±2.2	89.5±0.4	

TABLE 23: Model performances of different Byzantine-resilient methods under different attacks (with Non-IID setting  $\beta = 0.1$  and 30 attackers for classification of MNIST).

		Krum [6]	GeoMeidan [13]	Median [68]	Trimmed [68]	Bulyan [21]	FLtrust [10]	DnC [52]	Kmeans [54]	FedCut (Ours)
M N I S T	No attack	88.9±0.3	92.2±0.2	85.2±0.2	84.8±0.7	86.0±0.2	88.8±0.4	92.2±0.3	92.1±0.4	92.4±0.1
	Lie [4]	89.1±0.1	82.2±0.6	82.3±1.5	81.6±1.0	83.8±0.8	88.9±0.5	92.3±0.3	92.3±0.2	92.2±0.0
	Fang-v1 [18]	89.3±0.2	51.0±3.1	35.3±7.0	34.3±2.9	78.1±0.4	78.3±3.3	92.2±0.2	92.3±0.1	92.2±0.0
	Fang-v2 [18]	33.5±6.9	40.6±3.3	40.6±4.4	34.9±3.3	14.9±3.3	81.7±1.6	84.4±1.8	87.4±0.5	92.3±0.1
	Same value [35]	88.9±0.6	82.4±0.7	55.7±0.3	53.7±2.8	85.5±1.2	88.8±0.8	92.3±0.2	92.2±0.1	92.2±0.1
	Gaussian [6]	89.2±0.3	92.3±0.1	87.1±0.7	87.4±0.4	85.7±0.4	87.7±0.6	74.0±1.7	20.3±4.4	92.3±0.0
	sign flipping [15]	89.0±0.6	91.2±0.3	87.2±0.3	87.5±0.5	86.0±0.7	75.4±0.6	83.1±1.5	64.7±9.1	91.5±0.9
	label flipping [15]	89.0±0.5	89.3±0.1	73.3±2.3	71.3±1.6	86.7±0.3	88.8±0.9	88.9±0.2	88.3±0.7	90.7±0.7
	micic [28]	73.4±5.4	82.9±1.4	83.1±3.1	87.7±0.3	72.5±8.6	90.8±0.5	91.8±0.3	91.9±0.2	92.2±0.1
	Collusion (Ours)	89.0±0.5	82.2±1.2	73.6±1.2	72.3±1.2	86.7±1.2	89.2±0.5	89.4±0.5	31.2±2.2	92.2±0.0
	Averaged	81.9±1.5	78.6±1.1	70.3±2.1	69.6±1.5	76.6±1.7	85.8±1.0	88.1±0.7	75.3±1.8	92.0±0.2
Worst-case	33.5±6.9	40.6±3.3	35.3±7.0	34.3±2.9	14.9±3.3	75.4±0.6	74.0±1.7	20.3±4.4	90.7±0.7	

TABLE 24: Model performances of different Byzantine-resilient methods under different attacks (with Non-IID setting  $\beta = 0.5$  and 30 attackers for classification of MNIST).

		Krum [6]	GeoMeidan [13]	Median [68]	Trimmed [68]	Bulyan [21]	FLtrust [10]	DnC [52]	Kmeans [54]	FedCut (Ours)
C I F A R 10	No attack	29.1±7.0	53.0±8.0	16.7±5.1	19.1±9.4	17.3±3.4	56.3±2.8	56.5±12.8	54.3±12.9	66.7±0.7
	Lie [4]	26.6±6.5	11.2±2.5	9.8±0.2	11.8±2.4	10.0±0.2	11.2±1.8	10.4±0.7	47.0±18.2	63.8±0.2
	Fang-v1 [18]	25.5±6.7	32.5±7.3	11.3±2.5	16.2±3.8	13.4±2.0	24.5±19.5	36.5±23.4	55.5±15.7	63.9±1.3
	Fang-v2 [18]	10.0±0.0	10.0±0.0	9.9±0.3	10.0±0.2	10.0±0.0	10.0±0.0	55.9±10.0	10.0±0.0	64.4±1.5
	Same value [35]	26.8±6.5	10.0±0.0	13.4±3.7	10.0±3.6	25.9±11.6	49.3±18.6	45.7±13.0	44.9±21.9	62.3±1.4
	Gaussian [6]	20.7±9.9	27.6±20.3	16.6±2.5	27.9±11.9	11.7±2.0	55.5±2.0	26.3±7.9	13.3±1.3	61.6±0.8
	sign flipping [15]	27.6±8.3	28.1±17.9	16.5±3.8	25.6±6.9	14.6±4.7	37.4±23.2	14.3±3.4	11.2±1.5	60.5±1.3
	label flipping [15]	20.3±10.1	41.6±8.5	14.9±3.4	22.1±6.2	12.7±2.9	52.3±2.5	43.1±10.6	24.9±24.8	54.8±1.4
	micic [28]	22.3±10.7	52.6±1.7	15.2±2.4	21.3±7.2	13.3±1.5	10.0±0.0	50.6±12.0	42.6±28.2	63.4±0.9
	Collusion (Ours)	28.6±6.7	10.0±0.1	9.8±0.3	9.9±0.4	13.2±3.4	55.4±3.1	29.5±7.8	10.1±0.2	62.0±1.1
	Averaged	23.8±7.2	27.7±6.6	13.4±2.4	17.4±5.2	14.2±3.2	36.2±7.4	36.9±10.2	31.4±12.5	62.3±1.1
Worst-case	10.0±0.0	10.0±0.0	9.8±0.2	9.9±0.4	10.0±0.2	10.0±0.0	10.4±0.7	10.0±0.0	54.8±1.4	

TABLE 25: Model performances of different Byzantine-resilient methods under different attacks (with Non-IID setting  $\beta = 0.1$  and 6 attackers for classification of CIFAR10).

		Krum [6]	GeoMeidan [13]	Median [68]	Trimmed [68]	Bulyan [21]	FLtrust [10]	DnC [52]	Kmeans [54]	FedCut (Ours)
C I F A R 10	No attack	25.2±16.8	55.9±13.0	18.5±10.2	59.0±13.7	17.7±7.4	62.9±0.2	59.9±15.2	56.9±16.3	66.7±1.6
	Lie [4]	37.5±9.1	10.0±0.0	10.0±0.1	11.7±2.9	10.7±1.2	16.7±7.6	10.0±0.0	31.5±30.8	67.3±0.5
	Fang-v1 [18]	35.2±10.5	49.9±16.7	15.1±3.1	23.2±5.0	15.8±3.6	43.5±29.0	56.2±17.1	56.4±16.0	64.1±0.7
	Fang-v2 [18]	10.0±0.0	10.0±0.0	13.8±2.4	13.1±6.4	10.0±0.1	10.0±0.0	63.3±4.0	15.9±4.8	65.4±0.6
	Same value [35]	37.8±8.9	15.1±8.8	10.2±0.3	10.7±1.2	37.1±16.4	59.5±0.7	58.3±15.3	56.2±17.1	62.9±0.9
	Gaussian [6]	37.5±11.5	56.1±14.2	13.7±3.0	47.9±27.7	15.2±4.6	62.3±1.6	26.6±8.4	12.6±0.5	64.9±1.2
	sign flipping [15]	36.3±11.1	51.1±20.8	17.0±2.2	41.7±12.1	16.2±3.1	60.8±0.6	17.4±1.4	20.6±9.5	63.8±0.6
	label flipping [15]	20.1±18.1	47.1±23.7	14.5±5.6	42.3±9.4	12.8±4.5	58.5±2.3	48.3±13.6	50.6±16.3	55.7±2.7
	micic [28]	40.0±3.4	60.7±5.4	22.7±2.0	62.1±1.8	17.7±1.7	10.0±0.0	63.2±1.6	45.5±30.8	67.1±1.4
	Collusion (Ours)	39.2±10.8	10.0±0.0	10.0±0.1	10.2±0.5	14.1±4.8	62.3±0.2	14.1±4.0	9.9±0.2	66.2±0.6
	Averaged	31.9±10.0	36.6±10.3	14.6±2.9	32.2±8.1	16.7±4.7	44.7±4.2	41.7±8.1	35.6±14.2	64.4±1.1
Worst-case	10.0±0.0	10.0±0.0	10.0±0.1	10.2±0.5	10.0±0.1	10.0±0.0	10.0±0.0	9.9±0.2	55.7±2.7	

TABLE 26: Model performances of different Byzantine-resilient methods under different attacks (with Non-IID setting  $\beta = 0.5$  and 6 attackers for classification of CIFAR10).



## APPENDIX C

### PROOF

We consider a *horizontal federated learning* [66], [40] setting consisting of one server and  $K$  clients. We assume  $K$  clients<sup>7</sup> have their local dataset  $\mathcal{D}_i = \{(\mathbf{x}_{i,j}, y_{i,j})\}_{j=1}^{n_i}$ ,  $i = 1 \cdots K$ , where  $\mathbf{x}_{i,j}$  is the input data,  $y_{i,j}$  is the label and  $n_i$  is the total number of data points for  $i_{th}$  client. The training in federated learning is divided into three steps which iteratively run until the learning converges:

- The  $i_{th}$  client takes empirical risk minimization as:

$$\min_{\mathbf{w}_i} F_i(\mathbf{w}_i, \mathcal{D}_i) = \min_{\mathbf{w}_i} \frac{1}{n_i} \sum_{j=1}^{n_i} \ell(\mathbf{w}_i, \mathbf{x}_{i,j}, y_{i,j}), \quad (10)$$

where  $\mathbf{w}_i \in \mathbb{R}^d$  is the  $i_{th}$  client's local model weight and  $\ell(\cdot)$  is a loss function that measures the accuracy of the prediction made by the model on each data point.

- Each client sends respective local model updates  $\nabla F_i$  to the server and the server updates the *global model*  $\mathbf{w}$  as  $\mathbf{w} = \mathbf{w} - \eta \frac{1}{K} \sum_{i=1}^K \nabla F_i$ , where  $\eta$  is learning rate.
- The server distributes the updated global model  $\mathbf{w}$  to all clients.

We assume a malicious threat mode where an unknown number of participants out of  $K$  clients are Byzantine, i.e., they may upload arbitrarily corrupt updates  $\mathbf{g}_b$  to degrade the global model performance (MP). Under this assumption, behaviours of Byzantine clients and the rest of benign clients can be summarized as follows:

$$\mathbf{g}_i = \begin{cases} \nabla F_i & \text{Benign clients} \\ \mathbf{g}_b & \text{Byzantine clients} \end{cases} \quad (11)$$

Moreover, we regard model updates contributed by  $K$  clients as an undirected graph  $G = (V, E)$ , where  $V = v_1, \dots, v_K$  represent  $K$  model updates,  $E$  is a set of weighted edge representing similarities between uploaded model updates corresponding to clients in  $V$ . We assume that the graph  $G = (V, E)$  is weighted, and each edge between two nodes  $v_i$  and  $v_j$  carries a non-negative weight, e.g.,  $A_{ij} = \exp(-\|\mathbf{g}_i - \mathbf{g}_j\|^2 / 2\sigma^2) \geq 0$ , where  $\mathbf{g}_i$  is uploaded gradient for  $i_{th}$  client and  $\sigma$  is the Gaussian scaling factor. Let  $G_R = (V_R, E_R)$  and  $G_B = (V_B, E_B)$  respectively denote two subgraphs of  $G$  representing benign and Byzantine clients.

#### C.1 Proof of Proposition 1

**Lemma 1.** [58] *Let  $G$  be an undirected graph with non-negative weights. Then the multiplicity  $c$  of the eigenvalue 1 of  $L$  equals the number of connected components  $B_1, \dots, B_c$  in the graph,*

**Remark 5.** *The analysis given in [42], [58] shows that one could estimate  $c$  by counting the number of eigenvalues equaling 1 as Lemma 1*

**Lemma 2** ([57]). *Let  $\lambda$ ,  $Y$  and  $\delta$  be eigenvalue, principle eigenvectors and the eigengap of  $L$  separately. Assume a matrix small perturbation for  $L$  as  $\tilde{L} = L + E$  so that  $\|E\|^8$  is small enough, let  $\tilde{\lambda}$ ,  $\tilde{Y}$  be eigenvalue and principle eigenvectors of  $\tilde{L}$ , then*

$$\|\lambda - \tilde{\lambda}\| \leq \|E\| \quad (12)$$

7. In this article we use terms "client", "node", "participant" and "party" interchangeably.

8.  $\|\cdot\|$  in the paper represents the  $\ell_2$  norm

$$\|Y - \tilde{Y}\| \leq \frac{4\|E\|}{\delta - \sqrt{2}\|E\|} \quad (13)$$

**Remark 6.** *From the perturbation theory, Lemma 2 demonstrates the stability of eigenvectors when there is a small perturbation of block diagonal adjacency matrix.*

**Assumption 5.** *Assume the difference of local gradients  $\nabla F_i$  and the mean of benign model update  $\nabla F = \frac{1}{|V_R|} \sum_{i \in V_R} \nabla F_i$  is bounded ( $V_R$  is the set of benign clients), i.e., there exists a finite  $\kappa$ , such that*

$$\|\nabla F_i - \nabla F\| \leq \kappa.$$

**Remark 7.**  $\kappa$  in Assumption 5 has also been used earlier to bound heterogeneity in datasets [37]; Specifically, when the data is homogeneous, we have  $\kappa = 0$  in Assumption 5.

**Proposition 4.** *Suppose  $K$  clients consist of  $m$  benign clients and  $q$  attackers ( $q < m - 1$ ). If Assumption 5 holds for Non-collusion and Collusion-diff attacks, then only the first  $c$  eigenvalues are close to 1 and*

- $c = 1 + q < \frac{K}{2}$  for Non-collusion attacks provided that  $\|\mathbf{g}_b - \nabla F\| \gg \kappa$  and malicious updates ( $\mathbf{g}_b$ ) are far away from each other;
- $c = 1 + B < \frac{K}{2}$  for Collusion-diff attacks provided that malicious updates form  $B$  groups and  $\|\mathbf{g}_b - \nabla F\| \gg \kappa$ ;
- $c > \frac{K}{2}$  for Collusion-mimic attacks that  $\|\mathbf{g}_b - \nabla F\| < \kappa$  and malicious updates are almost identical.

*Proof.* For Non-Collusion attack,  $\|\mathbf{g}_b - \nabla F\| > \kappa$  and malicious updates ( $\mathbf{g}_b$ ) are far away from each other. Therefore, we define normalized adjacency matrix  $A$  in the ideal case is block-wised where benign clients form a block with no relations to other attackers. Consequently, we obtain the largest  $c$  eigenvalues of  $A$  are 1 according to Lemma 1, where  $c = 1 + q < \frac{K}{2}$ . In general, normalized adjacency matrix  $\tilde{A} = A + E$ . Based on conditions that malicious updates ( $\mathbf{g}_b$ ) are far away from each other and  $\|\mathbf{g}_b - \nabla F\| \gg \kappa$ , we have  $\tilde{A}_{ij} = \exp(-\|\mathbf{g}_b - \nabla F_i\|/\sigma^2)$  is small, so  $\|E\|$  is small. Consequently, according to Lemma 2,

$$\tilde{\lambda} - \lambda \leq \|E\| \quad (14)$$

As a result, we obtain the first  $q$  eigenvalues of  $\tilde{A}$  are close to 1 due to the small  $\|E\|$ .

Similarly, we have  $c = 1 + B < \frac{K}{2}$  for Collusion-diff attack; the first  $c$  eigenvalues of  $\tilde{A}$  are close to 1 for Collusion-mimic attack, and  $c \geq m + 1 > \frac{K}{2}$ .  $\square$

**Remark 8.** *Proposition 4 illustrates that the eigenvalue 1 has multiplicity  $c$ , and then there is a gap to the  $(c + 1)_{th}$  eigenvalue  $\lambda_{c+1} < 1$ . Therefore, we can use the position of the obvious eigengap to elucidate the number of community clusters<sup>9</sup>. Moreover, Proposition 4 demonstrates the different positions of obvious eigengap for Non-collusion, Collusion-diff and Collusion-mimic attacks.*

9. We use the largest eigengap to determine the community clusters

## C.2 Proof of Proposition 2

**Lemma 3.** Minimizing  $\sum_{i=1}^c W(B_i, \bar{B}_i)/\text{vol}(B_i)$  over all  $c$ -partition  $V = B_1 \cup \dots \cup B_c$  is equivalent with maximizing  $\text{tr}(H^T D^{-1/2} A D^{-1/2} H)$  over  $\{H | H \in \mathbb{R}^{K \times c}, H^T H = I\}$ , where  $W(B_i, B_j) := \sum_{i \in B_i, j \in B_j} A_{ij}$  and  $\text{tr}$  represents the trace of matrix.

*Proof.* Define  $\mathbf{f}_i = (f_{i1}, \dots, f_{iK})^T$

$$f_{ij} = \begin{cases} \sqrt{\frac{1}{\text{vol}(B_i)}}, & v_j \in B_i \\ 0, & v_j \notin B_i \end{cases} \quad (15)$$

Then

$$\begin{aligned} \mathbf{f}_i^T (D - A) \mathbf{f}_i &= \frac{1}{2} \sum_{m=1}^K \sum_{n=1}^K A_{mn} (f_{im} - f_{in})^2 \\ &= \frac{1}{2} \left[ \sum_{v_m \in B_i, v_n \notin B_i} A_{mn} (f_{im} - f_{in})^2 \right. \\ &\quad \left. + \sum_{v_n \in B_i, v_m \notin B_i} A_{mn} (f_{im} - f_{in})^2 \right] \\ &= \frac{1}{2} \left[ \sum_{v_m \in B_i, v_n \notin B_i} A_{mn} \left( \sqrt{\frac{1}{\text{vol}(B_i)}} - 0 \right)^2 \right. \\ &\quad \left. + \sum_{v_n \in B_i, v_m \notin B_i} A_{mn} \left( 0 - \sqrt{\frac{1}{\text{vol}(B_i)}} \right)^2 \right] \\ &= W(B_i, \bar{B}_i) / \text{Vol}(B_i), \end{aligned} \quad (16)$$

where  $W(B_i, B_j) := \sum_{i \in B_i, j \in B_j} A_{ij}$ . Moreover, we have  $\mathbf{f}_i^T \mathbf{f}_i = 1/\text{vol}(B_i)$ . Thus,

$$\sum_{i=1}^c W(B_i, \bar{B}_i) / \text{Vol}(B_i) = \sum_{i=1}^c \mathbf{f}_i^T (D - A) \mathbf{f}_i = \text{tr}(F^T (D - A) F), \quad (17)$$

where  $F$  is matrix combining all  $\mathbf{f}_i$ . Let  $F = D^{-1/2} H$ , then  $H^T H = I$  and

$$\begin{aligned} \min_{(B_1 \cup \dots \cup B_c) = V} \sum_i W(B_i, \bar{B}_i) / \text{Vol}(B_i) &= \min_F \text{tr}(F^T (D - A) F) \\ &= \min_H \text{tr}(H^T D^{-1/2} (D - A) D^{-1/2} H) \\ &= c - \max_H \text{tr}(H^T D^{-1/2} A D^{-1/2} H) \end{aligned} \quad (18)$$

In federated learning, clients would send the updates to the server in each iteration, thus we consider the graph for all iterations as follows:

**Definition 5.** (Spatial-Temporal Graph) Define a Spatial-Temporal graph  $G = (V, E)$  as a sequence of snapshots  $\langle G^1, \dots, G^t \rangle$ , where  $G^t = (V, E^t)$  is an undirected graph at iteration  $t$ .  $V$  denotes a fixed set of vertexes representing model updates belonging to  $K$  clients.  $E^t$  is a set of weighted edge representing similarities between model updates corresponding to clients in  $V$  at iteration  $t$ , where related adjacency matrix of the graph is  $A^t$ .

The  $c$ -partition Ncut for Spatial-Temporal Graph is thus defined as follows:

**Definition 6.** ( $c$ -partition Ncut for Spatial-Temporal Graph) Let  $G = (V, E)$  be a Spatial-Temporal graph as Def. 5. Denote the  $c$ -partition for graph  $G$  as  $V = B_1 \cup \dots \cup B_c$  and  $B_i \cap B_j = \emptyset$  for any  $i, j$ ,  $c$ -partition Ncut for Spatial-Temporal Graph aims to optimize:

$$\min_{(B_1 \cup \dots \cup B_c) = V} \sum_{t=1}^T \sum_{i=1}^c \frac{W^t(B_i, \bar{B}_i)}{\text{Vol}^t(B_i)}, \quad (19)$$

where  $\bar{B}_i$  is the complement of  $B_i$ ,  $W^t(B_i, B_j) := \sum_{v_i \in B_i, v_j \in B_j} A_{ij}^t$ , and  $A_{ij}^t$  is edge weight of  $B_i$  and  $B_j$ , and  $\text{Vol}^t(B_i) := \sum_{v_i \in B_i} \sum_{v_j \in V} A_{ij}^t$

**Proposition 5.** FedCut (Algo. 2) solves the  $c$ -partition Ncut in Eq. (19).

*Proof.* Firstly, according to the line 2 in Algo. 2,

$$\begin{aligned} \tilde{L}^t &= \frac{t-1}{t} \tilde{L}^{t-1} + \frac{1}{t} L^t \\ &= \frac{t-1}{t} \left( \frac{t-2}{t-1} \tilde{L}^{t-2} + \frac{1}{t-1} L^{t-1} \right) + \frac{1}{t} L^t \\ &= \frac{t-2}{t} \tilde{L}^{t-2} + \frac{1}{t} (L^{t-1} + L^t) \\ &= \dots \\ &= \frac{1}{t} \sum_{i=1}^t L^i, \end{aligned} \quad (20)$$

where  $L^i = D^{-1/2} A^i D^{-1/2}$ . Furthermore, according to Lemma 3,

$$\begin{aligned} \min_{(B_1 \cup \dots \cup B_c) = V} \sum_{t=1}^t \sum_{i=1}^c \frac{W^t(B_i, \bar{B}_i)}{\text{Vol}^t(B_i)} &= \min_H \sum_{i=1}^t \text{tr}(H^T D^{t-1/2} (D^t - A^t) D^{t-1/2} H) \\ &= \min_H \text{tr}(H^T \left( \sum_{i=1}^t D^{t-1/2} (D^t - A^t) D^{t-1/2} \right) H) \\ &= \min_H \text{tr}(H^T \sum_{i=1}^t L^t H) \\ &= \min_H \text{tr}(H^T \tilde{L}^t H) t, \end{aligned} \quad (21)$$

where  $H^T H = I$ . By the Rayleigh-Ritz theorem [39] it can be seen immediately that the solution of  $\min_H \text{tr}(H^T \tilde{L}^t H) t$  is given by the  $H$  which is the eigenvector corresponding to the  $c$  largest eigenvalue of  $\tilde{L}^t$ . Thus we prove that FedCut aims to solve the  $c$ -partition Ncut in Eq. (19) for Spatial-Temporal graph among  $t$  iterations.  $\square$

## C.3 Proof of Theorem 1

**Assumption 6.** For malicious updates  $\mathbf{g}_b$  provided that  $\|\mathbf{g}_b - \nabla F\| > \kappa$ , the difference between the mean of benign updates and colluders' updates has at least  $C\kappa$  distance, where  $C$  is a large constant, i.e.,

$$\|\mathbf{g}_b - \nabla F\| > C\kappa.$$

**Lemma 4** ([42]). Let adjacency matrix  $A$ 's off-diagonal blocks  $A^{ij}$ ,  $i \neq j$  be zero (block diagonal matrix). Also assume that each cluster is connected. Then there exists  $c$  orthogonal vectors  $r_1, \dots, r_c$

( $r_i^T r_j = 1$  if  $i = j$ , 0 otherwise) so that top  $c$  eigenvectors ( $Y \in \mathbb{R}^{K \times c}$ ) of normalized adjacency matrix satisfy

$$y_j^{(i)} = r_i, \quad (22)$$

for all  $i = 1, \dots, c, j = 1, \dots, n_i$ , where  $y_j^{(i)}$  represents  $j_{th}$  rows in  $i_{th}$  clusters of  $Y$ . In other words, there are  $c$  mutually orthogonal points on the surface of the unit  $c$ -sphere around which  $Y$ 's rows will cluster. Moreover, these clusters correspond exactly to the true clustering of the original data.

**Lemma 5** (Theorem 4.14 in [43]). *Defined  $Y$  same as Lemma 4, the Kmeans algorithm that clusters  $\tilde{Y} = Y + E_1$  into  $c$  groups returns an optimal solution of cost at most  $\frac{1-\epsilon^2}{1-32\epsilon^2}\epsilon^2$  with probability  $1 - \tilde{O}(\sqrt{\epsilon})$ , where  $\epsilon = \|E_1\|$*

**Remark 9.** 1) Lemma 4 illustrates the clustering accuracy of NCut is 100% in clustering top  $c$  eigenvectors when adjacency matrix is the block diagonal matrix.

2) Lemma 5 shows Kmeans clustering for eigenvectors  $Y$  still reach optimal clustering with a large probability when eigenvectors  $Y$  has a small perturbation.

**Theorem 3.** *Suppose an  $0 < \alpha < \frac{1}{2}$  fraction of clients are Byzantine attackers. If Assumption 5 and 6 holds, we can find the estimate of  $\hat{\mathbf{g}}$  of  $\bar{\mathbf{g}}$  according to line 12 in Algo. 1 and with the probability  $1 - \tilde{O}(\sqrt{Z_1})$ , such that  $\|\hat{\mathbf{g}} - \bar{\mathbf{g}}\| \leq \tilde{O}(C\alpha\kappa)$ , where  $Z_1 = \frac{4K\sqrt{Z\frac{C^2}{4}}}{\delta - K\sqrt{2Z\frac{C^2}{4}}}$ ,  $Z = \exp(-2\kappa^2/\sigma^2)$ .*

*Proof.* Suppose the server receives first  $(K - q)$  correct gradients  $\{\mathbf{g}_1, \dots, \mathbf{g}_{K-q}\}$  with mean  $\bar{\mathbf{g}}$ . Therefore, we have

$$\|\mathbf{g}_i - \mathbf{g}_j\| \leq \|\mathbf{g}_i - \bar{\mathbf{g}}\| + \|\mathbf{g}_j - \bar{\mathbf{g}}\| \leq 2\kappa, \quad (23)$$

for any  $1 \leq i, j \leq K - q$ . Thus we have  $A_{ij} \geq \exp(-2\kappa^2/\sigma^2) \triangleq Z$  ( $0 < Z < 1$ ), for any  $1 \leq i, j \leq K - q$ .

Moreover, for any updated gradients of clients in different party (such as  $\mathbf{g}_i, \mathbf{g}_j$ ), according to Assumption 6, we have

$$\|\mathbf{g}_i - \mathbf{g}_j\| \geq C\kappa. \quad (24)$$

Consequently,  $A_{ij} < \exp(-C^2\kappa^2/(2\sigma^2)) = Z\frac{C^2}{4}$ , for any  $i, j$  in different parties.

On one hand, if  $A_{ij} = 0$ , for any  $i, j$  in different parties, then the adjacency matrix  $A$  is block diagonal matrix so we could apply Lemma 4 to get 100% clustering accuracy for solving FedCut ( $c$ -partition NCut for Spatial-temporal Graph) in  $t_{th}$  iteration, i.e., server would select clusters ( $\mathcal{T}$ ) with largest number of clusters. Since  $\alpha < 0.5$ , the clusters with largest number must include all benign updates and malicious updates that  $\|\mathbf{g}_b - \bar{\mathbf{g}}\| < \kappa$ . As a result,

$$\|\hat{\mathbf{g}} - \bar{\mathbf{g}}\| \leq \frac{q\|\mathbf{g}_b - \bar{\mathbf{g}}\|}{K} \leq \tilde{O}\left(\frac{q\kappa}{K}\right) \quad (25)$$

On the other hand, in general case that adjacency matrix  $\tilde{A}_{ij} > 0$ , for any  $i, j$  in different parties, set  $\tilde{A} = A + E$ , where  $A$  is block diagonal matrix and  $E$  is perturbation matrix. For the large  $C$ ,  $Z\frac{C^2}{4}$  is small enough. Consequently, we have

$$\begin{aligned} \|Y - \tilde{Y}\| &\leq \frac{4\|E\|_2}{\delta - \sqrt{2}\|E\|_2} \\ &\leq \frac{4K\sqrt{\alpha(1-\alpha)Z\frac{C^2}{4}}}{\delta - K\sqrt{2\alpha(1-\alpha)Z\frac{C^2}{4}}} \triangleq Z_1. \end{aligned} \quad (26)$$

The first inequality is according to Lemma 2 and second is due to  $\|E\|_2 \leq K\sqrt{\alpha(1-\alpha)}\sqrt{Z\frac{C^2}{4}}$ . according to Lemma 5, we could obtain the optimal clustering with probability  $1 - \tilde{O}(\sqrt{Z_1})$ . Similarly, we have

$$\|\hat{\mathbf{g}} - \bar{\mathbf{g}}\| \leq \frac{q\|\mathbf{g}_b - \bar{\mathbf{g}}\|}{K} \leq \tilde{O}\left(\frac{q\kappa}{K}\right) \quad (27)$$

for line 12 in Algo. 1 with probability  $1 - \tilde{O}(\sqrt{Z_1})$ , where

$$Z_1 = \frac{4K\sqrt{\alpha(1-\alpha)Z\frac{C^2}{4}}}{\delta - K\sqrt{2\alpha(1-\alpha)Z\frac{C^2}{4}}}, \quad Z = \exp(-2\kappa^2/\sigma^2). \quad \square$$

#### C.4 Proof for Theorem 2

Following definitions of federated learning introduced in [66], [40], we consider a *horizontal federated learning* setting consisting of one server and  $K$  clients. We assume  $K$  clients have their local dataset  $\mathcal{D}_i, i = 1 \dots K$ . In each step,  $i_{th}$  client minimizes the local risk function as  $\min_{\mathbf{w}_i} F_i(\mathbf{w}_i) = \min_{\mathbf{w}_i} \frac{1}{|\mathcal{D}_i|} \sum_{j=1}^{|\mathcal{D}_i|} F_i(\mathbf{w}, \mathbf{x}_{i,j})$ , where  $\mathbf{x}_{i,j} \in \mathcal{D}_i, j \in [|\mathcal{D}_i|]$ . Then clients send the updates  $\mathbf{g}_i = \nabla F_i(\mathbf{w}_i)$  to the server and server aggregate the gradients to update the global model  $\mathbf{w}$ , finally the server distribute the  $\mathbf{w}$  to all clients (see details in Algo. 1). Specifically, for  $t + 1$  iteration, server update the global model  $\mathbf{w}_{t+1}$  as:

$$\mathbf{w}^{t+1} = \mathbf{w}^t - \eta \hat{\mathbf{g}}^t \quad (28)$$

**Assumption 7.** *The stochastic gradients sampled from any local dataset have uniformly bounded variance over  $\mathcal{D}_i$  for all clients, i.e., there exists a finite  $\sigma_0$ , such that for all  $x \in \mathcal{D}_i, i \in [K]$ , we have*

$$\mathbb{E}_j \|\nabla F_i(\mathbf{w}, x_{i,j}) - \nabla F_i(\mathbf{w})\|^2 \leq \sigma_0^2. \quad (29)$$

**Remark 10.** *The difference between Assumption 5 and 7 is that the former bounds the variance across gradient estimates within the same client while the latter bounds the variance between model updates across clients.*

**Assumption 8.** *We assume that  $F(x)$  is  $L$ -smooth and has  $\mu$ -strong convex.*

**Lemma 6** ([7]). *If  $F$  is  $L$ -smooth, then for all  $\mathbf{w}^*$  (optimal solution w.r.t  $F$ ), then:*

$$\frac{1}{2L} \|\nabla F(x)\|^2 \leq F(\mathbf{w}) - F(\mathbf{w}^*) \leq \frac{L}{2} \|\mathbf{w} - \mathbf{w}^*\|^2 \quad (30)$$

**Theorem 4.** *Suppose an  $0 < \alpha < \frac{1}{2}$  fraction of clients are corrupted. For a global objective function  $F : \mathbb{R}^d \rightarrow \mathbb{R}$ , the server distributes a sequence of iterates  $\{\mathbf{w}^t : t \in [0 : T]\}$  (see Algo. 1) when run with a fixed step-size  $\eta < \min\{\frac{1}{4L}, \frac{1}{\mu}\}$ . If Assumption 5, 6, 7 and 8 holds, the sequence of average iterates  $\{\mathbf{w}^t : t \in [0 : T]\}$  satisfy the following convergence guarantees<sup>10</sup>:*

$$\|\mathbf{w}^T - \mathbf{w}^*\|^2 \leq (1 - \frac{C_1\mu}{L})^T \|\mathbf{w}^0 - \mathbf{w}^*\|^2 + \frac{\Gamma}{\mu^2}, \quad (31)$$

where  $\Gamma = \tilde{O}(\sigma_0^2 + \kappa^2 + C^2\alpha^2\kappa^2)$ ,  $b$  is batch size and  $\mathbf{w}^*$  is the global optimal weights in federated learning.

10. There are some modifications for theorem 2 compared to main text, please refer to Theorem 2 here instead of main text

*Proof.* Note that  $\mathbf{w}^t = \frac{1}{K} \sum_{i=1}^K \mathbf{w}_i^t$ , so we have:

$$\begin{aligned}
\mathbf{w}^{t+1} &= \mathbf{w}^t - \eta \hat{\mathbf{g}}^t \\
&= \mathbf{w}^t - \eta \nabla F(\mathbf{w}^t) + \eta \nabla F(\mathbf{w}^t) - \eta \frac{1}{K} \sum_{i=1}^K \nabla F_i(\mathbf{w}^t) \\
&\quad + \eta \frac{1}{K} \sum_{i=1}^K \nabla F_i(\mathbf{w}^t) - \eta \hat{\mathbf{g}}^t \\
&= \underbrace{[\mathbf{w}^t - \eta \nabla F(\mathbf{w}^t)]}_{=:U_1} + \underbrace{\eta \left[ \frac{1}{K} \sum_{i=1}^K (\nabla F(\mathbf{w}^t) - \nabla F_i(\mathbf{w}_i^t)) \right]}_{=:U_2} \\
&\quad + \underbrace{\eta \left[ \frac{1}{K} \sum_{i=1}^K \nabla F_i(\mathbf{w}_i^t) - \hat{\mathbf{g}}^t \right]}_{=:U_3}
\end{aligned} \tag{32}$$

Therefore,

$$\mathbf{w}^{t+1} - \mathbf{w}^* = [U_1 - \mathbf{w}^*] + \eta U_2 + \eta U_3 \tag{33}$$

Taking norm on both sides and then squaring:

$$\begin{aligned}
\|\mathbf{w}^{t+1} - \mathbf{w}^*\|^2 &= \|U_1 - \mathbf{w}^*\|^2 + \eta^2 \|U_2 + U_3\|^2 \\
&\quad + 2\eta \langle U_1 - \mathbf{w}^*, U_2 + U_3 \rangle
\end{aligned} \tag{34}$$

Taking use of  $2 \langle \mathbf{a}, \mathbf{b} \rangle \leq \|\mathbf{a}\|^2 + \|\mathbf{b}\|^2$ , we have

$$\begin{aligned}
2\eta \langle U_1 - \mathbf{w}^*, U_2 + U_3 \rangle &= 2 \langle \sqrt{\frac{\eta\mu}{2}}(U_1 - \mathbf{w}^*), \sqrt{\frac{\eta}{\mu}}(U_2 + U_3) \rangle \\
&\leq \frac{\eta\mu}{2} \|U_1 - \mathbf{w}^*\|^2 + \frac{2\eta}{\mu} \|U_2 + U_3\|^2
\end{aligned} \tag{35}$$

Combining Eq. (34) and (35), we have:

$$\begin{aligned}
\|\mathbf{w}^{t+1} - \mathbf{w}^*\|^2 &\leq \left(1 + \frac{\eta\mu}{2}\right) \|U_1 - \mathbf{w}^*\|^2 \\
&\quad + \left(\eta^2 + \frac{2\eta}{\mu}\right) \|U_2 + U_3\|^2 \\
&\leq \left(1 + \frac{\eta\mu}{2}\right) \|U_1 - \mathbf{w}^*\|^2 \\
&\quad + \left(2\eta^2 + \frac{4\eta}{\mu}\right) \|U_2\|^2 + \left(2\eta^2 + \frac{4\eta}{\mu}\right) \|U_3\|^2
\end{aligned} \tag{36}$$

Substituting the values of  $U_1, U_2$  and  $U_3$  into Eq. (34), taking expectation w.r.t. the stochastic sampling of gradients by clients, we could get:

$$\begin{aligned}
\|\mathbf{w}^{t+1} - \mathbf{w}^*\|^2 &\leq \left(1 + \frac{\eta\mu}{2}\right) \|\mathbf{w}^t - \eta \nabla F(\mathbf{w}^t) - \mathbf{w}^*\|^2 \\
&\quad + \left(2\eta^2 + \frac{4\eta}{\mu}\right) \left\| \frac{1}{K} \sum_{i=1}^K (\nabla F(\mathbf{w}^t) - \nabla F_i(\mathbf{w}_i^t)) \right\|^2 \\
&\quad + \left(2\eta^2 + \frac{4\eta}{\mu}\right) \left\| \frac{1}{K} \sum_{i=1}^K \nabla F_i(\mathbf{w}_i^t) - \hat{\mathbf{g}}^t \right\|^2
\end{aligned} \tag{37}$$

Now we bound each of the three terms on the RHS of Eq. (37) separately as follows:

**Firstly**, since  $F$  is  $\mu$  strong convex,  $\langle \mathbf{w}^* - \mathbf{w}^t, \nabla F(\mathbf{w}^t) \rangle \geq$

$F(\mathbf{w}^*) - F(\mathbf{w}^t) - \frac{\mu}{2} \|\mathbf{w}^* - \mathbf{w}^t\|^2$ . Also, according to Lemma 6, we have:

$$\begin{aligned}
&\|\mathbf{w}^t - \eta \nabla F(\mathbf{w}^t) - \mathbf{w}^*\|^2 \\
&= \|\mathbf{w}^t - \mathbf{w}^*\|^2 + \eta^2 \|\nabla F(\mathbf{w}^t)\|^2 \\
&\quad + 2\eta \langle \mathbf{w}^* - \mathbf{w}^t, \nabla F(\mathbf{w}^t) \rangle \\
&\leq (1 - \mu\eta) \|\mathbf{w}^t - \mathbf{w}^*\|^2 + \left(\eta^2 - \frac{\eta}{L}\right) \|\nabla F(\mathbf{w}^t)\|^2 \\
&\leq (1 - \mu\eta) \|\mathbf{w}^t - \mathbf{w}^*\|^2,
\end{aligned} \tag{38}$$

where the last inequality is due to  $\eta < \frac{1}{4L}$ . **Secondly**,

$$\begin{aligned}
&\left\| \frac{1}{K} \sum_{i=1}^K (\nabla F(\mathbf{w}^t) - \nabla F_i(\mathbf{w}_i^t)) \right\|^2 \\
&\leq \frac{1}{K^2} \sum_{i=1}^K \|\nabla F(\mathbf{w}^t) - \nabla F_i(\mathbf{w}_i^t)\|^2 \\
&\leq \frac{2}{K^2} \sum_{i=1}^K [\|\nabla F(\mathbf{w}^t) - \nabla F(\mathbf{w}_i^t)\|^2 \\
&\quad + \|\nabla F(\mathbf{w}_i^t) - \nabla F_i(\mathbf{w}_i^t)\|^2] \\
&\leq \frac{2L^2}{K^2} \sum_{i=1}^K \|\mathbf{w}^t - \mathbf{w}_i^t\|^2 + 2\kappa^2
\end{aligned} \tag{39}$$

Note that

$$\|\mathbf{w}^t - \mathbf{w}_i^t\|^2 = \left\| \frac{1}{K} \sum_{k=1}^K (\mathbf{w}_k^t - \mathbf{w}_i^t) \right\|^2 \leq \frac{1}{K} \sum_{k=1}^K \|\mathbf{w}_k^t - \mathbf{w}_i^t\|^2 \tag{40}$$

Moreover, for the batch data  $\mathcal{S}$ , we have

$$\begin{aligned}
\|\mathbf{w}_k^t - \mathbf{w}_i^t\|^2 &= \frac{\eta^2}{|\mathcal{S}|} \left\| \sum_j (\nabla F_i(\mathbf{w}_i^t, x_{ij}) - \nabla F_k(\mathbf{w}_k^t, x_{kj})) \right\|^2 \\
&\leq \frac{\eta^2}{|\mathcal{S}|} \sum_j \|\nabla F_i(\mathbf{w}_i^t, x_{ij}) - \nabla F_k(\mathbf{w}_k^t, x_{kj})\|^2 \\
&\leq \frac{5\eta^2}{|\mathcal{S}|} \sum_j [(\|\nabla F_i(\mathbf{w}_i^t, x_{ij}) - \nabla F_i(\mathbf{w}_i^t)\|^2) \\
&\quad + (\|\nabla F_k(\mathbf{w}_k^t) - \nabla F_k(\mathbf{w}_k^t, x_{kj})\|^2) \\
&\quad + (\|\nabla F_i(\mathbf{w}_i^t) - \nabla F(\mathbf{w}_i^t)\|^2) + (\|\nabla F(\mathbf{w}_i^t) - \nabla F(\mathbf{w}_k^t)\|^2) \\
&\quad + (\|\nabla F(\mathbf{w}_k^t) - \nabla F_k(\mathbf{w}_k^t)\|^2)] \\
&\leq 5\eta^2 [\sigma_0^2 + \sigma_0^2 + 4\kappa^2 + L^2 \|\mathbf{w}_i^t - \mathbf{w}_k^t\|^2 + 4\kappa^2]
\end{aligned} \tag{41}$$

The second inequality is due to the Cauchy-Schwarz inequality. The Third inequality is because of Lemma 7, Assumption 5 and 8. Then we transfer  $\|\mathbf{w}_i^t - \mathbf{w}_k^t\|^2$  to RHS of Eq. (41), we derive:

$$(1 - 5\eta^2 L^2) \|\mathbf{w}_i^t - \mathbf{w}_k^t\|^2 \leq 5(2\sigma_0^2 + 8\kappa^2) \tag{42}$$

Thus

$$\|\mathbf{w}_i^t - \mathbf{w}_k^t\|^2 \leq \frac{5(2\sigma_0^2 + 8\kappa^2)}{(1 - 5\eta^2 L^2)} \tag{43}$$

Combining Eq. (39), (40) and (43), we obtain

$$\begin{aligned} & \left\| \frac{1}{K} \sum_{i=1}^K (\nabla F(\mathbf{w}^t) - \nabla F_i(\mathbf{w}_i^t)) \right\|^2 \\ & \leq \frac{2L^2}{K^2} \frac{5K^2(2\sigma_0^2 + 8\kappa^2)}{(1 - 5\eta^2)} + 2\kappa^2 \\ & = \frac{10L^2(2\sigma_0^2 + 8\kappa^2)}{(1 - 5\eta^2L^2)} + 2\kappa^2 \end{aligned} \quad (44)$$

**Thirdly**, according to Theorem 3, we obtain

$$\left\| \frac{1}{K} \sum_{i=1}^K \nabla F_i(\mathbf{w}_i^t) - \hat{\mathbf{g}}^t \right\| \leq \tilde{\mathcal{O}}(\alpha^2 \kappa^2) \quad (45)$$

**Finally**, Noted that  $1 - 5\eta^2L^2 > \frac{1}{2}$  and  $(1 + \frac{\eta\mu}{2})(1 - \mu\eta) < 1 - \frac{\mu\eta}{2}$  when  $\eta < \frac{1}{4L}$ . And if  $\eta + \frac{2}{\mu} < \frac{3}{\mu}$ , i.e.,  $\eta < \frac{1}{\mu}$ , we bounded Eq.(37) as:

$$\begin{aligned} \|\mathbf{w}^{t+1} - \mathbf{w}^*\|^2 & \leq (1 + \frac{\eta\mu}{2})(1 - \mu\eta)\|\mathbf{w}^t - \mathbf{w}^*\|^2 \\ & + (2\eta^2 + \frac{4\eta}{\mu})\left(\frac{10L^2(2\sigma_0^2 + 8\kappa^2)}{(1 - 5\eta^2L^2)} + 2\kappa^2\right) + (2\eta^2 + \frac{4\eta}{\mu})\tilde{\mathcal{O}}(\alpha^2 \kappa^2) \\ & \leq (1 - \frac{\mu\eta}{2})\|\mathbf{w}^t - \mathbf{w}^*\|^2 + (2\eta^2 + \frac{4\eta}{\mu})\left(\frac{10L^2(2\sigma_0^2 + 8\kappa^2)}{(1 - 5\eta^2L^2)} + 2\kappa^2\right) \\ & + (2\eta^2 + \frac{4\eta}{\mu})\tilde{\mathcal{O}}(\alpha^2 \kappa^2) \\ & \leq (1 - \frac{\mu\eta}{2})\|\mathbf{w}^t - \mathbf{w}^*\|^2 + \frac{240\eta}{\mu}(\sigma_0^2 + 4\kappa^2) + \frac{12\kappa^2\eta}{\mu} \\ & + (\frac{6\eta}{\mu})\tilde{\mathcal{O}}(\alpha^2 \kappa^2) \end{aligned} \quad (46)$$

Therefore, we could use Eq. (46) by induction for  $t = 1, \dots, T - 1$  to obtain

$$\begin{aligned} & \left\| \mathbf{w}^T - \mathbf{w}^* \right\|^2 \\ & \leq (1 - \frac{\eta\mu}{2})^T \|\mathbf{w}^0 - \mathbf{w}^*\|^2 + \left[ \frac{240\eta}{\mu}(\sigma_0^2 + 4\kappa^2) + \frac{12\kappa^2\eta}{\mu} \right. \\ & \left. + (\frac{6\eta}{\mu})\tilde{\mathcal{O}}(C^2\alpha^2\kappa^2) \right] / (\frac{\mu\eta}{2}) \\ & = (1 - \frac{\eta\mu}{2})^T \|\mathbf{w}^0 - \mathbf{w}^*\|^2 + \tilde{\mathcal{O}}(\sigma_0^2 + \kappa^2 + \alpha^2\kappa^2) / \mu^2 \\ & \leq (1 - \frac{C_1\mu}{L})^T \|\mathbf{w}^0 - \mathbf{w}^*\|^2 + \frac{1}{\mu^2}\Gamma \end{aligned} \quad (47)$$

where  $\Gamma = \tilde{\mathcal{O}}(\sigma_0^2 + \kappa^2 + \alpha^2\kappa^2)$  and  $C_1$  is a constant.  $\square$